EPIGENETIC PROGRAMMING OF CHIMERIC ANTIGEN RECEPTOR (CAR) T CELLS

by

Nayan Jain

A Dissertation

Presented to the Faculty of the Louis V. Gerstner, Jr.

Graduate School of Biomedical Sciences,

Memorial Sloan Kettering Cancer Center

in Partial Fulfillment of the Requirements for the Degree of

Doctor of Philosophy

New York, NY

September, 2022

Michel W. Sadelain, MD, PhD
Dissertation Mentor

Date

To my family, Rajesh, Veena, and Palak.

ABSTRACT

Chimeric antigen receptor (CAR) T cells have induced remarkable responses in patients with hematological malignancies but so far, their efficacy has been limited in solid tumors. There is, therefore, a need to engineer CAR T cells to endow them with enhanced anti-tumor function.

Multiple studies have shown that T cell effector differentiation and eventual dysfunction are associated with transcriptional and epigenetic changes acquired over time. Here, we report divergent effects of modulating the epigenetic landscape of human CAR T cells by disruption of two different epigenetic factors: *TET2*, a methylcytosine dioxygenase and *SUV39H1*, a histone methyltransferase.

Disruption of *TET2* initially enhances *in vivo* (murine NSG model bearing human acute lymphoblastic leukemia cell line, NALM6) anti-tumor efficacy of T cells in a CAR design dependent manner. However, over time, substantial antigen-independent clonal CAR T cell expansions develop, resulting in multi-organ infiltration and death. Functional characterization of these proliferative CAR T cells revealed near total loss of effector function. Molecular characterization revealed that CAR expression and biallelic *TET2* disruption are necessary to achieve sustained proliferation. Further transcriptional and genome accessibility characterization revealed that *TET2* disruption in CAR T cells results in an establishment of an epigenetic state that allows for the AP-1 factor, BATF3, to drive

MYC expression which drives sustained antigen-independent proliferation in TET2 deficient CAR T cells.

In the aforementioned murine model, we find that disruption of *SUV39H1* in human CAR T cells improves their anti-tumor efficacy. This enhanced anti-tumor efficacy is associated with improved early expansion and long-term persistence of *SUV39H1*-edited CAR T cells. Paired genome accessibility and transcriptional analysis on *SUV39H1*-edited and unedited CAR T cells revealed epigenetic changes associated with SUV39H1 loss that promote expression of memory associated transcription factors (*TCF1*, *LEF1* and *KLF2*) and curtail T cell dysfunction. We find that robust long-term expression of memory factors in *SUV39H1*-edited CAR T cells allows for their improved metabolic fitness and enhances their ability to reject tumor upon multiple *in vivo* tumor rechallenges. Long-term (200 days) follow up of mice treated with *SUV39H1*-edited CAR T cells found no evidence of toxicity as was observed in mice treated with *TET2*-edited CAR T cells.

In summary, our findings illustrate the therapeutic promise of CAR T cell epigenetic programming as well as highlights potential toxicities that might emerge on modulating certain epigenetic factors.

ACKNOWLEDGEMENTS

There is a Hindi proverb that roughly translates to “A community raises the kid”. It perfectly surmises my PhD experience. I have been a recipient of far more than my fair share of generosity in my life so far, particularly during my time at Sloan. I can only hope to pay it forward to the best of my abilities.

I want to express my gratitude to Michel for being such a wonderful mentor. His trust in my abilities to tackle difficult questions, and constant motivation, had a profound impact on my personal growth. His emphasis on continuing to push the boundaries of what we know (and what we think we know!) had a deep impact on shaping my approach to research.

I was so fortunate to share the lab with so many great people. It is always difficult settling in a new city, but I was lucky to have so many people in the lab make me feel so comfortable, both in the lab and outside. In particular, I want to thank Jorge, Judith, Justin, Lisa, Mohamad, and Sjoukje for their advice, and patience in answering my incessant questions. I also want to thank past and current PhD students in the lab- Anton, Ashlesha, Theodore, Pieter and Ophelie. A special thank you to Zeguo Zhao who has been such a great partner in research over the years, and a great tennis coach!

I want to thank my committee members, Dr. Morgan Huse and Dr. Ming Li for their advice and guidance through my PhD.

I want to express my gratitude to students in the GSK community. In particular to my classmates – Ben, Chris, Jake, Michelle, Nick, Steve, Xiaoyi and Yuchen. It was such a great fun, sharing classes with all of them and learning from each other's diverse experiences. Thank you for all the good times and conversations over the last few years.

I want to thank the GSK administration for all their hard work in creating such a wonderful community. Thank you – Iwona Abramek, Ivan Gerena, Maria Torres, and David McDonagh. Thank you to our assistant dean, Linda Burnley. Our current dean, Michael Overholtzer, and former dean, Ken Marians.

I want to thank my extended family in the US for all the great trips over the last few years and making me feel so at home.

I want to thank my friends from India for all the great conversations and support. As we navigate through life, their experiences have been a window to all sorts of interesting worlds – consulting, engineering, finance, oil and gas, physics, start-ups.

To my parents, thank you for all your sacrifices and endless patience. You continue to inspire me by your example of selflessness, and incredible work ethic. To my

sister, thank you for all the thoughtful care packages and cards over the years. Your love and support mean everything.

LIST OF TABLES

LIST OF FIGURES

LIST OF ABBREVIATIONS

ACT: adoptive cell therapy

ALL: acute lymphocytic leukemia

AML: acute myeloid leukemia

BED: biallelic editing

CAR: chimeric antigen receptor

CCR: chimeric costimulatory molecule

CD: cluster of differentiation

CLL: chronic lymphocytic leukemia

CRS: cytokine release syndrome

DLI: donor leukocyte infusion

DN: dominant negative

ETD: edited gene

FDA: food and drug association

FFluc: firefly luciferase

GvHD: graft versus host disease

HLA: human leukocyte antigen

i.p.: intraperitoneal

i.v.: intravenous

Ig: immunoglobulin

IL: interleukin

KO: knockout

LAK: lymphokine activated killer cell

pMHC: peptide-major histocompatibility complex

scFv: small chain variable fragment

TCR: T cell receptor

TIL: tumor-infiltrating lymphocyte

TLR: toll-like receptor

VST: virus-specific T cell

WT: wild-type

CHAPTER 1

Introduction

Cancer predates humanity, with cancerous growth discovered in dinosaur fossils[1]. Some of the earliest written records of cancer in humans' dates to ancient Egypt that were discovered in the 19th century, especially the Edwin Smith and George Ebers papyri that describe surgical, pharmacological, and magical treatments[2]. Today, cancer is the second most common cause of death in the United States after Heart disease, with 1.9 million diagnoses and 609,360 deaths in 2022[3]. Cancer treatment can be categorized in one of the 9 categories – 1) Chemotherapy 2) Hormone Therapy 3) Hyperthermia 4) Immunotherapy 5) Photodynamic Therapy 6) Radiation Therapy 7) Stem Cell Transplant 8) Surgery 9) Targeted Therapy (National Cancer Institute). This thesis focuses on a special class of immunotherapy – chimeric antigen receptor (CAR) T cell therapy. Virchow in 1863 had observed infiltration of neoplastic tissues with leukocytes[4]. The earliest documented case of immunotherapy can be traced to William Coley in 1891[5]. Coley injected live and inactivated *Streptococcus pyogenes* and *Serratia marcescens* in patients with inoperable tumors (mainly bone and sarcomas)[6]. Despite reporting good results, Coley's Toxins as they came to be known, were viewed by skepticism amongst his peers. The unfavorable contemporary view of the methodology, along with the emergence of radiation therapy led to it being discontinued from use[7]. The 20th Century saw a transformation in our understanding of biology and medicine. Fundamental discoveries in immunology were made – particularly in the nature of cells (and their function) that compose the immune system. Our

understanding of tumor immunology has also evolved significantly since Coley first conducted his trials on patients. These advances in fundamental biology, immunology and tumor biology have allowed us to progress from treating cancer patients by infecting them with bacteria to inducing long-term durable remission by genetically engineering immune cells to target tumor.

T cells - introduction

The cells of the immune system originate from a common pluripotent stem cell progenitor called the hematopoietic stem cell (HSC) (Figure 1.1). HSCs predominantly reside in the bone marrow. HSCs differentiate to give rise to progenitors of the lymphoid and myeloid lineage (Figure 1.1). The myeloid progenitor gives rise to variety of cell types including basophils, dendritic cells, eosinophils, erythrocytes, macrophages, mast cells, megakaryocytes, and neutrophils (Figure 1.1). The common lymphoid progenitor on the other hand gives rise to 3 main cell types – B cells, natural killer (NK) cells and T cells (Figure 1.1). B cells mature in the bone marrow[8]. NK cells also largely mature in the bone marrow[8]. However, there are reports in humans and mice that suggest NK cells can mature in secondary lymphoid tissues (SLTs) including tonsils, spleen, and lymph nodes[9]. Precursor T cells egress from the bone marrow and undergo maturation in the thymus[8]. B and T cells upon maturation differ from NK cells in one significant way, they bear a receptor (B-cell receptor (BCR) in B cells, and T-cell receptor (TCR) in T cells) that confers them specificity towards an antigen[8]. Henceforth, we will focus on T cells.

Commitment to the T cell lineage only occurs after entry into the thymus (overview in Figure 1.2). The thymic development of T cells can roughly be classified into 3 distinct states – 1) Commitment to T cell lineage. 2) Divergence between αβ and γδ lineage. 3) CD4/CD8 lineage differentiation of αβ T cells[10]. 1) Commitment to T cell lineage. This process starts post entry of uncommitted progenitors to the thymus which suppresses genes associated with myeloid lineage[10]. Double negative (DN) thymocytes ($CD4^-CD8^-$) are committed to T

cell lineage through Notch1 (in cooperation with Runx1, GATA-3 and E-box proteins) signaling upon interaction with its ligand Delta-like 4 (DL4) on thymic stroma[11,12]. 2) Divergence between αβ and γδ lineage. Bulk of post-thymic mature T cells are of αβ lineage, with γδ T cells constituting about 0.5-5% of mature T cells[13]. These identities are established through TCR rearrangement during DN3 stage of the thymic development. Most rearrangements do not lead to a productive TCR, resulting in cell death[8]. This checkpoint for αβ precursors is called as β-selection[8]. Thymocytes at this stage signal through their rearranged TCRβ chain, CD3 chains and pre-TCRα which binds to TCRβ in the absence of a rearranged TCRα[8]. Cells that pass this stage then enter a proliferative state where they become double positive (DP) for CD4 and CD8[8]. They also initiate TCRα gene rearrangement. γδ T cells differ from αβ T cells in that there is no pre-γδ TCR[10]. γδ T cell selection therefore depends on signal strength of γδ receptor, they do not progress to DP state and remain in DN state[10]. 3) CD4/CD8 lineage differentiation of αβ T cells. Due to the intrinsic randomness of TCR specificity, most DP thymocytes fail to interact with self-peptide:MHC (pMHC) complexes and die by neglect[10]. Another subset of DP thymocytes that have overt reaction to pMHC also undergo TCR-induced programmed cell death[10]. Thymocytes with some, but not overt, reactivity to pMHC are then directed to either the CD4 (helper) or CD8 (cytotoxic) lineage[10]. CD4 T cells recognize peptides that are presented on MHC class II while CD8 T cells recognize peptides that are presented on MHC class I[8]. Although there is still some debate on how CD4/8 lineage choice is determined, the current favored model posits differences in kinetics of MHC class II and MHC class I induced TCR signaling affects expression of lineage determining transcription

factors ThPOK (CD4) and Runx3 (CD8)[14]. Once the CD4/8 lineage determination of thymocytes is made, both lineages rely on the transcription factor KLF2 for thymic egress and entry into the blood stream[15].

T cell - anti-tumor immunity

Mature CD4/CD8 thymocytes that have entered the bloodstream and not yet encountered their cognate antigen are referred to as naïve T cells[8]. Naïve T cells constantly surveil the body through the lymphatic system, a vast network of organized tissue that can be broadly divided into primary lymphoid organs (bone marrow and thymus) and secondary lymphoid organs (lymph nodes, spleen, and mucosal lymphoid tissues)[8]. Antigen is taken up primarily by dendritic cells and macrophages which then travel to draining lymph node to present the antigen to T and B cells[8]. Upon recognizing their cognate antigens, CD4/8 T cells rapidly undergo proliferation and differentiation to become activated $CD4^+$ T cells that produce cytokine to “help” B and $CD8^+$ T cells or activated $CD8^+$ T cells that recognize and kill cells displaying their cognate antigen[8].

Immune activation can occur in the context of an infection or tumor. Tumors, due to their unique biology, can sometimes generate antigens that the immune system can recognize as foreign, these antigens are called as neo-antigens[16]. The presence of neo-antigens in a cancer type is corelated with the mutation burden of the tumor[16]. Associations between activated immune system and anti-tumor response were described over a century ago but the role of T cells in mediating anti-tumor responses was not appreciated until 1970s[17].

Subsequently, infiltrating cytotoxic and helper lymphocytes in tumors were found to be associated with tumor regression in humans [18,19]. In parallel, discoveries of potent negative regulators of T cell activation, Cytotoxic T-lymphocyte-associated protein 4 (CTLA4) and Programmed cell death protein 1 (PD-1) were made in 1987[20] and 1992[21]. Many additional negative regulators of T cell activation have since been found. These molecules are collectively known as checkpoint inhibitors. Antagonist antibodies targeting CTLA4, and PD-1 have shown efficacy in a wide range of tumors, particularly in patients with high mutation burden, but their efficacy has been limited in tumors with low mutation rate that are less immunogenic[22].

Anti-tumor adoptive cell therapy

Another approach towards generating immune responses against tumors is to directly infuse tumor reactive T cells in patients. Murine studies in the 1950s had shown that adoptive transfer of immune cells can mediate tumor rejection. Adoptive transfer of autologous patient-derived leukocytes was first done by Southam et al. in 1966[23]. Although no statistical significance was achieved, the data was suggestive of lymphocytes having a growth inhibitory effect on cancer cells[23]. Contemporaneously, observations of anti-tumor effects were also noted in allogeneic transplant setting[24,25]. However, the anti-tumor effects of these early adoptive cell therapies (ACT) were not consistent and sometime lead to lethal graft versus host disease (GVHD)[26]. The discovery and characterization of TCR and cytokines (particularly interleukin 2) in the early 80s[27] allowed better *ex vivo* expansion of cells for ACT. These cells were named lymphokine activated killer cells (LAK) and constituted a heterogenous mix of non-specific

T cells, tumor reactive T cells and NK cells[26]. However, the frequency of tumor reactive T cells in peripheral blood is very low, and even after expansion may fail to reach critical numbers to mediate effective anti-tumor response[26]. Isolation and expansion of T cells from surgical explants instead of peripheral blood yielded superior anti-tumor response[28]. Three major limitations of these adoptive cell therapies are: 1) In the case of allogenic ACT, there is a risk of donor T cells that can cause GVHD which can sometimes even be fatal. 2) ACT relies on the presence of tumor reactive T cells in the starting product, either from the patient or donor. 3) If the tumor reactive T cells are of low cytotoxic potential, the chances of inducing effective anti-tumor response are limited[26]. These shortcomings led to research in ways to engineer T cells to redirect their specificities and thus overcome the reliance on naturally occurring tumor reactive T cells to mediate anti-tumor effects.

Engineering T cells – introduction to technologies

Early efforts in T cell engineering focused on transducing human tumor infiltrating lymphocytes with neomycin-resistance cassette by γ-retroviral vector to monitor the survival and trafficking of TILs *in vivo*[29]. Both γ-retroviral[30-32] and lentiviral vectors[33-36] were used for introducing transgenes in human and murine T cells. γ-retrovirus and lentivirus can provide stable expression of transgenes. There are, however, some important differences between these two methods of viral delivery systems – 1) γ-retroviruses can be produced at high titers from a stable producer line while lentiviral vectors require large-scale transfections, DNA removal and downstream vector purification and concentration[37]. 2) Lentiviral vectors can transduce non dividing cells (though

not all quiescent cells) whereas retroviral vectors can only infect diving cells expressing the viral receptors[37]. 3) While both viral vectors integrate in a semi-random manner, γ-retroviruses tend to favor transcriptional start sites (TSS) while lentiviral integrations are clustered in gene body of actively transcribing genes[38]. Due to the intrinsic randomness of vector integration, there is a risk of oncogenic transformation due to inadvertent disruption of a tumor suppressor or activation of oncogene by the viral vector. Indeed, treatment of X-linked severe combined immunodeficiency by γ-retroviral gene transfer of $CD34^+$ HSCs resulted in uncontrolled vector-induced leukemia through enhancer-mediated mutagenesis in 25% of patients[39]. Clonal expansions due to lentiviral integrations have also been reported[40,41,42]. Self-inactivating (SIN) lentiviral vectors were shown to have a lower risk of insertional oncogenesis than gammaretroviral vectors in side-by-side comparisons of model systems[43]. Mature T cells, however, appear to be resistant to oncogenesis, even when T cell oncogenes are transduced by retroviral vectors[44].

Non-viral gene delivery systems in human T cells have also grown in popularity in recent years due to the development of efficient electroporation protocols for DNA, RNA, and proteins that allow for their transient expression[38]. Co-transfection of piggyBac or Sleeping Beauty transposase allow for non-viral integration of transgene into T cells[45,46].

The advent of various genome editing technologies has allowed for more precise engineering of T cells. Genome editing technologies that mediate site-directed double strand DNA break can result in either non-homologous end

joining (NHEJ), or homology directed repair (HDR). NHEJ results in insertions or deletions at the site of editing. HDR, on the other hand, relies on homology from the sister chromatid to repair the targeted DNA. Therefore, if the transgene is designed to bear homology to the site of edit or is naturally homologous, one can co-opt HDR to induce the integration of a gene of interest at a defined site in the genome.

TCR based adoptive cell therapy

Retro- and lenti-viral vectors have been primary means of encoding exogenous TCRs to redirect T cell specificity. More recently, targeted integration of transgenic TCR into a genomic safe harbor site (genomic region where viral vector integration is unlikely to cause oncogenesis), including TCR locus has been achieved[47]. The anti-NY-ESO-1 TCR has demonstrated promising anti-tumor efficacy with minimal toxicities[48]. However, other clinical trials including MART-1[49], gp100[50], and CEA[51] have resulted in moderate to severe on-target off-tumor toxicities. Unexpected off-target toxicities can also occur in engineered T cells with transgenic TCR. Pairing between the exogenous TCR and endogenous TCR can lead to mispaired TCR heterodimers leading to reactivity to self-antigens as these heterodimers have not undergone thymic selection. This issue can now be circumvented with endogenous TCR ablation by gene editing. However, the overarching issue with TCR based cancer immunotherapy is that it is still restricted by human leukocyte antigen (HLA)-type. As we will see in the next section, synthetic immunoglobulin based chimeric receptors can allow us to overcome this limitation imposed by HLA.

Chimeric antigen receptor (CAR) T cells

TCR bears structural homology to the immunoglobulin, especially in its antigen recognition domain. The first chimeric TCR molecules involved recombining the immunoglobulin VH and VL rearranged gene segments to the C-region exons of the TCR α and β chains[52,53] to redirect the specificity of T cell hybridoma. These molecules could recognize and kill cells that express their immunoglobulin antigen in an HLA independent manner. The next evolution in these early designs involved fusion of single-chain antibody segment to the cytoplasmic region of CD3 zeta via a short spacer to the transmembrane[54]. These designs are now collectively referred to as first generation CARs (Figure 1.3). While they could induce cytolysis in target antigen presenting cells in an HLA independent manner, they could not confer the proliferation and persistence that are required for sustained T cell response against tumors *in vivo*[55].

The ability of CAR molecules to confer properties of proliferation and persistence increased significantly by the addition of costimulatory domains[56,57]. Although cytokines were known for promoting proliferation in T cells, the discovery of CD28 as a costimulatory molecule required for full T activation was much later[58]. Subsequently, a host of costimulatory molecules have been characterized. They are broadly divided into either the CD28 family or the tumor necrosis factor receptor superfamily (TNFSF)[59]. CARs containing costimulatory domains are classified as the second generation of CAR design (Figure 1.3). CD28 or 41BB (TNSF9) or both costimulatory domains comprise about ~95% of all CAR designs used currently in the clinic[60].

CD19 paradigm

The choice of CD19 as a target antigen was critical in success of early CAR designs[26]. CD19 is a 95kD glycoprotein consisting of a transmembrane domain, a cytoplasmic C-terminus, and extracellular N-terminus[61]. CD19 expression is restricted to the B-cell lineage, where it plays an important role in B-cell development by modulating the pre-BCR/BCR signals[62]. In mature B-cells, it signals through multi-component complex consisting of complement receptor CD21, the tetraspanin membrane protein CD81 (TAPA-1), and the interferon-induced transmembrane protein 1, CD225[61]. Due to the important role of CD19 in B cell development and function, expression of CD19 is robust in B-cell lineage and only lost during plasma cell differentiation[61,62]. As would be expected, CD19 is expressed in most B cell lineage leukemias and lymphomas[63].

The first study to report durable (~300 days) anti-tumor response in a murine xenograft model of human cancer was reported by Brentjens et al. in 2003[64]. Treatment of Raji (Burkitts Lymphoma) and NALM6-CD80 (Acute lymphoblastic leukemia cell line) bearing severe combined immunodeficiency (SCID)-Beige mice with first generation CD19 targeting CAR (19z1) resulted in improved survival of mice, with some mice maintaining durable (~300 days) remission. However, 19z1 CAR T cells require CD80 mediated *in vivo* costimulation either through endogenous expression of CD80 (Raji) or through engineered CD80 expression (NALM6-CD80) on the tumor line. Subsequent studies showed that second generation CAR T cells with either CD28[65,66] or 4-1BB[67,68] costimulation could mediate durable long-term remission in murine xenograft models of

human leukemia/lymphoma where tumor lines do not express ligands for costimulatory receptors on T cells. These pre-clinical murine studies laid the foundation for subsequent clinical trials involving CD19-targetted CAR T cells.

Kochenderfer et al. reported in 2010 a single patient who was treated with anti-CD19 targeted second generation CAR T cells containing the CD28 costimulation domain[69]. Follow-up scans revealed partial remission of the lymphoma that lasted 32 weeks[69]. Reports on larger cohorts of patients (Acute lymphoblastic leukemia [ALL]/Chronic lymphocytic leukemia [CLL]) treated with either 4-1BB based[70] (3 patients) or CD28 based[71] (10 patients) second generation CD19 CAR T cells were subsequently published demonstrating sustained ani-tumor response, with 2/3 CLL patients treated by Kalos et al. achieving a complete response[70]. These reports were especially impressive as patients in these cohorts had received multiple rounds of prior treatments. Subsequently, these therapies received FDA approval for adult patients with relapsed and/or refractory (R/R) B cell lymphomas[72], children and young adults aged <25 years with R/R B-ALL[73].

Treatment and long-term follow up of patients from the early clinical trials has revealed novel insights into the properties of CD19 targeted CAR T cells. Some patients experienced symptoms like fever, hypotension, hypoxia, and neurological effects such as ataxia and aphasia associated with elevated serum cytokine levels including interferon-γ and interleukin-6 which corelates with peak CAR T cell expansion[74-76]. These spectra of symptoms are collectively termed as cytokine release syndrome (CRS) and can be life-threating if not

controlled[77]. Anti–interleukin-6-receptor antagonist, Tocilizumab, is usually effective in the management of severe cytokine release syndrome induced by CAR T cells[74,78]. Glucocorticoids are administered if no response to interleukin-6 receptor blockade is observed[77]. More recently, blockade of IL-1 has been reported as a therapeutic intervention strategy to curb CRS without compromising on CAR T cell therapeutic efficacy[79]. Due to the expression of CD19 on normal B-cells, B-cell aplasia and hypogammaglobulinemia is also observed but these conditions are manageable with immunoglobulin therapy[80].

Another feature of CAR T cell therapy that has emerged in over a decade since the first patients were treated has been the impressive durability of response, with the earliest patients maintaining remission for over 10 years now[81]. The response rates have consistently been well over 50% in B-cell leukemias and lymphomas[77] (Table 1.1).

Table1.1: CAR T cell response rates in Leukemia/lymphoma

Cancer Type	Response Rates
Adult B-cell Acute Lymphoblastic Leukemia (B-ALL)	83-93%[74,82,83]
Pediatric B-ALL	68-90%[73,84-86]
Chronic Lymphocytic Leukemia (CLL)	57-71%[77]
Diffuse Large B-cell Lymphoma (DLBCL)	64-86%[72,82,87,88]
Follicular Lymphoma	71%[88]
Transformed Follicular Lymphoma	70-83%[72,82,88]

However, still a large fraction of patients will have poor primary response upon CAR T cell infusion or eventually relapse[73,83,89]. Lack of primary response in CAR T cell therapy can be attributed to multiple reasons. In one of the earliest CAR T cell clinical trials, Brentjens et al. noted no anti-tumor response in CLL patients that received CAR T cells without a pre-conditioning regimen of lymphodepletion chemotherapy[71]. Thereafter, lymphodepletion pre-conditioning became a part of the standard CAR T cell therapy protocol. Since most patients receive autologous CAR T cells, the intrinsic quality of patient T cells can be an important determinant of anti-tumor response. In a retrospective analysis of CLL patients who received CD19-targetted 4-1BB CAR T cells, Fraietta et al. reported that CAR T cells in the infusion product of complete-responders was enriched in memory-related genes, including IL-6/STAT3 signatures, whereas T cells from nonresponders had higher expression of genes associated with effector differentiation, glycolysis, exhaustion, and apoptosis[90]. Deng et al. reported that large B cell lymphoma (LBCL) patients who achieved compete response when treated with CD19-targetted CD28 CAR T cells had three three-fold higher frequencies of CD8 T cells expressing memory signatures than patients with partial response or progressive disease[91]. CD8 T cell exhaustion was associated with poor molecular response[91]. Tumor-intrinsic features can also lead to lack of efficacy of CAR T cells. Impaired death receptor signaling on ALL cells has been reported in pre-clinical models as a mechanism of primary resistance to CD19-targetted 41BB costimulation CAR T cells[92]. This was mediated by inherent resistance to T-cell cytotoxicity which led to persistent antigenic stimulation of CAR T cells leading to their dysfunction[92].

CD19 loss/downregulation represents another major mechanism of resistance. Sotillo et al. reported hemizygous deletions spanning the *CD19* locus and *de novo* frameshift and missense mutations in exon 2 of *CD19* in some relapse samples[93]. Alternative splicing resulting in CD19 mRNA that lacked exon 2 were also identified in a relapsing patient[93]. This alternative spliced CD19 mRNA resulted in a N-terminally truncated CD19 variant, which fails to trigger killing by CD19-targetted CAR[93]. Gardner et al. reported that 2/7 B-ALL patients (harboring rearrangement of the mixed lineage leukemia (*MLL*) gene) relapsed after having achieved CR with a CD19 negative acute myeloid leukemia (AML) that was clonally related to their B-ALL[94]. Ruella et al. reported that an accidental transduction of a single leukemic B cell by the CAR vector during CAR T cell manufacturing resulted in epitope-masking and resistance to CD19 targeted CAR therapy[95]. Hamieh et al. described a reversible CD19 loss in tumor cells through trogocytosis, where CD19 is transferred from the tumor to T cells resulting in low levels of CD19 on the tumors and T cell fratricide killing[96]. Trogocytosis affects both CD28 and 4-1BB based CAR designs albeit to different degrees, but it can be offset by cooperative killing and combinatorial targeting[96]. Multiple clinical trials are currently underway that involve targeting another antigen in addition to CD19 to overcome the issue of CD19 loss or downregulation[97,98].

Advances in CAR therapy – receptor design

Since the description of CD28 and 4-1BB costimulated second generation CAR designs over 2 decades ago, several design modifications have been reported

to improve upon these foundational second-generation CAR designs. Building upon evidence that above a certain threshold, activation by antibody-like receptors may negatively affect T cell function[99], Ghorashian et al. designed a low-affinity CD19 CAR that improved expansion and persistence while limiting severe CRS in pediatric patients[100]. Several studies have reported that the same epitope can activate CAR T cells more efficiently when expressed in a membrane-proximal manner as opposed to membrane-distal[101]. Therefore, tailoring the extracellular spacer sequence to position the scFv for efficient T cell activation in the context of epitope location is another avenue for improving CAR design. CARs with short extracellular spacer have been reported to improve T cell effector function when targeting membrane-distal epitope[102] while CARs with longer extracellular spacer result in superior T cell effector function when targeting a membrane-proximal epitope[103]. The hinge-transmembrane (H/T) region of the CAR has also been reported to affect the antigen sensitivity of T cells[104]. Majzner et al. reported that CD28-H/T lowers the antigen sensitivity threshold of 4-1BB costimulated CAR as compared to CD8-H/T region[104].

Costimulatory domains play an important role in determining the properties of CAR transduced T cells. CARs containing CD28-costimulatory domain impart a stronger effector function[105], higher antigen sensitivity and glycolysis in T cells[106] as compared to 4-1BB containing CARs. On the other hand, 4-1BB CARs impart stronger proliferation[105] and improved persistence and mitochondrial biogenesis[106]. Several modifications in the intracellular domains intended to improve the function of both CD28 and 41BB encompassing CARs

have been reported. Feucht et al., reported on 4 mutant CD3z molecules that had various combinations of immunoreceptor tyrosine-based activation motifs (ITAMs) mutated, namely X23, 1XX, X2X, and XX3[107]. 1XX outperformed all 5 (including wild type CD3z) CD19-targetted CD28-CAR designs in a xenograft model of human B-ALL[107]. Guedan et al. reported a mutant CD28 costimulatory domain where asparagine was replaced by phenylalanine (CD28-YMFM)[108]. This mutation led to reduced T cell differentiation and improved CAR T cell persistence[108]. Majzner et al. reported that addition of another ITAM to 4-1BB CAR enhances their recognition of low-antigen density cells[104]. Combining both CD28 and 4-1BB costimulatory domains in the same CAR (third generation CAR design) was surprisingly found to have poorer anti-tumor efficacy than CD28-CAR in murine xenograft model of human B-ALL[105].

Multiple studies have reported on co-expression of either a natural or synthetic co-stimulatory receptor (CCR)/ligand to improve CAR T cell function. Zhao et al. reported that co-expression of 41BBL in CD28-CARs enhanced their proliferation, persistence, and anti-tumor efficacy in a murine xenograft model of human B-ALL[105]. CD28-CAR T cells expressing CD40 ligand (CD40L) displayed superior anti-tumor activity in a syngeneic murine leukemia/lymphoma model and protected against tumor antigen escape by promoting a CD40 mediated endogenous anti-tumor response[109]. Co-expression of a CCR targeting CD38 enhanced the avidity and cytotoxicity of BCMA and CD19 targeted CAR T cells[110]. In addition, CARs and CCRs can be designed to provide complementary CD28 and 4-1BB costimulation for increased cytokine secretion, and improved expansion and persistence *in*

vivo[110]. Dominant negative (DN) receptors particularly targeting inhibitory receptors such as PD-1[111] have also been employed to improve CAR T cell function. These receptor (in the case of DN inhibitory receptors) lack the intracellular signaling domains and therefore lack the inhibitory signaling that ensues upon their cognate ligand binding. DN inhibitory receptors (when co-expressed with CAR) therefore compete with the endogenous inhibitory receptors and limit inhibitory signaling in CAR T cells. A variation of this design where instead of total absence of cytoplasmic signaling moieties, costimulatory signaling is provided through inhibitory ligand binding is called a switch receptor. The PD-1 switch receptor, where the PD-1 extracellular domain is fused to a CD28 intracellular signaling domain was reported to enhance CAR T cell efficacy in a preclinical murine model[112]. Another approach has been to engineer CAR T cells to secrete stimulatory cytokines to promote not only their proliferation and persistence but also modulate the tumor microenvironment to promote tumor eradication[113]. This approach might be particularly applicable in the context of solid tumors that are associated with immune suppressive microenvironment. Numerous cytokines and chemokines have been reported to augment CAR T cell function. Examples include IL12[114,115], IL15[116,117], IL18[118,119], IL7[120] and CCL19[120], IL33[121], IL36γ[122]. Alternatively, CAR T cell function can also be improved by expression of a transcription factor. Lynn et al. reported over-expression of *cJUN* in human CAR T cells enhanced their expansion and functional persistence in pre-clinical tumor models[123]. Seo et al. reported over-expression of BATF in murine CAR T cells promoted production of effector cytokines and supported formation of long-lived memory T cells in syngeneic tumor models[124].

Our understanding of the molecular underpinnings of CAR T cell dysfunction has improved significantly over the last 15 years aided by the developments in the field of T cell biology. This has led to strategies that involve modulating (either increasing or disrupting) the expression of defined factors to allow for improved CAR T cell function.

Advances in CAR therapy – genome engineering

A complementary approach to over-expression of genetic factors that promote T cell function is to limit the factors that are negative regulators of T cell function. There are multiple ways of suppressing a factor, such as by expressing a dominant negative variant (i.e.: PD-1 DN). Another would be to express a short hairpin RNA (shRNA) against a target gene of interest to limits its expression. Expressing a PD-1 shRNA along with the CAR has been reported to result in improved CAR T cell anti-tumor efficacy in multiple xenograft models of human tumors[125]. A third way is to edit the target gene of interest to disrupt the generation of functional protein. Different classes of site-specific DNA nucleases including meganucleases[126], Transcription Activator-like Effector Nucleases (TALENs)[127] and clustered regularly interspaced short palindromic repeats (CRISPR) and associated Cas9 nuclease (CRISPR-Cas9)[128] systems have been used to edit the genome of CAR T cells. Amongst these site-specific genome editing systems, CRISPR-Cas9 is generally favored for its ease of use and high degree of programmability. There are 2 major classes of genes that have been targeted by genome editing tools for CAR T cell therapy. One includes genes such as T cell receptor α and β chains (*TRAC*, *TRBC*), and β_2 microglobulin (B2M). These genes are of interest for development of allogeneic

CAR T cell products. The disruption of *TRAC* and *TRBC* is to prevent GVHD while the disruption of B2M is to prevent the rejection of donor CAR T cells by the host T cells. Eyquem et al. took this approach a step further by targeting the CAR vector into the TRAC locus by using CRISPR-Cas9 for *TRAC* editing and adeno-associated virus (AAV) for CAR delivery into human peripheral T cells[129]. The CAR in this case is inserted into the *TRAC* locus and is expressed under the control of the endogenous *TRAC* promoter. Eyquem et al. further showed that CD19-targeted CD28-costimulated CAR T cells when expressed from the *TRAC* locus (*TRAC*-1928z T cells) outperformed conventional γ-retroviral CD19-targeted CD28-costimulated (Rv-1928z) CAR T cells in a murine xenograft model of human B-ALL. Functional and mechanistic studies showed that *TRAC*-1928z CAR T cells have reduced tonic CAR signaling due to effective internalization and more physiological re-expression upon repeated antigen exposure which results in delaying T cell effector differentiation and eventual dysfunction[129]. Another class of genes that have been commonly targeted in CAR T cells include well known T cell inhibitory molecules such as PD-1[130], LAG-3[131], TOX[132], TOX2[132], NR4A (1, 2, and 3)[132], and TGF-β receptor II (*TGFBR2*)[133]. CRISPR-Cas9 screens in CAR T cells have also found novel negative regulators of CAR T cell function such as REGNASE-1[134], p38[135], and TLE4[136] and IKZF2[136].

Advances in CAR therapy – epigenetic programming

So far, the introduction has focused on modulating the expression of transcriptional factors and inhibitory receptors to limit terminal effector differentiation and delay the onset of dysfunction in CAR T cells. An alternate

approach is to epigenetically program CAR T cells to limit terminal effector differentiation. The motivation behind this approach lies in a series of reports that characterized the epigenetic changes associated with T cell differentiation and dysfunction. Youngblood et al., reported that HIV-specific PD1^{high} CD8^{+} T cells that have undergone chronic TCR stimulation are unmethylated at the PD-1 transcriptional regulatory locus as compared to naïve T cells[137]. In a subsequent study, Youngblood et al. showed that memory-precursor virus specific CD8^{+} T cells acquired de novo methylation at naïve-associated genes and demethylate effector genes[138]. Furthermore, conditional deletion of de novo methyltransferase, DNA methyltransferase 3a (Dnmt3a), at an early stage of effector differentiation resulted in reduced methylation of naive-associated genes[138]. While the two studies discussed above reported locus accessibility differences arising out of the DNA methylation state, locus accessibility can also be affected by chromatin modifications. By profiling canonical active (H3K27ac) and repressive (H3K27me3) chromatin marks in memory precursor and terminally differentiated effector CD8^{+} T cells during viral infection, Gray et al. reported increased H3K27me3 marks on numerous pro-memory and pro-survival genes in terminally differentiated effectors indicative of lineage restriction[139]. Memory precursors on the other hand maintain permissive chromatin at both pre-memory and pro-survival genes[139]. Furthermore, a role of polycomb repressive complex 2 (PRC2) was shown in mediating epigenetic silencing of memory genes[139]. Profiling chromatin accessibility (assay for transposase-accessible chromatin, ATACseq) over time in CD8^{+} T cells as they differentiate from naïve to effector and ultimately become dysfunctional in a syngeneic tumor model revealed distinct chromatin states and surface markers

that distinguished reprogrammable from non-reprogrammable PD1^{hi} dysfunctional T cells[140]. Subsequently, Feldman et al. reported on distinct T cell chromatin states associated with CD8^{+} memory T cell state in patients who respond to checkpoint immunotherapy [n= 35 for anti-PD-1, n=11 for anti-CTLA4+PD-1, and n=2 for anti-CTLA4][141]. Ghoneim et al., showed de novo DNA methylation of memory genes results in terminal T cell differentiation both, in murine chronic virus infection model and tumor model[142]. Furthermore, this DNA methylation mediated silencing of memory genes makes T cell unresponsive to PD-L1 blockade[142]. More recently, deletion of DNMT3A in CAR T cells was shown to enhance their proliferation and anti-tumor efficacy through upregulation of interleukin-10[143].

Motivation for thesis studies

Given the role of epigenetics in defining and maintaining T cell state, and the emerging evidence that memory T cell signatures in pre-infusion CAR T cells are associated with better clinical outcomes[90.91]. The overarching aim in this thesis was to modulate the epigenetic state of the CAR T cells to limit their terminal differentiation and enhance their anti-tumor efficacy. We chose to disrupt two different epigenetic factors -1) Ten-eleven translocation 2 (*TET2*). 2) Suppressor of variegation 3-9 1 (*SUV39H1*).

TET proteins (3 members: *TET1*, *TET2*, *TET3*) sequentially oxidize 5-methylcytosine (5mC), they are therefore involved in mediating the intermediate reactions involved in removal of the 5-methyl group from cytosine[144]. TET2 loss in HSCs results in their aberrant expansion and myeloid skewing[145]. Our

interest in disrupting *TET2* in CAR T cells was due to a series of murine studies and a clinical observation in a CLL patient treated with CAR T cells. In murine $CD4^+$ T cells, *TET2* has been shown to interact with Th1 and Th17 lineage determining transcription factors and promote their effector cytokine expression[146]. TET2 loss has also been shown to promote memory formation in virus specific murine $CD8^+$ T cells[147]. More recently, a report by Fraietta et al. described the emergence of a dominant CAR T cell clone in a patient treated with a lentiviral 4-1BB CAR vector where the CAR vector integrated into the *TET2* locus resulting in its disruption[42,148]. These findings collectively led us to hypothesize that the disruption of *TET2* would promote memory formation in CAR T cells and improve their anti-tumor efficacy. Since CAR designs differ in the rate of differentiation that they impart to the T cells, we further hypothesized that the effect of *TET2* disruption on memory formation would not be uniform across different CARs. We, first assess the effect of *TET2* disruption on the widely used CD28 and 4-1BB based second generation CAR T cells. We then expand the scope of the study to include analysis of *TET2* disruption on other CD28-based CAR designs. Two chapters are dedicated to this study (Chapters 3 and 4).

SUV39H1 belongs to SUV39 sub-family (*SUV39H1*, *SUV39H2*) of lysine methyl transferases (KMT)[149]. KMTs have been implicated in Th1/2 lineage plasticity[150], TCR signaling[151], and T cell terminal differentiation[139]. *SUV39H1* (and *H2*) are H3K9 site-specific histone methyltransferases[149]. *SUV39H1* has previously been reported to play an important role in controlling Th2 lineage commitment[149]. More recently, disruption of *SUV39H1* in murine OT-1

transgenic $CD8^+$ T cells was reported to result in defective effector differentiation due to improper silencing of memory associated genes[152]. This led us to evaluate the disruption of *SUV39H1* in human CD28-CAR T cells, with the hope that disruption of *SUV39H1* would limit their strong effector differentiation and eventual dysfunction by promoting the expression of memory associated genes leading to an improved anti-tumor efficacy. Chapter 5 is dedicated to this study.

Chapter 3: Disruption of *TET2* enhances T cell anti-tumor efficacy in a CAR dependent manner

In this chapter we develop the reagents for disruption of *TET2* in human T cells. We then assess the effect of disruption of *TET2* on T cells expressing different CARs on parameters such as proliferation, differentiation, and anti-tumor efficacy in a murine xenograft model of B-ALL. We describe the unexpected emergence of a hyper-proliferative CAR T cell population that becomes apparent long after tumor clearance.

Chapter 4: BATF3/MYC axis drives hyper-proliferation of TET2 deficient CAR T cells

In this chapter we perform functional and molecular characterization studies on the hyper-proliferative CAR T cell population. These studies led to the discovery of an auto-regulatory feed forward loop allowing for a BATF3 driven MYC dependent proliferation of TET2 deficient CAR T cells.

Chapter 5: *SUV39H1* disruption enhances functional persistence of CD28 costimulated CAR T cells

We assess the effect of SUV39H1 disruption on proliferation, differentiation, and anti-tumor efficacy of CD28-costimulated CAR T cells in a murine xenograft model of B-ALL. We then perform transcriptional and chromatin accessibility studies to characterize the underlying molecular mechanism mediating the functional differences that we observe due to SUV39H1 deficiency in CD28-CAR T cells.

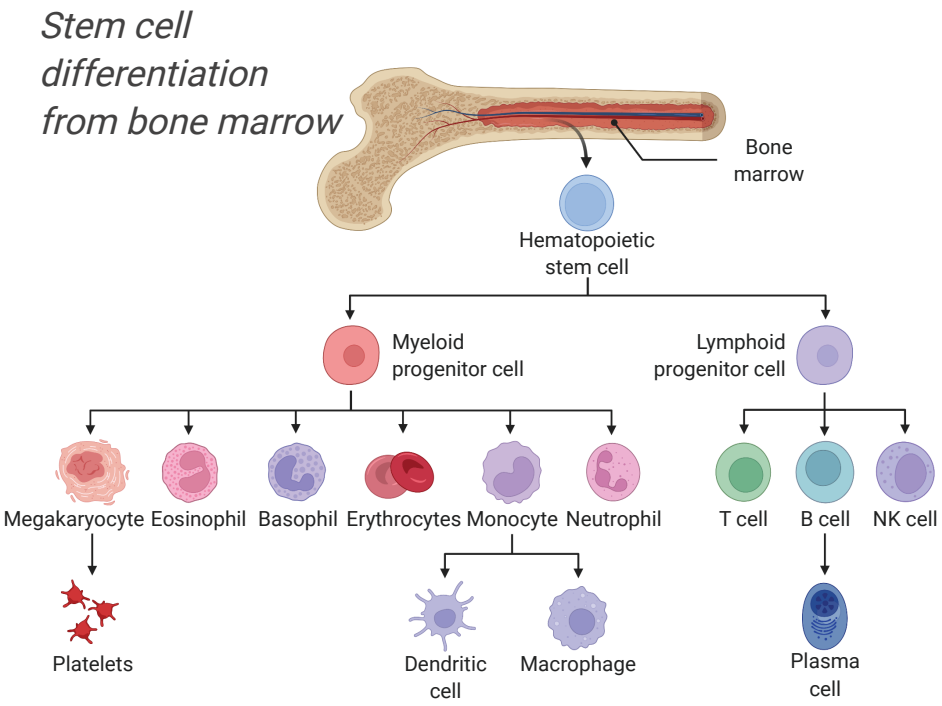

Figure 1.1: Hematopoietic stem cell differentiation

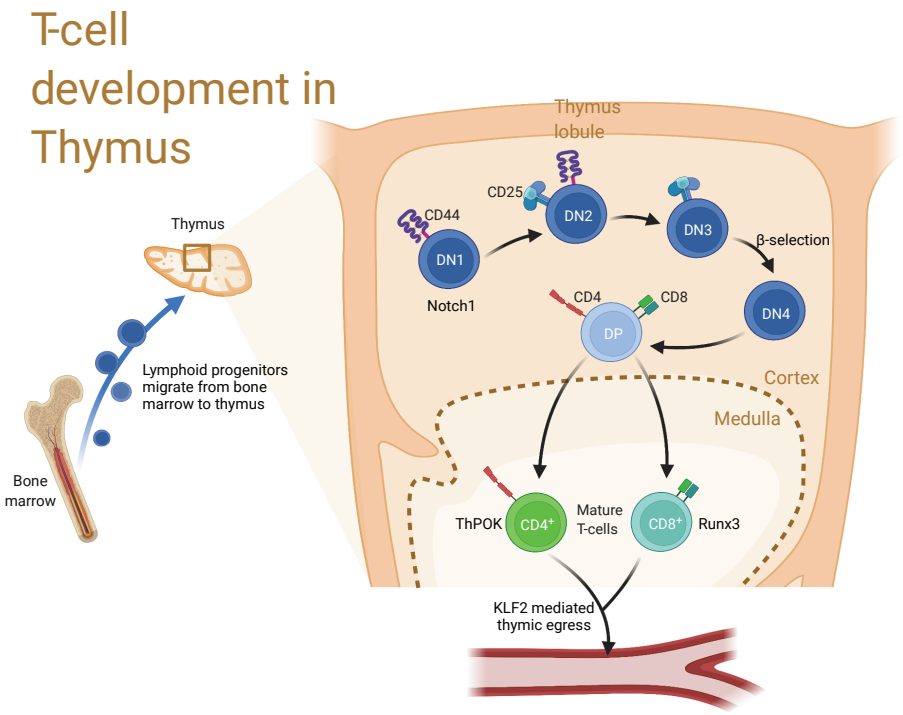

Figure 1.2: T-cell development in the thymus

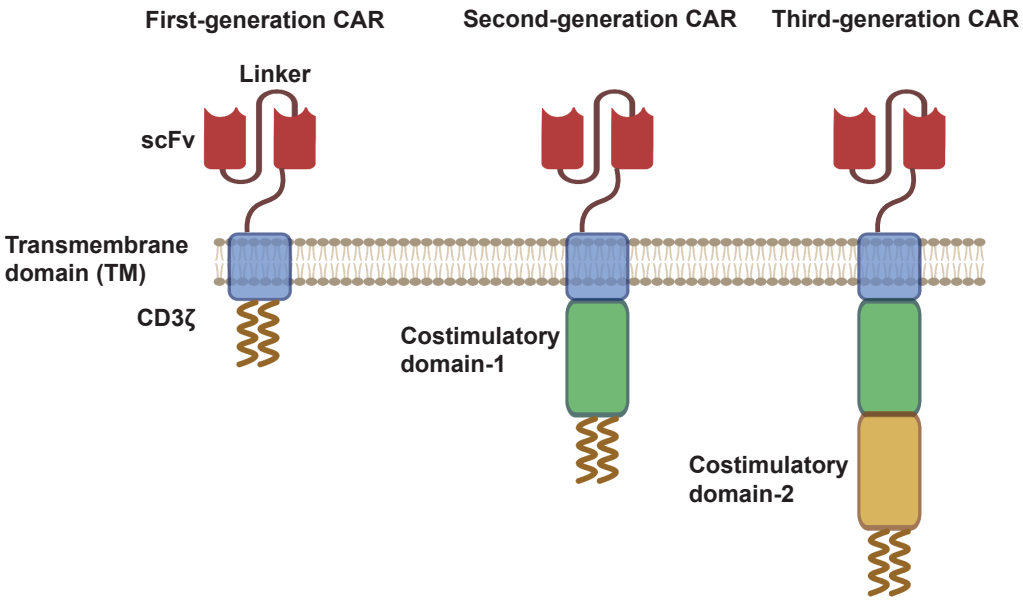

Figure 1.3: Evolution of CAR design

CHAPTER 2

Materials and Methods

Retroviral vector constructs and retroviral production

Plasmids encoding the retroviral vector were prepared using standard molecular biology techniques[153]. LNGFR (A truncated and mutated TNF-R family homolog[154]) was used as a control molecule to ensure comparable CAR expression levels from different bicistronic vectors. Synthesis of Rv-1928z, Rv-19BBz, and Rv-1928z+41BBL, has been previously described[64,66,105]. Pd28z+41BBL CAR is derived from a previously described CAR[155]. VSV-G pseudotyped retroviral supernatants derived from transduced gpg29 fibroblasts (H29) were used to construct stable retroviral-producing cell lines as previously described[155].

AAV targeting for *TRAC*-1928z

The *TRAC* gRNA targets a sequence upstream of the transmembrane domain of the TCRα[129]. This domain is required for the TCRα and β assembly and surface expression. Both, non-homologous end joining (NHEJ) and integration of the CAR by Homology directed repair (HDR) at this locus would then efficiently disrupt the TCR complex. *TRAC*-1928z is based on the pAAV-GFP backbone (Cell Biolabs). It contains 1.9 kb of genomic *TRAC* flanking the gRNA targeting sequence, a self-cleaving P2A peptide in frame with the first exon of TRAC followed by the 1928z CAR used in clinical trials.

Isolation and expansion of human T cells

Buffy coats from anonymous healthy donors were purchased from the New York Blood Centre (institutional review board-exempted). All blood samples were handled following the required ethical and safety procedures. Peripheral blood mononuclear cells were isolated by density gradient centrifugation. T cells were then purified by using the Pan T Cell Isolation Kit (Miltenyi Biotec). T cells were stimulated with CD3/CD28 T cell Activator Dynabeads (Invitrogen) at 1:1 ratio and cultured in RPMI+10% Fetal Bovine Serum (FBS), 5 ng ml−1 interleukin-7 (IL7) and 5 ng ml−1 IL15 (Miltenyi Biotec) for retroviral transduction (Rv-CAR) and gene targeting (*TRAC*-1928z) experiments. The culture medium was changed every 2 days. The cells were cultured at 10^6 cells per ml.

Mouse systemic tumor model

We used 6- to 12-week-old NOD/SCID/IL-2Rγ null (NSG) mice (The Jackson Laboratory), under a protocol approved by the Memorial Sloan Kettering Cancer Centre (MSKCC) Institutional Animal Care and Use Committee. All relevant animal use guidelines and ethical regulations were followed.

NALM6 Model

NALM6 expressing firefly luciferase-GFP (FFLuc-GFP) were described previously[66]. NSG mice were inoculated with 5e5 NALM6 cells by tail vein injection, CAR T cells were then injected 4 d later at varying doses. Bioluminescence imaging was performed using the IVIS Imaging System

(PerkinElmer) with the Living Image software (PerkinElmer) for the acquisition of imaging datasets.

PC3-PSMA Model

Prostate cancer cell line, PC3, were injected via tail vein in NSG mice at a dose of 2e6/mouse. PC3 cells express firefly luciferase-GFP, which enable tumor monitoring through bioluminescence. CAR T cells were injected after 30 days.

Secondary transplant of *TET2$_{bed}$* CAR T cells

A day prior to the transplant, NSG mice were irradiated with a cumulative dose of 200 cGy. 2e6 *TET2$_{bed}$* CAR T cells were then injected through tail vein. For IL2 treatment group, mice received 1000U of IL2 twice a week (Intra-peritoneal). For IL7+IL15 treatment group, IL7 was subcutaneously injected at 0.5ug/mouse/week. IL-15 and IL-15ra were pre-incubated at 1:6 weight ratio at 37^{o}C for 30 minutes before injection (IP) in mice at a dose of 2.5ug (1L-15) +15ug (IL-15ra)/week1[56]. Mice received exogenous cytokines for 60 days.

Cytotoxicity assays

The cytotoxicity of T cells transduced with a CAR was determined by luciferase-based assay. NALM6 expressing firefly luciferase-GFP served as target cells. The effector and tumour cells were co-cultured at indicated E/T ratio in the black walled 96 well plates in triplicate manner with 1e5 target cells in a total volume of 100 µl/well. Target cells alone were planted at the same cell density to determine the maximal luciferase expression (relative light units; RLUmax). 18 hr later, 100 µl luciferase substrate (Bright-Glo, Promega) was directly added

to each well. Emitted light was measured by luminescence plate reader or Xenogen IVIS Imaging System (Xenogen) with Living Image software (Xenogen) for acquisition of imaging data sets. Lysis was determined as: [1 − (RLUsample)/ (RLUmax)] × 100.

DNA/RNA simultaneous extraction

Cell pellets were resuspended in RLT buffer and nucleic acids were extracted using the AllPrep DNA/RNA Mini Kit (QIAGEN catalogue # 80204) according to the manufacturer's instructions. RNA was eluted in nuclease-free water and DNA in 0.5X Buffer EB. Phase separation in cells lysed in TRIzol Reagent (ThermoFisher catalogue # 15596018) was induced with chloroform. RNA was precipitated with isopropanol and linear acrylamide and washed with 75% ethanol. The samples were resuspended in RNase-free water.

Flow cytometry

Flow cytometry analysis was performed on Aurora (Cytek), and LSRFortessa (BD). All antibodies used in this study are listed in reagent table. Countbright beads (Invitrogen) were used to determine the absolute number of cells according to the manufacturer's protocol. Flow cytometry analysis was done on FlowJo. Cell sorting was performed by a BD FACSAria cell sorter.

CRISPR sequencing

Genomic DNA was isolated using DNeasy Blood & Tissue Kits (Qiagen). Primers were designed to amplify the region encompassing the site of CRISPR/Cas9 editing with the following guidelines – size (200-280 bp),

CRISPR/Cas9 edit site within the first 100bp from one end of the PCR. The PCR product was then sent for next generation sequencing for 100,000-300,000 reads per product. The editing efficiency was then determined through CRISPRESSO.

Transcriptome sequencing

After RiboGreen quantification and quality control by Agilent BioAnalyser, 2ng total RNA with RNA integrity numbers ranging from 7.3 to 9.7 underwent amplification using the SMART-Seq v4 Ultra Low Input RNA Kit (Clonetech catalogue # 63488), with 12 cycles of amplification. Subsequently, 10ng of amplified cDNA was used to prepare libraries with the KAPA Hyper Prep Kit (Kapa Biosystems KK8504) using 12 cycles of PCR. Samples were barcoded and run on a HiSeq 4000 in a PE50 run, using the HiSeq 3000/4000 SBS Kit (Illumina). An average of 40 million paired reads were generated per sample and the percent of mRNA bases per sample ranged from 31% to 69%.

TCR sequencing

After PicoGreen quantification and quality control by Agilent BioAnalyser, 188-200ng of genomic DNA were split equally into six reactions and prepared using the immunoSEQ human TCRB Kit (Adaptive Biotechnologies) according to the manufacturer's instructions. Briefly, multiplex PCR was used to amplify the CDR3 region for 31 cycles. After clean-up, 2μL of PCR product was used as input into library preparation with 8 cycles of PCR. Barcoded samples were pooled by volume and sequenced using custom primers on a NextSeq 500 in a SR155 run, using the NextSeq 500/550 Mid Output Kit v2.5 (150 Cycles)

(Illumina). The loading concentration was 1pM and 20% spike-in of PhiX was added to the run to increase diversity and for quality control purposes. Raw BCL files were transferred to the immunoSEQ Analyser for processing and analysis.

Exome capture and sequencing

After PicoGreen quantification and quality control by Agilent BioAnalyser, 250ng of DNA were used to prepare libraries using the KAPA Hyper Prep Kit with 8 cycles of PCR. After sample barcoding, 100ng of library were captured by hybridization using the xGen Exome Research Panel v1.0 (IDT) according to the manufacturer's protocol. PCR amplification of the post-capture libraries was carried out for 8 cycles. Samples were run on a HiSeq 4000 in a PE100 run, using the HiSeq 3000/4000 SBS Kit (Illumina). Samples were covered to an average of 111X.

ATAC sequencing

Profiling of chromatin was performed by ATAC-Seq as described[51]. Briefly, 50,000 fresh T cells were washed in cold PBS and lysed. The transposition reaction containing TDE1 Tagment DNA Enzyme (Illumina catalogue # 20034198) was incubated at 37°C for 30 minutes. The DNA was cleaned with the MinElute PCR Purification Kit (QIAGEN catalogue # 28004) and material was amplified for 5 cycles using NEBNext High-Fidelity 2X PCR Master Mix (New England Biolabs catalogue # M0541L). After evaluation by real-time PCR, 8 additional PCR cycles were done. The final product was cleaned by aMPure XP beads (Beckman Coulter catalogue # A63882) at a 1X ratio, and size

selection was performed at a 0.5X ratio. Libraries were sequenced on a HiSeq4000 in a PE50 run, using the HiSeq 3000/4000 SBS Kit (Illumina). An average of 108 million paired reads were generated per sample.

ATAC-seq data analysis

Reads were trimmed for both quality (<=15) and Illumina adaptor sequences using Trim Galore v0.4.5 1,2 then aligned to human assembly hg38 using bowtie2 with the default parameters. Duplicated reads that have the same start site and orientation were removed using the Picard tool MarkDuplicates (http://broadinstitute.github.io/picard). Accessible regions were called using MACS2 v2.1.25 against standard input as the control (fold change > 2 and p value < 0.001). Regions overlapping with genomic 'blacklisted' regions (http://mitra.stanford.edu/kundaje/akundaje/release/blacklists/hg38human/hg38.blacklist.bed.gz) were removed. The peaks from all samples were then merged within 500 bp to create a full peak atlas. Raw read counts were tabulated over this peak atlas using featureCounts. All genome browser tracks were normalized to a sequencing depth of ten million mapped reads. Peaks were annotated using linear genomic distance, with a gene assigned to a peak if it was within 50 kb up- or down- stream of the gene start or end, respectively. Raw read counts in the peak atlas were normalized in DESeq2 prior differential and motif analyses. Differential peaks were then identified between groups of interest. Significant differential regions were accepted with fold change greater than 1.5 and adjusted p value less than 0.1.

S-EPTS/LM-PCR integration site analysis

Shearing-Extension Primer Tag Selection Ligation-Mediated PCR (S-EPTS/LM-PCR) is a shearing DNA based integration site (IS) analysis method in orientation to the original EPTS/LM-PCR. S-EPTS/LM-PCR starts with shearing of genomic DNA to an intended length of 500 bp using the Covaris M220 instrument. Sheared DNA is split into three equal replicates (500 ng each) and purified, followed by primer extension using two vector, long-terminal-repeat-specific biotinylated primers. The extension product is purified, and biotinylated DNA is being captured by paramagnetic beads. The captured DNA is ligated to linker cassettes including a molecular barcode, and the ligation product is amplified in an exponential PCR using biotinylated vector- and linker-cassette-specific primers. Biotinylated PCR-products are magnetically captured, washed, and used as template for amplification in a second exponential PCR with barcoded primers allowing sequencing by MiSeq technology (Illumina). Final preparation for sequencing is done as previously described[157,158]. Applied DNA double barcoding allows parallel sequencing of multiple samples in a single sequencing run while minimizing sample cross-contamination. Amplicons are then sequenced on the MiSeq instrument using V2 Reagent Kit (Illumina).

Exome computational analysis

Raw sequence data were trimmed according to sequence quality (Phred) and only sequences showing complete identity in both molecular barcodes (linker cassette barcode, sequencing barcodes) were further analysed. An in-house semi-automated bioinformatical data mining pipeline was used to analyse the

data[159]. In brief, quality filtered sequences were trimmed (vector- and linker cassette specific parts removed) and only sequences that showed at least 18 nucleotides of expected, vector-specific sequence were analysed further to ensure the analysis of true vector-genome junctions. Such trimmed sequences were further filtered in a way that only sequences equal or larger than 25 bp were aligned to the human genome (UCSC assembly release number hg38, version 3) by Burrows-Wheeler Aligner (BWA) MEM algorithm for the initial alignment. It was subsequently followed by mapping of potential IS sequences with BLAST, where minimum alignment identity percentage of 95% is employed, while nearby genes and other integrating features were annotated as previously described according to RefSeq database. The relative sequence count of each detected IS was calculated in relation to all sequences attributed to corresponding sample.

Cytokine measurements

CAR T cells were cultured with irradiated fibroblast cell line, 3T3, that was engineered to express CD19. They assay was carried out in a 24-well flat bottom plate. 5e5 CAR T cells (concentration 1e6/ml) were plated with 1.5e5 3T3-CD19. The media was collected after 24 hours and supernatant cytokines were measured using cytometric bead arrays (BD) for human IL2, IFNγ, TNF and Granzyme B (GzmB) as per the manufacturer's instructions.

Seahorse assay

Seahorse 96 well plates were coated with 20 ul Poly-L-lysine (50ug/ml) for 20-30 mins at room temperature. CAR T cells were suspended in appropriate mito

stress test (DMEM with Glutmax, pyruvate, and glucose) and glycolysis stress test (DMEM with Glutmax and pyruvate) medium. Poly-L-lysine was aspirated, and the plate was washed with 200ul distilled water. 2e5 cells were added to each well. The plate was then run as per manufacturer's instructions.

Statistical analysis

All statistical analyses were performed using the Prism 9 (GraphPad) software. No statistical methods were used to predetermine sample size. Statistical tests are provided in the figure legends. Kolmogorov–Smirnov test was used to determine p values in GSEA analysis. *p<0.05, **p<0.01, ***p<0.0001, ****p<0.00001.

Table 2.1 Reagents and other Resources

REAGENT or RESOURCE	SOURCE	IDENTIFIER
Antibodies		
Mouse anti-human CD62L BV421	BD	Cat# 563862, RRID:AB_2738455
Mouse anti-human LAG3 BV605	BD	Cat# 745160, RRID:AB_2742761
Mouse anti-human CD45RA BV605	BD	Cat# 562886, RRID:AB_2737865
Mouse anti-human CD4 BUV395	BD	Cat# 563550, RRID:AB_2738273
Mouse anti-human CD45 BV711	BD	Cat# 564357, RRID:AB_2744404
Mouse anti-human CD8 BV510	BD	Cat# 563919, RRID:AB_2722546
Mouse anti-human CD3 BUV737	BD	Cat# 612750, RRID:AB_2870081
Mouse anti-human CD19 BUV496	BD	Cat# 564655, RRID:AB_2744311
Mouse anti-human CD271 PE	BD	Cat# 557196, RRID:AB_396599
Mouse anti-human PD1 PE	Biolegend	Cat# 329906, RRID:AB_940483
Mouse anti-human Tim3 BV785	Biolegend	Cat# 345032, RRID:AB_2565833
Mouse anti-human CCR7 PE	Biolegend	Cat# 353204, RRID:AB_10913813

Mouse anti-human CD271 AF647	Biolegend	Cat# 345114, RRID:AB_2572059
Goat Anti-Mouse IgG Antibody AF647	Jackson ImmunoResearch	Cat# 115-606-072
Mouse anti-human CD27 BV421	Biolegend	Cat#302824
Mouse anti-human IL-7Rα PE	Biolegend	Cat#351304
Chemicals, peptides, and recombinant proteins		
(+)-JQ-1	MedChem Express	Cat# HY-13030
Dexamethasone	Millipore Sigman	Cat# D4902-25MG
Recombinant Human IL-15 R alpha Fc Chimera (HEK293), CF	RnD systems	Cat# 7194-IR-050
Cytokines		
Human IL-7, premium grade	Miltenyi Biotec	Cat# 130-095-361
Human IL-15, premium grade	Miltenyi Biotec	Cat# 130-095-762
Critical commercial assays		
immunoSEQ human TCRB Kit	Adaptive Biotechnologies	N/A
MiSeq Reagent Kits v2	Illumina	Cat# MS-102-2001
SMART-Seq v4 Ultra Low Input RNA Kit	Clonetech	Cat# 63488
KAPA Hyper Prep Kit	Kapa Biosystems	Cat# KK8504
TruSeq Methyl Capture EPIC LT Library Prep Kit	Illumina	Cat# FC-151-1002
TDE1 Tagment DNA Enzyme	Illumina	Cat# 20034198
aMPure XP beads	Beckman Coulter	Cat# A63882
xGen Exome Research Panel v1.0	IDT	N/A
Seahorse XF Cell Mito Stress Test Kit	Agilent Technologies	Cat# 103015-100
Seahorse XF Glycolysis Stress Test Kit	Agilent Technologies	Cat# 103020-100
Human IL-2 Flex Set (Bead A4)	BD	Cat# 558270
Human TNF Flex Set (Bead C4)	BD	Cat# 560112
Human IFN-g Flex Set (Bead B8)	BD	Cat# 560111
Human Granzyme B Flex Set (Bead D7)	BD	Cat# 560304
Experimental models: Cell lines		

FFLuc-GFP NALM6	In house	N/A
H29	In house	N/A
FFLuc-GFP PC3	In house	N/A
Experimental models: Organisms/strains		
NSG mice	The Jackson Laboratory	Stock# 005557 RRID:BCBC_4142
Oligonucleotides		
B2M (Hs00187842_m1)	Thermo Fischer Scientific	Cat# 4453320
MYC (Hs00153408_m1)	Thermo Fischer Scientific	Cat# 4453320
BATF3 (Hs00232744_m1)	Thermo Fischer Scientific	Cat# 4331182
TRAC gRNA CAGGGUUCUGGAUAUCUGU	Synthego	N/A
TET2 gRNA 1 UUAGUCUGUUGCCCUCAACA	Synthego	N/A
TET2 gRNA 2 GGUUCUGUCUGGCAAAUGGG	Synthego	N/A
SUV39H1 gRNA GCUGCAGGACCUGUGCCGCC	Synthego	N/A
Scrambled gRNA GCACUACCAGAGCUAACUCA	Synthego	N/A
CleanCap Cas9 mRNA	Trilink Biotechnologies	Cat # L-7206
Software and algorithms		
Prism 9	Graphpad	https://www.graphpad.com
FlowJo V10	BD	https://www.flowjo.com/
Spark	Tecan	https://lifesciences.tecan.com/multimode-plate-reader?p=Software
CaseViewer	3DHISTECH	https://www.3dhistech.com/solutions/caseviewer/
FIJI/ImageJ		https://imagej.nih.gov/ij/download.html
GENE-IS	In house	N/A
DESeq2	Love et al. 2014	https://bioconductor.org/packages/release/bioc/html/DESeq2.html

BWA	Li et al., 2009	http://maq.sourceforge.net/
Seurat	CRAN	https://cran.r-project.org/web/packages/Seurat/index.html
CRISPRESSO	Pinello et al. 2016	https://github.com/lucapinello/CRISPResso

CHAPTER 3

Disruption of *TET2* enhances T cell anti-tumor efficacy in a CAR dependent manner

Introduction

We utilized CRISPR/Cas9 genome editing system to engineer *TET2* disruption in human T cells. After testing multiple guides, we identified a guide RNA that can edit *TET2* with an efficiency of ~67% (Figure 3.1a). To assess the effect of *TET2* disruption on *in vivo* anti-tumor efficacy of CAR T cells, we chose the two FDA-approved CD28 or 4-1BB-based CD19 targeting CAR designs (Figure 3.1b). We injected immune deficient NSG mice with human lymphoblastic leukemia cell line, NALM6, to model human leukemia in mice (Figure 3.1c). CAR T cells were then injected at limiting doses to assess differences in their ability to eliminate tumor in mice (Figure 3.1c). Pre-infusion in mice, CAR T cell transduction efficiency and differentiation state is determined through flow cytometry (Figures 3.1d-e).

Results

The CAR determines anti-tumor potency gain of *TET2*-edited T cells

NALM6 bearing mice were treated with low dose unedited or *TET2*-edited Rv-1928z (1e5 CAR T cells/mouse) or Rv-19BBz (2e5 CAR T cells/mouse). No survival difference was observed between recipients of *TET2*-edited or unedited Rv-1928z CAR T cells (Figures 3.2a-c). In contrast *TET2*-edited Rv-19BBz CAR T cells prolonged survival of tumor bearing mice as compared to mice that were treated with unedited Rv-19BBz (Figures 3.2d-f). Increased anti-tumor efficacy in Rv-19BBz was associated with more CAR T cells both in the bone marrow and spleen (Day 21 p.i, Figures 3.2g-h). In contrast, Rv-1928z CAR T cell numbers were not significantly different between the unedited and *TET2*-edited group (Day 21 p.i, Figures 3.2g-h). Flow cytometry analysis of CAR T cells isolated from bone marrow revealed that *TET2* editing enhanced the $CCR7^+$ (A marker for memory T cell state) fraction of Rv-19BBz CAR T cells but not Rv-1928z CAR T cells (Day 21 p.i, Figures 3.2i-j). Analysis of inhibitory receptors did not show significant differences between unedited and *TET2*-edited groups for both CAR designs (Day 21 p.i., Figure 3.2k). These observations suggested that *TET2* editing can promote CAR T cell accumulation and differentiation, but these effects depend on the CAR design.

Murine studies show that TET2 loss in $CD8^+$ T cells enhance their memory fraction[147]. Since we observed *TET2* editing improved expansion and memory formation in Rv-19BBz but not in Rv-1928z, we wondered whether the strong induction of effector differentiation by Rv-1928z CAR does not allow improved memory formation by TET2 deficiency. To test this hypothesis, we extended

our study to include two alternate CD28 based CAR designs, Rv-1928z+41BBL and TRAC-1928z (Figure 3.3a). Co-expression of 41BBL with 1928z CAR design enhances T cell proliferation and reduced their effector differentiation which in turn leads to enhanced anti-tumor activity of Rv-1928z+41BBL CAR T cells over Rv-1928z CAR T cells. Targeting 1928z to the *TRAC* locus, limits tonic signaling and delays effector differentiation and eventually exhaustion by allowing for effective internalization and re-expression of the CAR following single or repeated exposure to antigen.

As with Rv-1928z and Rv-19BBz, *TET2* editing did not affect CAR transduction efficiency or pre-infusion T cell phenotype of either of these CAR T cell populations (Figures 3.3b-c). The anti-tumor efficacy of both *TET2*-edited Rv-1928z+41BBL and *TRAC*-1928z CAR T cells was increased relative to their non-edited counterparts (Figures 3.3d-g). Flow cytometry analysis of CAR T cells isolated from bone marrow revealed that *TET2* editing enhanced the $CCR7^{+}$ fraction of both Rv-1928z+41BBL and *TRAC*-1928z (Figure 3.3h). However, it was not statistically significant for Rv-1928z+41BBL CAR T cells (Day 21 p.i., Figures 3.3h-i). Analysis of inhibitory receptors did not show significant differences between unedited and *TET2*-edited groups for both Rv-1928z+41BBL and *TRAC*-1928z CAR T cells (Day 21 p.i., Figure 3.3j), similar to observations from Rv-1928z and Rv-19BBz. These findings indicated that CAR structure (Rv-1928z vs Rv-19BBz) and expression (Rv-1928z vs *TRAC*-1928z or Rv-1928z vs Rv-1928z+41BBL) play a critical role in determining whether therapeutic efficacy will be increased upon *TET2* disruption.

Emergence of a hyper-proliferative phenotype in *TET2*-edited CAR T cells

We observed clinical signs of distress after day 50 in mice treated with *TET2*-edited *TRAC*-1928z and Rv-1928z+41BBL CAR T cells, even though these mice were tumor-free by bioluminescence imaging (Figures 3.4a, 3.3e, 3.3g). Gross pathology revealed an enlarged spleen and liver, pale kidneys, and lungs with extensive T cell infiltration and absence of $CD19^+$ leukemia (Figure 3.4b). The infiltrating T cells were CAR^+ (Figure 4.3a) and $Ki67^+$ (Figure 3.4b). This prompted us to treat additional cohorts of mice with all four CAR designs (Rv-19BBz, Rv-1928z, Rv-1928z+41BBL, *TRAC*-1928z), administering slightly higher but still low T cell doses ($2\text{-}5x10^5$). Under these doses, mice treated with all 4 CAR designs maintain long term tumor remission allowing for long-term follow up (90 days, Figure 3.4c). Mice treated with Rv-CARs were euthanized on day 90 and *TRAC*-CAR T cells recipients on day 75. All CARs maintained long-term tumor remission post primary tumor clearance, which typically occurred within 17 days according to BLI. A considerable increase in bone marrow and splenic CAR T cell numbers was found in mice treated with *TET2*-edited Rv-19BBz, Rv-1928z+41BBL and *TRAC*-1928z CAR T cells compared to their unedited counterparts (Figure 3.4d). In contrast, CAR T cell numbers in *TET2*-edited and unedited Rv-1928z in both bone marrow and spleen were not significantly different (Figure 3.4d), except for a single mouse (1 out of 10) that showed increased number of CAR T cells. Flow cytometric analysis of CAR T cells isolated from bone marrow again showed increased CCR7 expression in *TET2*-edited Rv-19BBz, Rv- 1928z+41BBL and *TRAC*-1928z CAR T cells compared to their unedited counterparts, but not in *TET2*-edited Rv-1928z T cells (Figures 3.5a-b). Flow cytometry analysis of inhibitory receptors did not

reveal any significant differences between unedited and *TET2*-edited groups for all 4 CAR designs (Figure 3.5c). This long-term follow-up thus established that *TET2* editing may lead to pathological CAR T cell accumulation occurring weeks or months after tumor clearance, the magnitude and frequency of which depend on the CAR type.

Confirming the hyper-proliferative phenotype with a different *TET2* gRNA and another tumor model

To ascertain that our observation of hyper-proliferative phenotype was not model specific or an off-target effect of the gRNA, we setup a human prostate cancer model in NSG mice (Figure 3.6a). PC3-PSMA bearing mice were treated with a curative dose of PSMA targeting CD28-costimulated CARs that co-express the 41BB ligand (Pd28z+41BBL, 2e5/mouse) to allow for durable anti-tumor response and enable long-term monitoring of the mice. Peripheral bleeds were performed 30 days after CAR T cell injection. *TET2*-edited Pd28z+41BBL CAR T cells (both with the previously used gRNA-g1 and the new gRNA-g2) were present at almost ~10-fold higher numbers in the peripheral blood as compared to scrambled gRNA edited Pd28z+41BBL (Figure 3.6b). Splenic CAR T cell quantification of WT Pd28z+41BBL and *TET2*-edited Pd28z+41BBL (Top 5 with the highest peripheral Pd28z+41BBL CAR T cell counts) revealed 4/5 *TET2*-edited Pd28z+41BBL treated mice bearing over 100 million CAR T cells in their spleen at day 45 (Figure 3.6c). These findings collectively rule out the possibility that the late-stage hyper-proliferative phenotype is a CD19 model dependent or a guide RNA specific observation.

Discussion

TET2 deficiency in HSCs results in skewing towards myeloid lineage[145]. Murine TET2-deficient $CD8^+$ T cells studies were conducted in $CD4Cre^+$ conditional TET2 knockout (*TET2* cKO) mouse that lack TET2 in all mature αβ T cells[147]. However, no significant differences in T cell homeostasis were observed in *TET2* cKO mice. Frequencies and absolute numbers of thymic and peripheral T cells were not significantly different between WT and *TET2* cKO mice. Carty et al. reported that, following acute lymphocytic choriomeningitis virus (LCMV) infection, TET2-deficient $CD8^+$ T cells have enhanced memory percussor effector cell (MPEC) population and reduced short lived effector cell (SLEC) population during primary anti-viral response (Day 8 p.i.). However, early T cell expansion in response to viral infection was very similar between WT and TET2-deficient groups. Carty et al. reported no incidence of a hyper-proliferative phenotype over time in *TET2* cKO mice. Fraietta et al. also describe an improved expansion and expression of memory markers in 4-1BB co-stimulated human CAR T cells that co-express *TET2* shRNA over control shRNA co-expressing 4-1BB CAR T cells in an *in vitro* model of weekly stimulation[42]. Another report by Kong et al. describes inhibition of bromodomain and extra-terminal domain (BET) by pharmacological agent JQ1, reinvigorates CAR T cells (4-1BB costimulatory domain) derived from patients that showed partial or no anti-tumor response upon administration of autologous CAR T cells in part by inhibition of TET2[160]. Consistent with earlier observations, we observe that *TET2*-editing can increase expression of memory markers in human CAR T cells. However, we find that the degree to which *TET2*-editing can increase expression of memory markers depends on the CAR design (Rv-1928z vs Rv-

19BBz) and expression (Rv-1928z vs (*TRAC*-1928z, Rv-1928z+41BBL)). Notably, *TET2* disruption did not increase expression of CCR7 expression for Rv-1928z CAR T cells, likely due to the very strong induction of effector function in Rv-1928z CAR T cells. Variant CD28 CAR designs that limit induction of effector function (*TRAC*-1928z and Rv-1928z+41BBL) are, however, amenable to reprogramming by *TET2*-editing to increase expression of memory markers. The emergence of hyper-proliferation and associated pathology in T cells with *TET2*-editing has not been reported before. The clonal expansion reported by Fraietta et al. subsided after tumor clearance from ~95% of total CAR product (at the peak of anti-tumor response) to <1% of total CAR product (post resolution of the tumor). In the next chapter, we characterize the hyper-proliferative CAR T cells and identify the drivers of proliferation.

The empirical correlation between *TET2*-editing allowing for more $CCR7^+$ CAR T cells and enhanced anti-tumor efficacy across different CAR designs is intriguing and suggests crosstalk between T cell differentiation mechanisms mediated by TET2 deficiency and CAR signals. CCR7 (along with CD62L) is widely used as a marker for memory T cell subset. Multiple reports have shown that $CCR7^+/CD62L^+$ CAR T cells outperform $CCR7^-/CD62L^-$ CAR T cells in *in vitro* models of repeated stimulation and pre-clinical tumor models[161]. However, once the *TET2*-edited CAR T cells achieve hyper-proliferative state, they are unlikely to possess characteristics of memory T cells. We will test this hypothesis more directly in the next chapter.

In summary, we find that *TET2*-editing enhances anti-tumor activity and CCR7^{+} expression of T cells in a CAR dependent manner. However, over time *TET2*-edited CAR T cells enter a stage of hyper-proliferation in absence of detectable tumor burden. This unchecked proliferation results in pathology in mice.

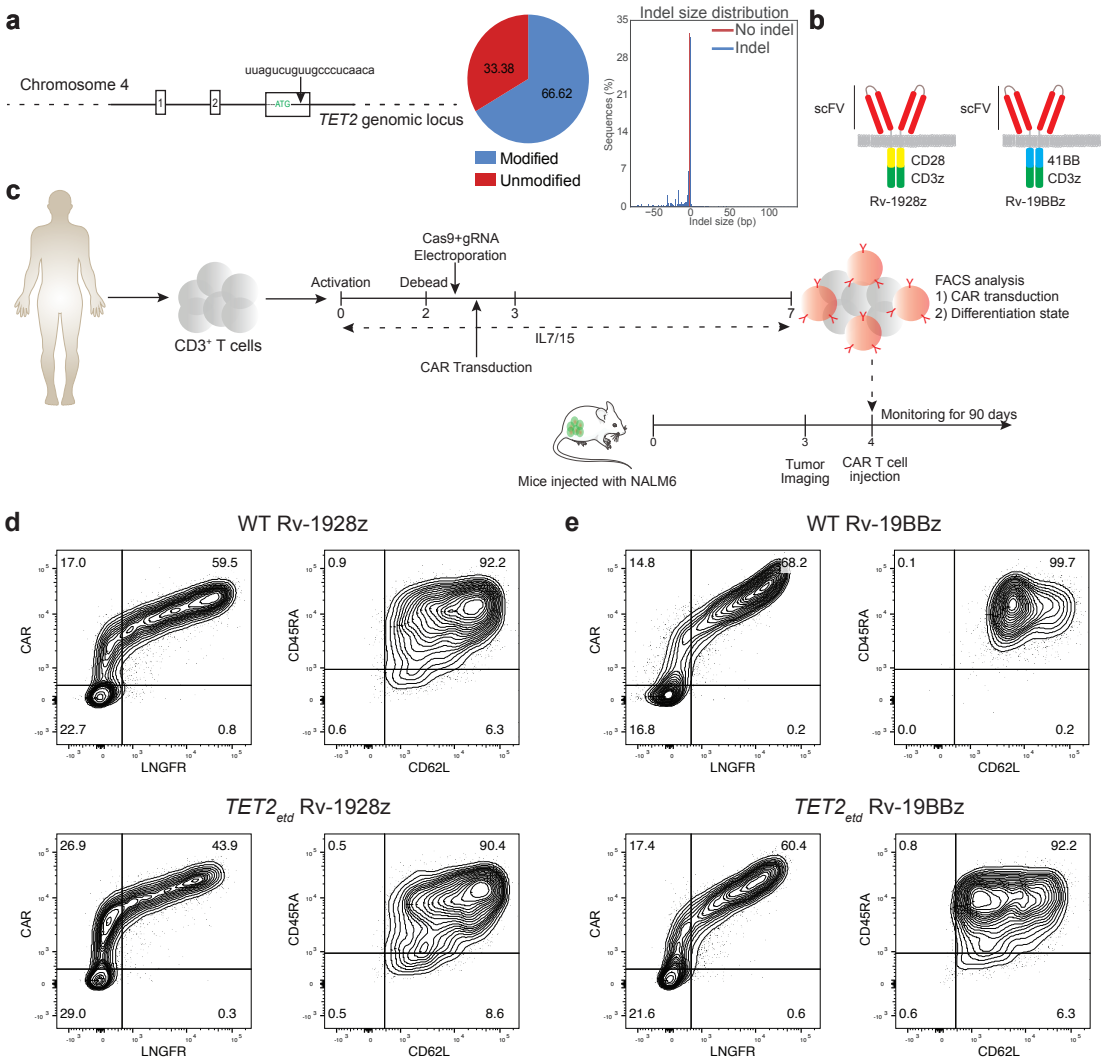

Figure 3.1: Schematics of CAR T cell generation and murine xenograft model.
a, gRNA targeting of *TET2* locus. **b,** Schematics of CD28 and 4-1BB CAR designs. **c,** Schematics of CAR T cell generation protocol and murine NALM6 model. **d-e,** CAR transduction efficiency and CAR T cell differentiation phenotyping pre-infusion in mice for Rv-1928z (**d**) and Rv-19BBz (**e**).

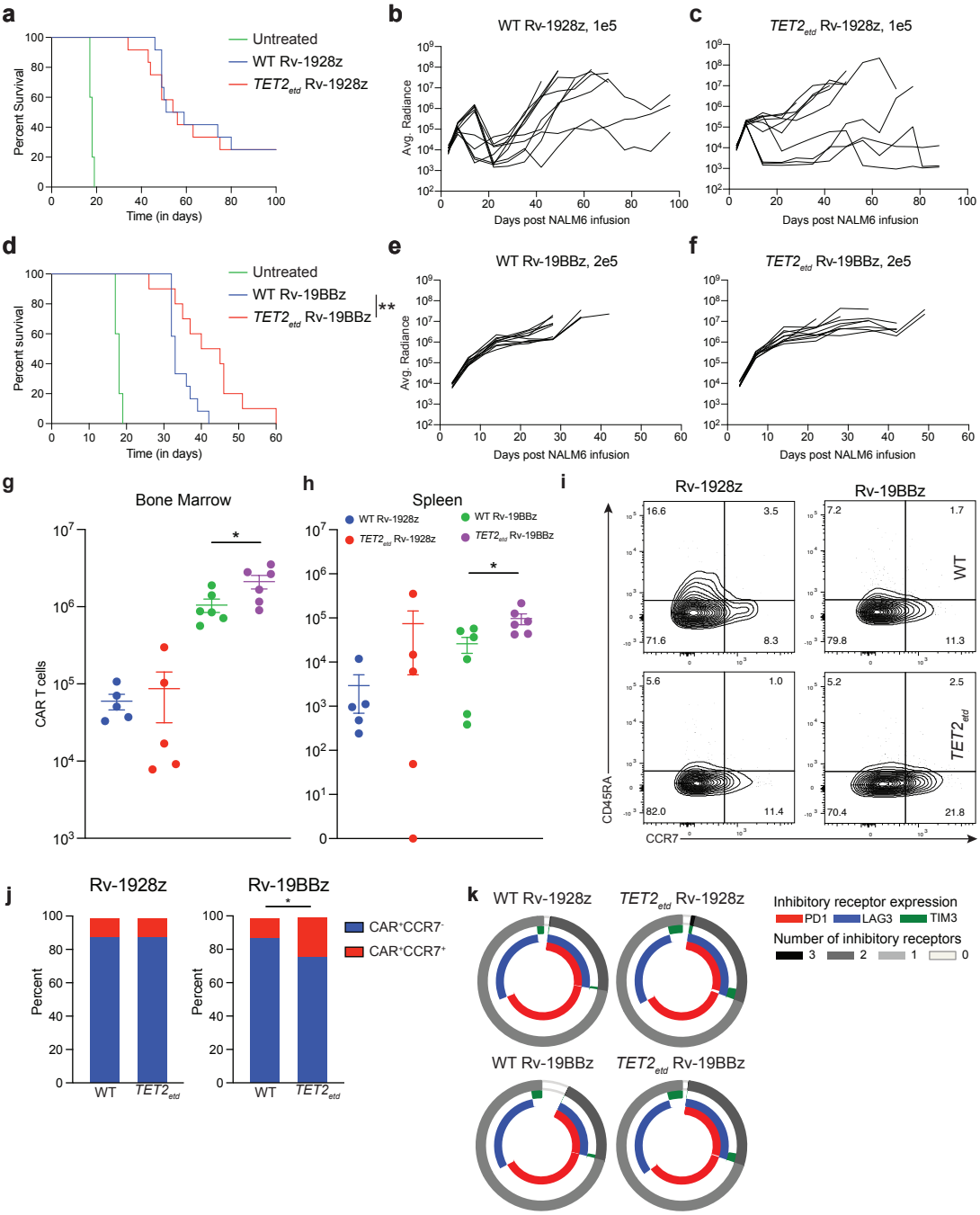

Figure 3.2: The CAR determines anti-tumor potency gain of *TET2*-edited T cells. **a-c,** Mice survival (**a**) and tumor radiance (**b,c**) under Rv-1928z (dose: 1e5, n=12) CAR T cell treatment. **d-f,** Mice survival (**d**) and tumor radiance (**e,f**) under Rv-19BBz (dose: 2e5, n=12) CAR T cell treatment. **g-h** Bone marrow (**g**) and splenic (**h**) CAR T cell quantification at 3 weeks post infusion. Data is represented as mean±SE. **i-j,** Differentiation phenotyping of bone marrow CAR T cells at week 3 post infusion (n=3). **k,** CAR T cell inhibitory receptor expression at week 3 post infusion from mouse bone marrow (n=3). p values were determined by log-rank Mantel–Cox test (**a,d**), Mann–Whitney test (**g,h**) and χ2 test (**j**).

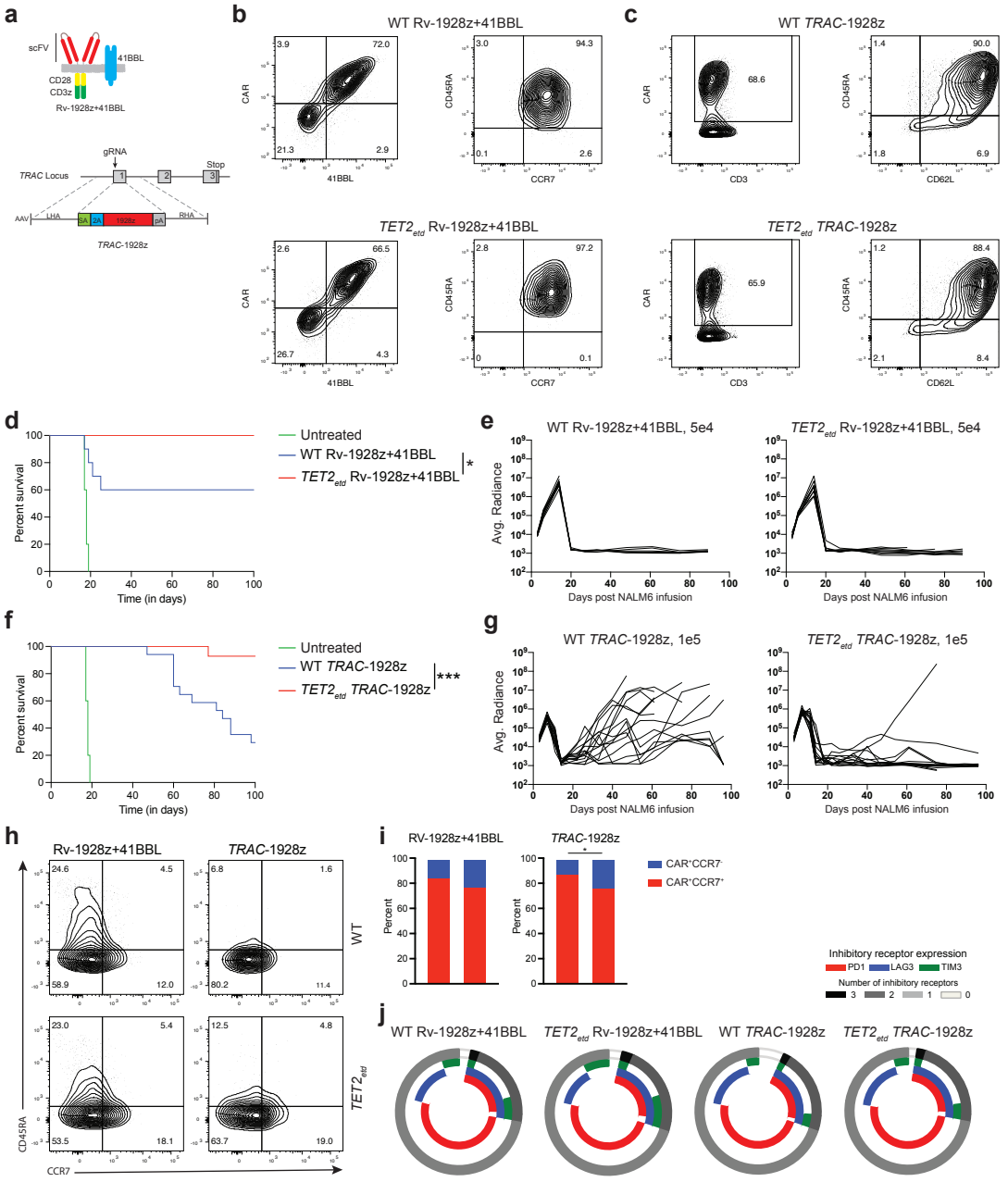

Figure 3.3: *TET2* editing enhances the anti-tumor efficacy of *TRAC*-1928z and Rv-1928z+41BBL CAR T cells.

a, Rv-1928z+41BBL (Top panel) and *TRAC*-1928z (Bottom panel) CAR designs. **b-c,** CAR transduction efficiency and CAR T cell differentiation phenotyping pre-infusion in mice for Rv-1928z+41BBL (**b**) and *TRAC*-1928z (**c**).**a-c,** Cancer-free mice survival (**d**) and tumor radiance (**e**) under Rv-1928z+41BBL (dose: 5e4, n=10) CAR T cell treatment. **f-g,** Cancer-free mice survival (**f**) and tumor radiance (**g**) under *TRAC*-1928z (dose: 1e5, n=15) CAR T cell treatment.**h-i,** Differentiation phenotyping of bone marrow CAR T cells at week 3 post infusion (n=3). **j,** CAR T cell inhibitory receptor expression at week 3 post infusion from mouse bone marrow (n=3).p values were determined by log-rank Mantel–Cox test (**d,f**) and χ2 test (**i**).

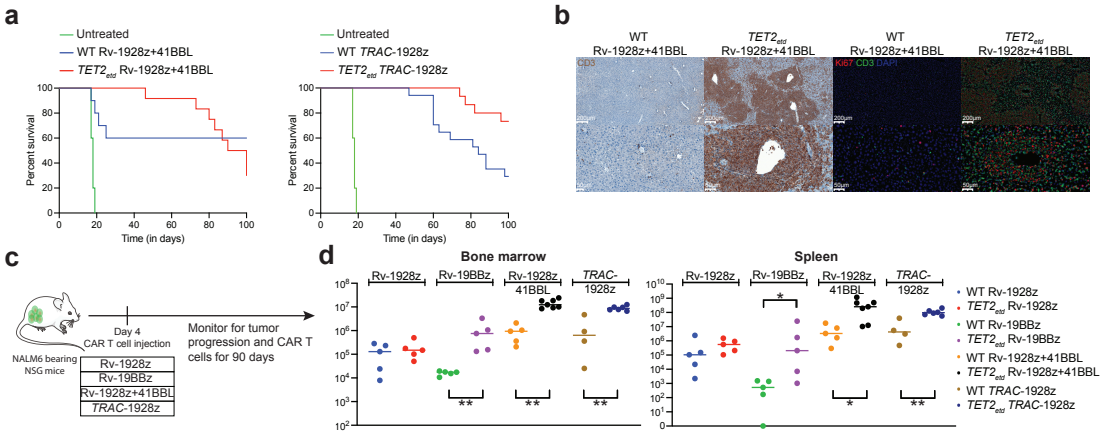

Figure 3.4: Effect of CAR design on long term T cell accumulation upon *TET2* editing. **a,** Overall survival of NALM6-bearing mice treated with Rv-1928z+41BBL (n=10) and *TRAC*-1928z (n=15). **b,** Immunohistochemistry and Immunofluorescence staining of a liver section of mice treated with WT Rv-1928z+41BBL and $TET2_{etd}$ Rv-1928z+41BBL at day 90. **c,** Schematics of long-term CAR T cell and tumor monitoring. Rv-1928z were used at 4e5, Rv-19BBz were used at 5e5, Rv-1928z+ 41BBL were used at 2e5 and *TRAC*-1928z CAR T cells were used at 4e5 dose. **d,** CAR T cell quantification in the bone marrow (left panel) and spleen (right panel). Bars show median values. Mann-Whitney test (**d**).

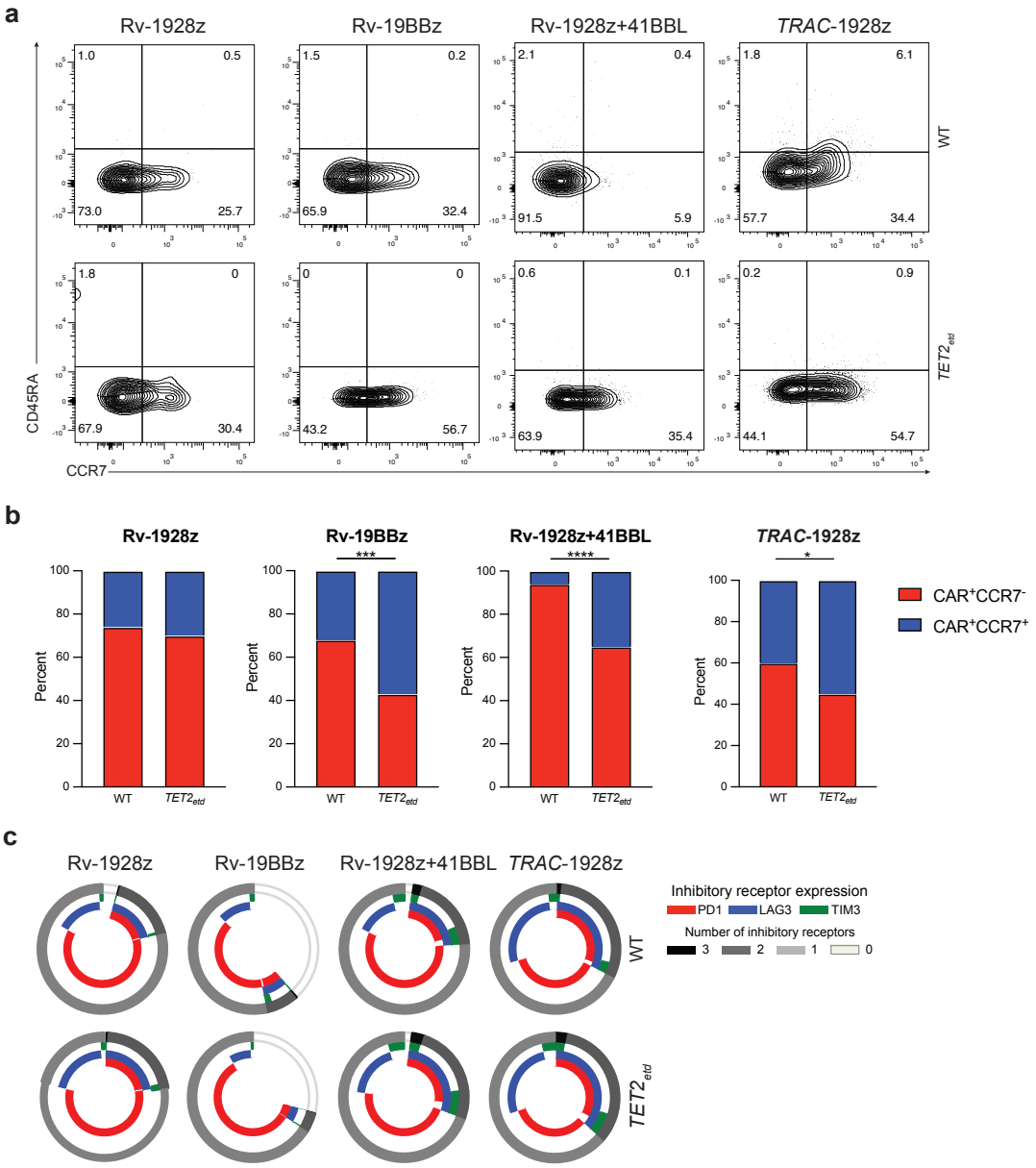

Figure 3.5: Long-term CAR T cell differentiation markers and inhibitory receptor expression upon *TET2* editing.
a-b, Differentiation phenotyping of retrovirally encoded CAR T cells (day 90) and *TRAC*-1928z CAR T cells (day 75) isolated from the bone marrow. **c,** Inhibitory receptor expression of bone marrow Rv-1928z, Rv-19BBz, Rv-1928z+41BBL (day 90) and *TRAC*-1928z (day 75) CAR T cells. p values were determined by χ2 test (**b**).

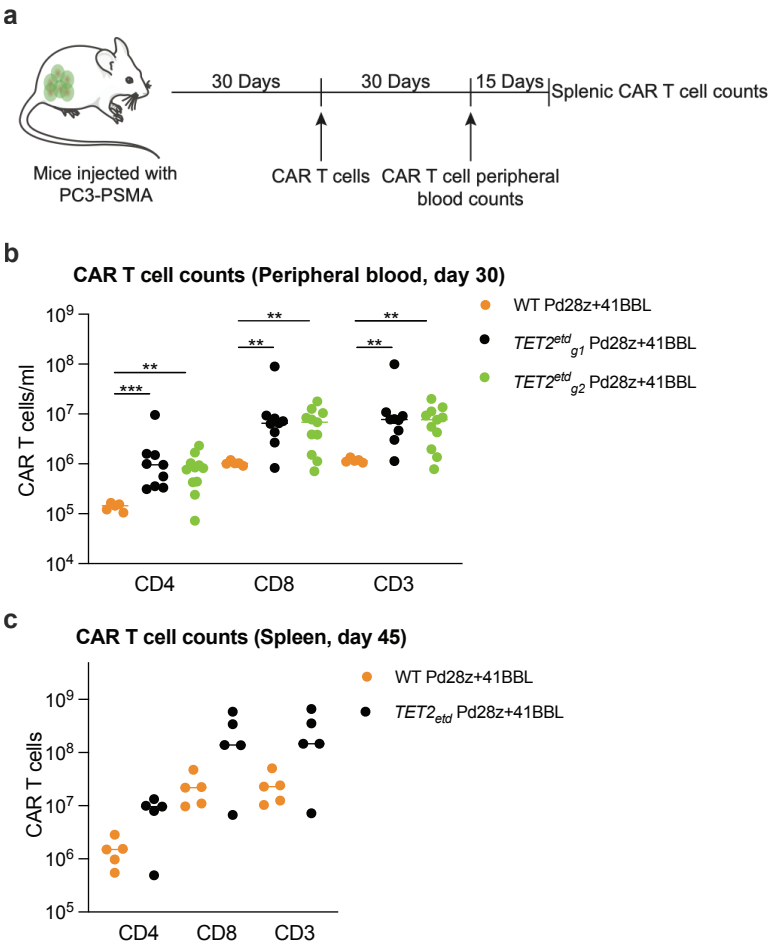

Figure 3.6: Effect of *TET2* editing on CAR T cell accumulation in a prostate cancer model.
a, Schematics of the prostate cancer experimental design. *TET2* was edited with the previously discussed gRNA (g1) and an alternative gRNA (g2). Pd28z+41BBL (PSMA targeted, CD28 costimulated CAR that coexpressess 41BBL ligand) was used in this study (Dose=2e5/mouse). **b,** CAR T cell counts in the peripheral blood 30 days post infusion of T cells. **c,** Mice with the top 5 CAR T cell peripheral counts at day 30 across both *TET2* targeting gRNA (g1 and g2) were euthanized at day 45 along with 5 scrambled gRNA treated Pd28z+41BBL mice and their splenic CAR T cell numbers were quantified. p values were determined by Mann-Whitney (**b**).

CHAPTER 4

BATF3/MYC axis drives hyper-proliferation of TET2-deficient CAR T cells

Introduction

In Chapter-3, we describe emergence of a hyper-proliferative T cell population, the frequency of which is dependent on the CAR. In this chapter, we further characterize the hyper-proliferative population. We first assess *TET2* allelic status of the hyper-proliferative populations since Cas9 nucleus can result in both monoallelic and biallelic editing at the gRNA target site. We then functionally address the cause of different frequencies of emergence of hyper-proliferative state across different CAR designs. Given that the hyper-proliferative population is largely $CCR7^{+}$, we assess the effector function of these CAR T cells. Finally, we perform a series of experiments to identify the drivers of proliferation in *TET2*-edited hyper-proliferative population.

Results

Achieving a hyper-proliferative state requires bi-allelic *TET2* disruption

All hyper-proliferative T cell populations identified were CAR^+. However, their TET2 allelic status was unknown. We hypothesized that there would be an enrichment for biallelic *TET2*-editing if total loss of TET2 is required for achieving hyper-proliferative state. We chose Rv-1928z and Rv-1928z+41BBL CAR designs to assess changes in *TET2*-editing over time. Pre-infusion Rv-1928z and Rv-1928z+41BBL CAR T cells had very similar *TET2*-editing efficiency (Figures 4.1a-b). By day 21 post infusion, we observed enrichment of TET2-editing for Rv-1928z+41BBL but not Rv-1928z (Figures 4.1c-e). In subsequent follow-up, large splenic T cell counts (>100e6, indicative of hyper-proliferative phenotype) were reached in 12/15 mice treated with *TET2*-edited Rv-1928z+41BBL, but only in 2 of 15 mice treated with *TET2*-edited Rv-1928z CART cells, detected by day 90 and 200, respectively. In the latter two cases (2-00 and 2-2), we found a 19bp deletion in both alleles in 2-2 (Figure 4.2a) and a large biallelic integration of a partial retroviral vector in 2-00 (Figure 4.2b). Five of the expanded *TET2*-edited Rv-1928z+41BBL populations harvested at day 90 were randomly selected for analysis and all were found to be nearly entirely (>98%) biallelically *TET2*-edited

(Figures 4.2c-g). We confirmed total ablation of TET2 on a protein level as well (Figure 4.2h). Thus, bi-allelic *TET2* editing ($TET2_{bed}$) is enriched over time, irrespective of CAR design, consistent with it being required for achieving a hyper-proliferative T cell state.

Multiple clones achieve hyper-proliferative status

We assessed clonal composition in the hyper-proliferative CAR T cell populations by TCRvβ sequencing. All 5 Rv-1928z+41BBL populations were multiclonal, with no clone constituting >50% of the total CAR product, except for sample 17-1 where a single clone accounted for ~82% of the CAR T cells (Left panel, Figures 4.2c-g). In contrast, both Rv-1928z populations (2-00 and 2-2) largely consisted in a single clone (>95%. Figures 4.2a-b), consistent with the lesser probability of 1928z CAR T cells achieving clonal expansion.

The lack of shared TCRs between different hyper-proliferative populations, the absence of GVHD in mice with hyper-proliferative CAR T cell population and the emergence of clonal dominance in *TRAC*-1928z CAR T cell-treated mice (Figure 4.2i), in which TCR expression has been disrupted (>90%) suggested that the TCR is not required for acquisition of a hyper-proliferative phenotype. To further exclude a role for TCR engagement in achieving sustained clonal expansion, we ablated TCR expression in conjunction with *TET2* disruption before transduction of Rv-1928z+41BBL and compared the frequency of emergence of the hyper-proliferative phenotype in recipient mice. Long-term follow up of TCR^{+}*TET2*-edited and TCR^{-}*TET2*-edited Rv-1928z+41BBL CAR T cells revealed no differences in frequency of CAR T cells achieving a hyper-proliferative state and their differentiation state (Figures 4.3a-c), confirming that antigen recognition by the TCR is not required for sustained proliferation.

Clonality and clonal persistence are imparted by the CAR

We hypothesized that the difference in clonal diversity amongst *TET2*-edited

hyper-proliferative Rv-1928z (Figures 4.2a-b) as compared to Rv-1928z+41BBL (Figures 4.2c-g), *TRAC*-1928z (Figure 4.2i), and Rv-19BBz (Figure 4.2j) owed to differences in T cell proliferation and persistence imparted by the CAR design. To this end, we introduced either Rv-1928z or Rv-1928z+41BBL in the same pool of *TET2*-edited T cells and compared the fate of common TCRvβ clonotypes expressing either CAR (Figure 4.4a). Pair-wise analysis revealed major differences in clonal evolution between Rv-1928z and Rv-1928z+41BBL from day 0 (pre-infusion CAR T cells) to day 21 (Figures 4.4b-c). This divergent evolution is illustrated by tracking the persistence of the 100 most frequent clones in the Rv-1928z pre-infusion cell population, all of which were also present in the Rv-1928z+41BBL pre-infusion product (Figure 4.4d). By day 21, most (70/100) of these clones were still detected in Rv-1928z+41BBL CAR T cells, while only 3/100 were detectable in recipients of Rv-1928z CAR T cells (Figure 4.4d). Retro-tracking clones present in hyper-proliferative populations (day 90) to pre-infusion, we found few persisting clones for Rv-1928z in contrast to Rv-1928z+41BBL (Figures 4.4e-f), even though both Rv-1928z and Rv-1928z+41BBL had similar pre-infusion clonal diversity (Figure 4.4g). The difference between Rv-1928z and Rv-1928z+41BBL in their respective clonal longevity was further evidenced by tracking the 100 most frequent clones from the pre-infusion Rv-1928z and Rv-1928z+41BBL CAR populations up to day 90. None were detected in Rv-1928z Figure 4.4h), whereas a few of the earliest clones detected on day 0 remained detectable in the day 90 Rv-1928z+41BBL population (Figure 4.4i), though they were not dominant (Figure 4.4j). Altogether, these observations confirmed that while biallelic *TET2*-editing is necessary for achieving sustained antigen-

independent proliferation, the frequency with which a T cell can establish a hyper-proliferative state is determined by the chimeric antigen receptor.

Uncoupling of proliferative and effector functions in persisting *TET2*$_{bed}$ CAR T cells

To assess the functional properties of the hyper-proliferative CAR T cell population, we first evaluated the cytolytic function of hyper-proliferative *TET2*$_{bed}$ CAR T cells. *TET2*$_{bed}$ CAR T cells demonstrated diminished cytolytic ability and failed to eliminate NALM6 both *in vitro* and *in vivo* (Figures 4.5a-c). For further molecular characterization, we focused on Rv-1928z+41BBL CAR T cells since the unedited Rv-1928z+41BBL CAR T cells persisted the most among the 4 tested CAR designs, thus providing a matched, unedited control. Transcriptional profiling of hyper-proliferative *TET2*$_{bed}$ and WT Rv-1928z+41BBL CAR T cells revealed an increased expression of cell cycle-related factors in the former (Figures 4.5d-e). In contrast, induction of effector cytokines (IL2, IFNγ, TNFα) was greater in WT Rv-1928z+41BBL CAR T cells than in *TET2*$_{bed}$ Rv-1928z+41BBL (Figure 4.5f). Collectively these observations establish that by day 90 *TET2*$_{bed}$ CAR T cells achieve a state of robust, sustained proliferation that is associated with poor effector function.

Hyper-proliferative CAR T cells do not harbor recurrent mutations and require cytokine support for secondary engraftment

Gene Set Enrichment analysis[162] (GSEA) did not show enrichment in central memory/stem cell memory signatures for *TET2*$_{bed}$ compared to WT Rv-1928z+41BBL (Figure 4.5g), despite the increased expression of CCR7 in

TET2-edited CAR T cells. Instead, we found enrichment in angioimmunoblastic T cell lymphoma (AITL) and HTLV1 driven T cell leukemia/lymphoma datasets (Figure 4.5h). TET2 loss along with acquired secondary mutations has been reported to cause myeloid and lymphoid malignancies[163]. Additionally, *TET2* and *TET3* deficient murine T cells cause proliferative disease upon secondary transplant[164,165]. This led us to gauge the proliferative potential of $TET2_{bed}$ CAR T cells upon secondary transplant and search for potential genetic drivers of proliferation.

We therefore investigated whether $TET2_{bed}$ clones harbored acquired mutations that could account for their clonal dominance. Whole exome sequencing was performed on three clones expressing different CARs (Figures 4.6a, c, e). Numerous non-synonymous point mutations were observed in all 3 dominant clones (Figures 4.6b, d, f). Analysis of translocations for these 3 samples only identified CAR (CD28/CD3z) fusions (Data not included). Some chromosomal amplifications and mega-base scale deletions were observed in a subset of the dominant clone population in samples 17-1 and 4-1 (Figures 4.6a, e). Given their lower frequency compared to that of the dominant clone, these gross chromosomal defects seem to be late occurring secondary events. For the retroviral encoded CARs in samples 17-1 and 2-2, we identified the sites of retroviral integration. None of them disrupted or integrated next to cancer-related genes associated with AITL or T cell lymphoma (Data not included). Altogether, we find that hyper-proliferative CAR T cells do not bear any conserved genetic mutation that could account for their dominance over other $TET2_{bed}$ CAR T cells.

Secondary transplant studies of *TET2*$_{bed}$ CAR T cells showed that they did not persist without exogenous IL7/15 supplementation (Figures 4.7a-b). Cell numbers, however, remained modest and were barely detectable at day 150 when the study reached its intended end point (Figure 4.7c). These findings indicate that *TET2*$_{bed}$ CAR T cells are unable to autonomously sustain their proliferation upon secondary transplant.

Establishment of a BATF3 driven MYC-dependent proliferative program

The lack of a conserved genetic driver of proliferation of *TET2*$_{bed}$ CAR T cells prompted us to study whether their epigenetic state enables sustained proliferation. Assay for Transposase-Accessible Chromatin using sequencing (ATAC-seq) analysis revealed significant differences between accessible chromatin regions of WT and *TET2*$_{bed}$ Rv-1928z+41BBL CAR T cells (Figure 4.8a). Activator protein (AP-1) family binding motif was the most significantly enriched motif in differentially open chromatin regions of *TET2*$_{bed}$ CAR T cells (Figure 4.8b). Paired transcriptional analysis revealed that, amongst the AP-1 factors, *BATF3* was the most significantly upregulated in *TET2*$_{bed}$ CAR T (Figure 4.8c). BATF3 has previously been implicated as a driver of proliferation in HTLV1-associated T cell leukaemia/lymphoma by inducing a *MYC* transcriptional program[166]. Distinct promoter and gene body regions of *BATF3*, with some encompassing consensus AP-1 binding motifs, were found to be more readily accessible in hyper-proliferative *TET2*$_{bed}$ Rv-1928z+41BBL CAR T cells compared to WT Rv-1928z+41BBL CAR T cells (Figures 4.8d-e). Furthermore, *TET2*$_{bed}$ Rv-1928z+41BBL CAR T cells showed a strong

enrichment in hallmark MYC targets when compared to WT Rv-1928z+41BBL CAR T cells (Figures 4.8f). These observations and the analogy to HTLV1-associated T cell leukaemia/lymphoma suggests that the BATF3/MYC axis may be essential for sustained antigen-independent proliferation in *TET2*$_{bed}$ CAR T cells.

JQ1 and dexamethasone inhibit *TET2*$_{bed}$ CAR T cell proliferation

JQ1 is an inhibitor of the BET protein BRD4 that has been previously shown to inhibit *BATF3* and *MYC* expression and inhibit ATLL cell growth[166]. Although JQ1 inhibited proliferation of all tested CAR populations, *TET2*$_{bed}$ CAR T cells were more sensitive to JQ1 treatment than pre-infusion *TET2*-edited CAR T cells (Figures 4.9a-b). This heightened sensitivity to JQ1 was associated with a greater suppression of *BATF3* and *MYC* expression in *TET2*$_{bed}$ CAR T cells (Figures 4.9d-e).

Dexamethasone has been shown to suppress AP-1 factors. Contrary to JQ1, dexamethasone did not limit proliferation of pre-infusion *TET2*-edited CAR T cells (Figures 4.9a-c). However, it did markedly inhibit proliferation of *TET2*$_{bed}$ CAR T cells (Figures 4.9a-c). This increased sensitivity to dexamethasone was associated with reduction of both *BATF3* and *MYC* expression in *TET2*$_{bed}$ CAR T cells (Figures 4.9d, 4.9f). In contrast, *MYC* expression was elevated in pre-infusion *TET2*-edited CAR T cells despite *BATF3* inhibition (Figures 4.9d, 4.9f). The differences in pattern of *MYC* expression between pre-infusion *TET2*-edited CAR T cells and *TET2*$_{bed}$ CAR T cells upon dexamethasone treatment suggests dependency of *MYC* expression on *BATF3* in *TET2*$_{bed}$ CAR T cells.

Discussion

In this chapter, we characterized the late-stage hyper-proliferative populations that emerge post tumor clearance in mice treated with *TET2*-edited CAR T cells. We find that hyper-proliferative populations are universally associated with biallelic editing of *TET2* and CAR expression (Figure 4.9g). We further show that TCR expression is dispensable for emergence of hyper-proliferative populations. TCRvβ sequencing of hyper-proliferative populations identified multiple T cell clones in mice treated with *TET2*-edited Rv-19BBz, Rv-1928z+41BBL and *TRAC*-1928z, while hyper-proliferative *TET2*-edited Rv-1928z CAR T cells were rare and monoclonal when they occurred. These observations suggest a probabilistic fate, wherein the chance of establishing a stable hyperproliferative state is low with Rv-1928z, only allowing rare breakthrough clones, and increased with CARs that promote greater persistence. Acquired secondary mutations were found in persisting T cells over time. However, we did not identify a recurrent mutation amongst different $TET2_{bed}$ CAR T cell populations. Instead, we identified an epigenetic profile pointing to key roles for AP-1 factors, including elevated *BATF3* expression.

AP-1 factors are critically involved in distinct T cell states[123,124,167-169]. High levels of BATF3, together with BATF, JunB and IRF4 are associated with human CAR T cell exhaustion[123]. On the other hand, *BATF* over-expression in murine CAR T cells enhances their anti-tumour activity[124], and *BATF3*[169] over-expression in OT-I T cells enhances their memory formation. $TET2_{bed}$ CAR T cells showed high *BATF3*, reduced *Jun*/*Fos* expression, and enhanced *MYC* accessibility for BATF3 binding, resulting in robust proliferation but diminished

effector function - a profile that differs from canonically defined T cell exhaustion and T cell memory.

AP-1 factors have also been implicated in oncogenesis[170]. *cJUN* and *BATF* over-expression can lead to uncontrolled proliferation[171,172]. BATF3 has been shown to drive proliferation in T cell leukaemia/lymphoma through MYC[166] or IL2R[173]. These diverse reports, and the hyper-proliferative CAR T cell phenotype we report here, underscore the potency of CAR T cell epigenetic programming but also the serious long-term safety concerns that may arise from manipulating *TET2* and possibly AP-1 factors.

TET2$_{bed}$ CAR T cells remained sensitive to dexamethasone, which lowered both *BATF3* and *MYC* expression in these cells. Dexamethasone sensitivity may account for the unexplained disappearance of a patient's TET2-deficient 19BBz T cell clone following corticosteroid administration to manage cytokine release syndrome[42]. However, prolonged *TET2$_{bed}$* CAR T cell clonal proliferation is prone to result in the accumulation of somatic mutations that may eventually become resistant to this elimination strategy. Screening for mutations in elderly subjects who are more likely to harbour *TET2* mutations[174] can reduce the risk of unintentionally generating *TET2$_{bed}$* CAR T cells. In addition, intentional disruption of *TET2* for CAR T therapy is likely to lead to an increased risk of T cell oncogenesis in subjects harbouring other oncogenic mutations such as in *DNMT3a*[175,176]. In summary, our findings demonstrate the potential of epigenetic reprogramming to augment CAR T cell potency but underscore the critical importance of CAR function and AP-1 factor regulation

in determining the fate of *TET2*-edited CAR T cells and the eventual risk of genomic instability.

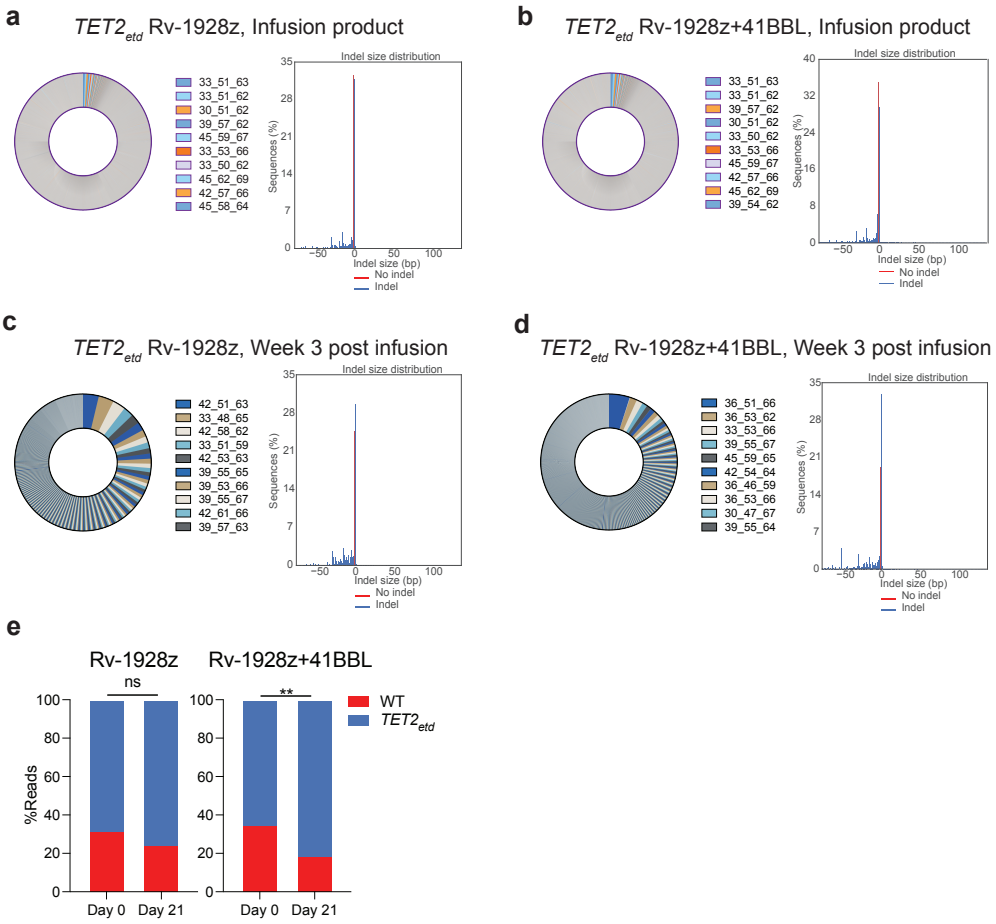

Figure 4.1: Enrichment rate of biallelic TET2 editing is dependent on the CAR design. **a,b,** Pre-infusion TCRvβ sequencing (left panel) and *TET2* status (right panel) of Rv-1928z (**a**) and Rv-1928z+41BBL (**b**). CAR T cells were generated from the same donor. **c,d,** TCRvβ sequencing (left panel) and *TET2* status (right panel) of Rv-1928z (**c**) andRv-1928z+41BBL (**d**) CAR T cells isolated at week 3 post infusion in mice. **e,** Enrichment of *TET2* editing from pre-infusion (day 0) in mice to day 21 in Rv-1928z and Rv-1928z+41BBL CAR T cells. p values were determined by χ2 test (**e**)

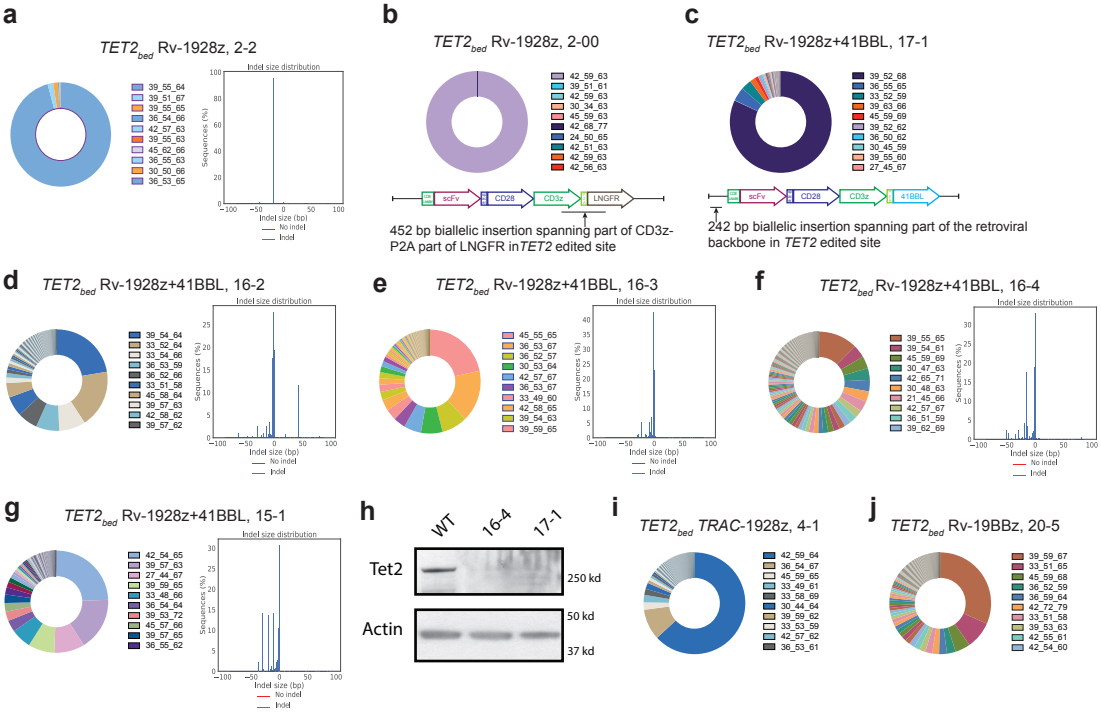

Figure 4.2: Hyper-proliferative *TET2*-edited CAR T populations are biallelically edited for *TET2*.

a,b TCRvβ sequencing (left panel) and *TET2* status (right panel) of hyper-proliferative Rv-1928z with a 19bp biallelic deletion (**a**) and a biallelic integration of the indicated segment for the retroviral vector (**b**). Both Rv-1928z are dominant for a single clone (>95% frequency of the top clone). **c-g,** TCRvβ sequencing (left panel) and *TET2* status (right panel) of hyper-proliferative Rv-1928z+41BBL CAR T cell populations. All are biallelically edited for *TET2*. 4/5 are oligoclonal. 17-1 clone was the Rv-1928z+41BLL hyper-proliferative CAR T cell population with a single clone at >50% frequency (**c**). **h,** TET2 western blot confirming total loss of TET2 in biallelically edited hyper-proliferative populations. **i-j,** Examples of oligoclonality in *TRAC*-1928z (**i**) and Rv-19BBz (**j**).

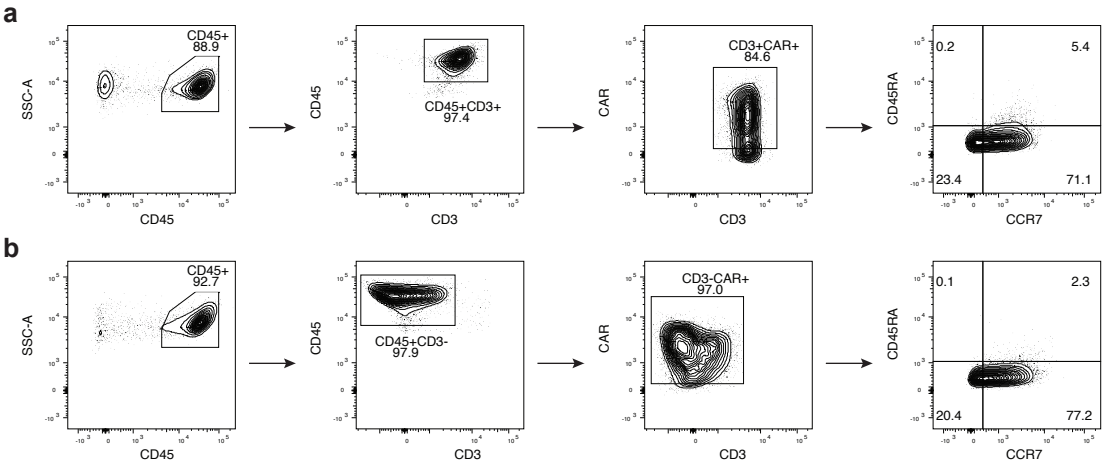

c

CAR T cell	Donor 1	Donor 2
TCR^{+}*TET2*$_{etd}$ Rv-1928z+41BBL	8/10	4/5
TCR^{-}*TET2*$_{etd}$ Rv-1928z+41BBL	7/10	4/5

Figure 4.3: TCR is dispensable for emergence of hyper-proliferative phenotype in *TET2*-edited Rv-1928z+41BBL CAR T cells.
a-b, Differentiation phenotyping in TCR^{+}*TET2*$_{etd}$ Rv-1928+41BBL (**a**) and TCR^{-}*TET2*$_{etd}$ Rv-1928z+41BBL (**b**). **c,** Summary of emergence of hyper-proliferative phenotype post CAR T cell infusion in mice for different donors. Mice were monitored for 90 days. 2e5 CAR T cells were used for both the groups.

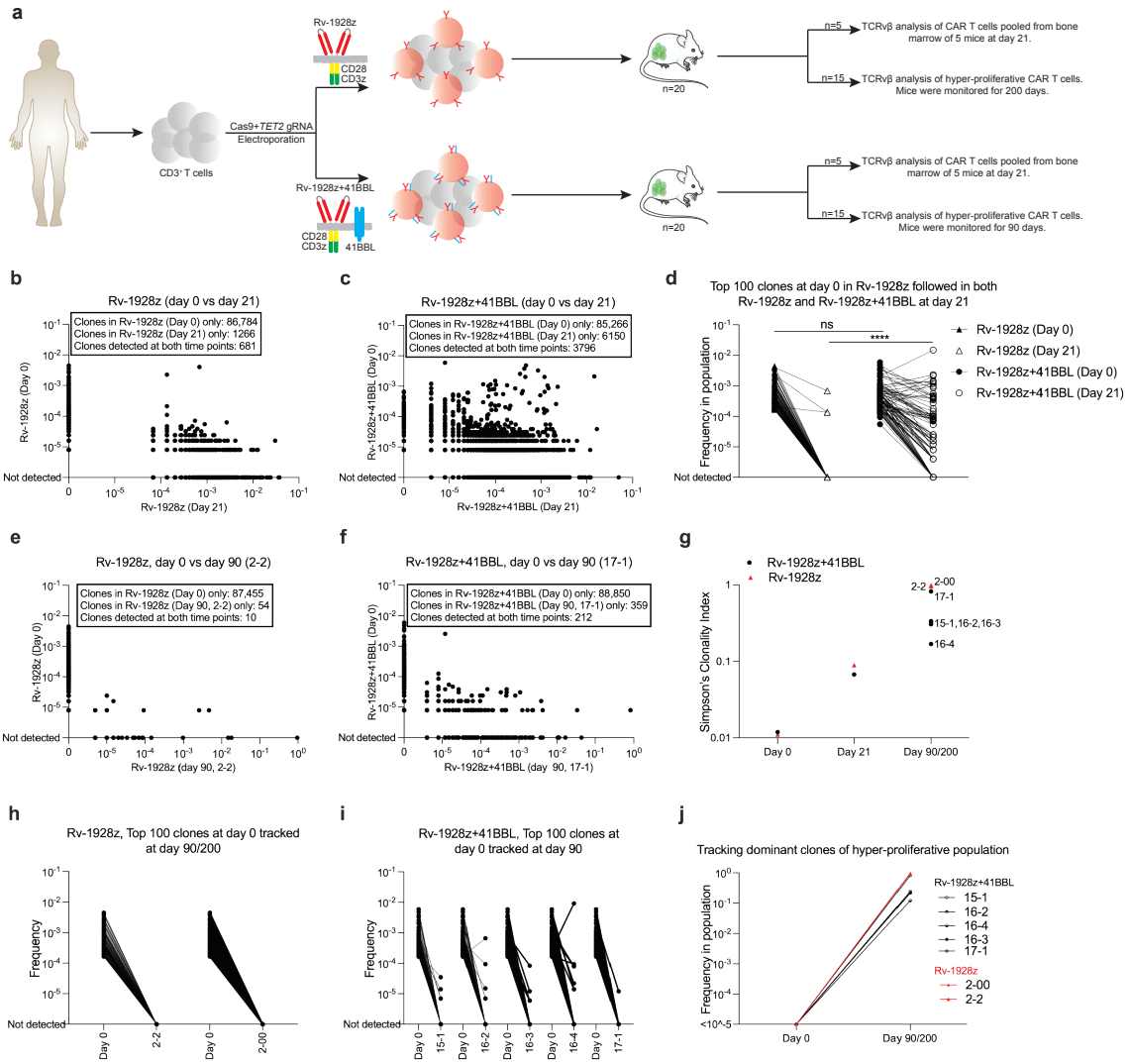

Figure 4.4: Properties of the chimeric antigen receptor design determine composition of *TET2*$_{bed}$ hyper-proliferative populations.

a, Rv-1928z or Rv-1928z+41BBL CAR T cells were generated from the same donor to assess the effect of CAR design on clonal persistence. 5 Mice were euthanized at day 21 to assess clonal diversity post tumor clearance. 15 mice were followed for emergence of a hyper-proliferative phenotype. **b-c,** Pair-wise analysis of Rv-1928z (**b**) and Rv-1928z+41BBL (**c**) at day 0 and day 21. **d,** Top 100 Rv-1928z clones at infusion were mapped in the Rv-1928z+41BBL infusion product. These clones were then assessed at day 21 for both the CAR receptors. **e-f,** Pair-wise analysis (day 0 vs day 90) of the lone hyper-proliferative population found at day 90 for Rv-1928z CAR receptor (**e**). Representative pair-wise analysis (day 0 vs day 90) of a Rv-1928z+41BBL hyper-proliferative population (**f**). Changes in clonality index over time in Rv-1928z and Rv-1928z+41BBL CAR T cells (**g**). **h-i,** Tracking the fate of the 100 most abundant pre-infusion clones in the hyper-proliferative populations of Rv-1928z (**h**) and Rv-1928z+41BBL (**i**). (**j**) Retro-tracking late-stage dominant clones in the infusion product (Day 0). All dominant clones were isolated at day 90 except for 2-00 which was isolated at day 200.

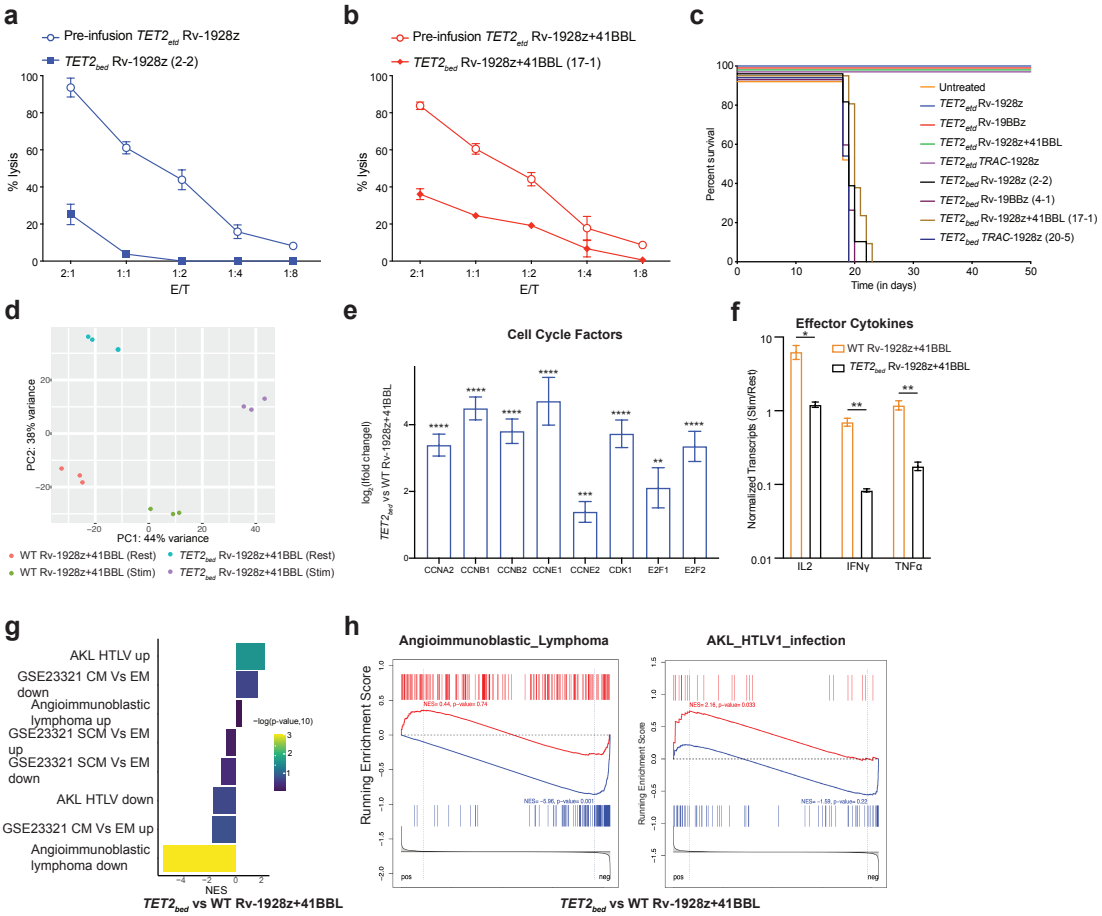

Figure 4.5: Loss of effector function in hyper-proliferative *TET2*$_{bed}$ CAR T cells. **a-b,** *In vitro* cytolytic activity assessment upon co-culture with NALM6 for 16-hrs as determined by luciferase activity for pre-infusion *TET2*-edited Rv-1928z and hyper-proliferative *TET2*$_{bed}$ Rv-1928z (2-2) (**a**) and pre-infusion *TET2*-edited Rv-1928z+41BBL and hyper-proliferative *TET2*$_{bed}$ Rv-1928z+41BBL (17-1) (**b**). **c,** NALM6 bearing NSG mice were either treated with 5e5 hyper-proliferative *TET2*$_{bed}$ Rv-1928z (n=7), Rv-19BBz (n=3), Rv-1928z+41BBL (n=7) and *TRAC*-1928z (n=5) CAR T cells or pre-infusion *TET2*-edited Rv-1928z (dose: 4e5), Rv-19BBz (dose: 5e5), Rv-1928z+41BBL (dose: 2e5) and *TRAC*-1928z (dose: 4e5) (n=5 for all pre-infusion *TET2*-edited CAR T cells). **d,** Principal component analysis of resting and stimulated (24-hrs post co-culture with CD3/28 beads at 1:1 bead to cell ratio) of WT Rv-1928z+41BBL and *TET2*$_{bed}$ Rv-1928z+41BBL. **e,** Elevated levels of cell cycle factors in *TET2*$_{bed}$ Rv-1928z+41BBL as compared to WT Rv-1928z+41BBL. Data is represented as mean±SE (n=3). p values were determined by Wald test with FDR correction.**f,** Reduced induction of effector cytokines in response to CD3/28 bead stimulation in *TET2*$_{bed}$ Rv-1928z+41BBL as compared to WT Rv-1928z+41BBL. Data is represented as mean±SE (n=3). p values were determined by t-test with FDR correction. **g-h,** Geneset enrichment analysis (GSEA) reveals no enrichment in central memory (CM) and stem cell memory (SCM) compartments for *TET2*$_{bed}$ Rv-1928z+41BBL as compared to WT Rv-1928z+41BBL (**g**). Enrichment in Angioimmunoblastic Lymphoma (AITL) and HTLV-1 driven Adult T cell lymphoma/leukemia genesets of *TET2*$_{bed}$ Rv-1928z+41BBL (**h**).

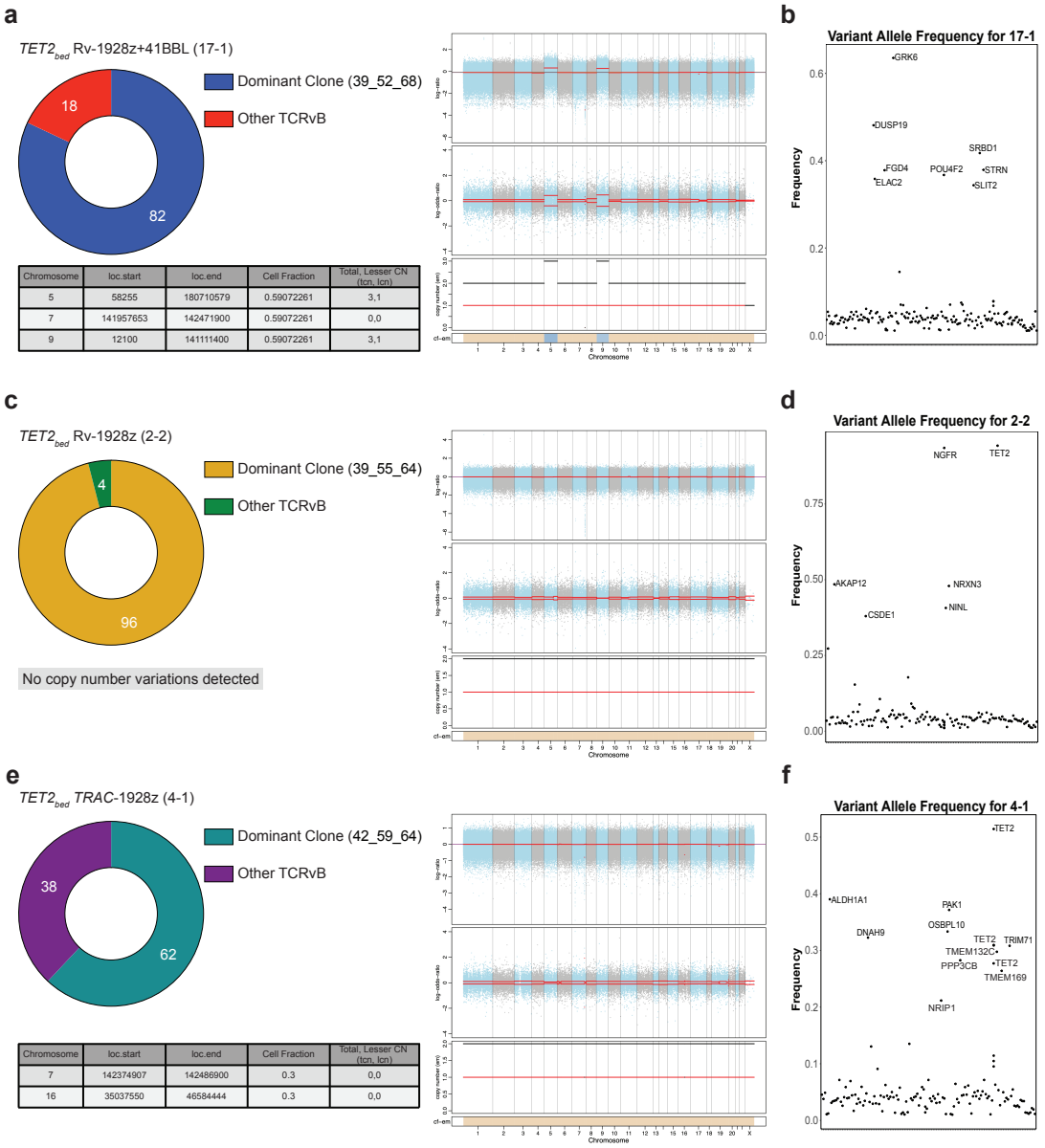

Figure 4.6: No conserved secondary genetic mutation between different hyper-proliferative *TET2*$_{bed}$ CAR T populations dominant for a single clone.
a, (Right panel) Copy number changes in *TET2*$_{bed}$ Rv-1928z+41BBL (17-1). The top panel displays log (ratio) denoted by "(logR)" with chromosomes alternating in the blue and gray. The middle panel displays log (odds-ratio) denoted by "(logOR)". Segment means are plotted in red lines. In the bottom panel total (black) and minor (red) copy number are plotted for each segment. The bottom bar shows the associated cellular fraction (cf). Dark blue indicates high cf. Light blue indicates low cf. Beige indicates a normal segment (total=2, minor=1). The table shows genetic events occurring at >0.1 cf. (Left panel) CAR T cell clonality as determined by vβ sequencing in *TET2*$_{bed}$ Rv-1928z+41BBL (17-1).**b,** Nonsynonymous acquired point mutations in *TET2*$_{bed}$ Rv-1928z+41BBL (17-1). Mutations that occur at a frequency > ((dominant TCRvβ frequency/2) -0.1) or >0.3 whichever is lower is annotated. **c,** (Right panel) Copy number changes in *TET2*$_{bed}$ Rv-1928z (2-2). (Left panel) CAR T cell clonality as determined by vβ sequencing in *TET2*$_{bed}$ Rv-1928z (2-2). **d,** Nonsynonymous acquired point mutations in *TET2*$_{bed}$ Rv-1928z (2-2). **e,** (Right panel) Copy number changes in *TET2*$_{bed}$ *TRAC*-1928z (4-1). (Left panel) CAR T cell clonality as determined by vβ sequencing in *TET2*$_{bed}$ *TRAC*-1928z (4-1). **f,** Nonsynonymous acquired point mutations in *TET2*$_{bed}$ *TRAC*-1928z (4-1).

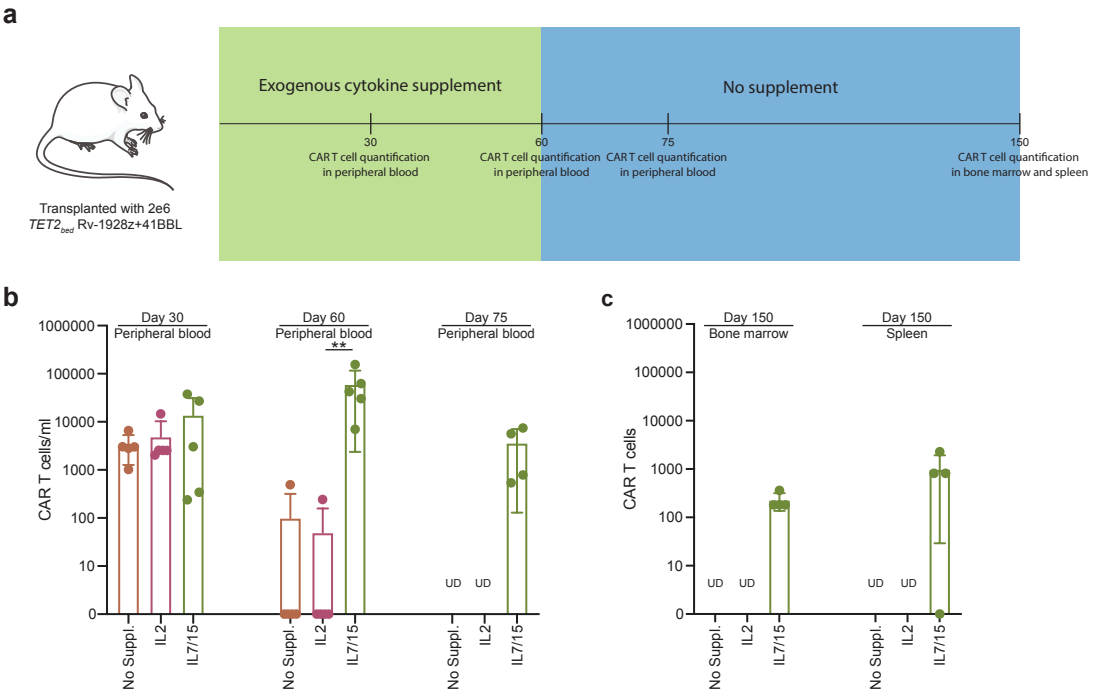

Figure 4.7: Hyper-proliferative *TET2*$_{bed}$ Rv-1928z+41BBL do not achieve uncontrolled proliferative state upon secondary transplant.

a, Schematics of secondary transplant of hyper-proliferative *TET2*$_{bed}$ Rv-1928z+41BBL cells. The exogenous cytokine supplement had to be stopped at day 60 due to deteriorating mice condition in response to frequent injections. **b,** CAR T cell quantification in peripheral blood under different exogenous supplementation at day 30, day 60 and day 75. Each dot represents a mouse. UD: undetected. **c,** CAR T cell quantification in bone marrow and spleen at day 150 post CAR T cell infusion. Data is represented as mean±SD (**b,c**). Mann–Whitney test (**b**).

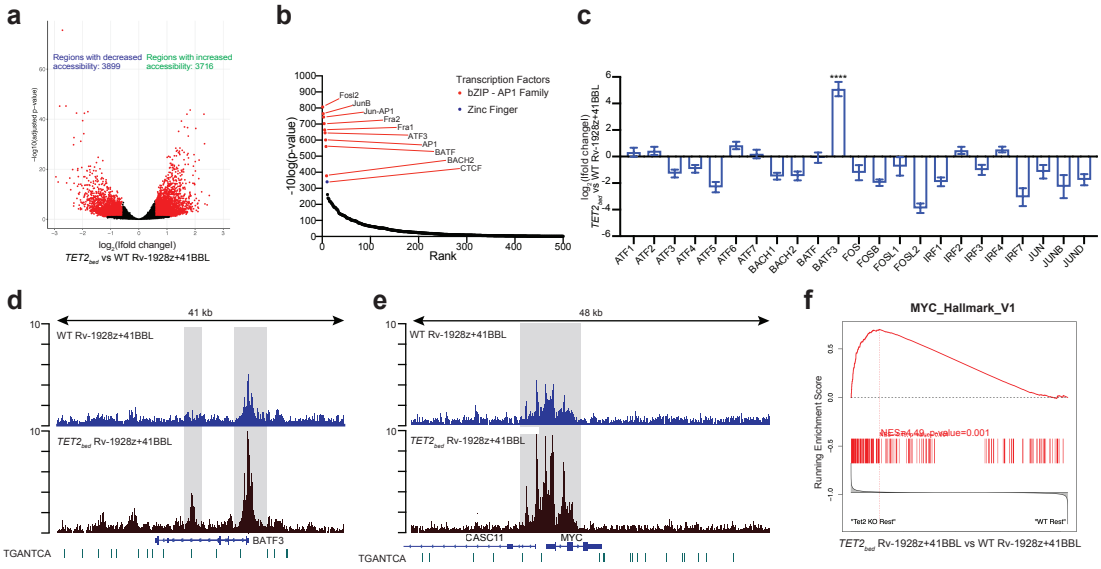

Figure 4.8: BATF3/MYC axis drives hyper-proliferation of *TET2*$_{bed}$ CAR T cells.
a, Differentially accessible genomic regions between *TET2*$_{bed}$ Rv-1928z+41BBL and WT Rv-1928z+41BBL. Both samples were isolated from mice at day 90. The red dots are peaks with Ifold changel >1.5 and (p_{adj}<0.1). **b,** AP1 binding motif was most significantly enriched in open chromatin region of *TET2*$_{bed}$ Rv-1928z+41BBL. Top 10 motifs are annotated. **c,** RNA expression of AP1-family transcriptional factors in *TET2*$_{bed}$ Rv-1928z+41BBL and WT Rv-1928z+41BBL. **d-e,**Increased genomic accessibility (Highlighted by grey background) in promoter and genebody regions of *BATF3* (**d**) and *MYC* (**e**). AP1 binding motif marked by green dashes. **f,** Geneset enrichment analysis reveals increased *MYC* signaling in *TET2*$_{bed}$Rv-1928z +41BBL as compared to WT Rv-1928z +41BBL.

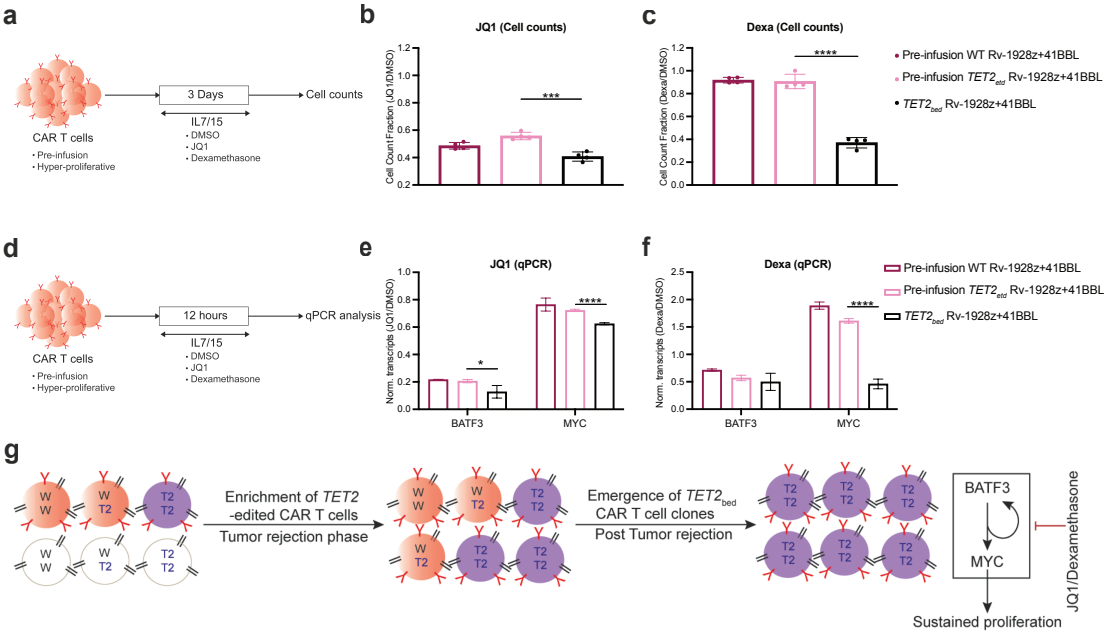

Figure 4.9: JQ1 and dexamethasone treatment inhibit *TET2*$_{bed}$ CAR T cell proliferation. **a-c,** Schematics of the cell proliferation assay (**a**). The cells were either treated with DMSO, JQ1 (500nM) or dexamethasone (dexa, 1µm). DMSO normalized cell counts for JQ1 (**b**) and dexa (**c**) treatment. p-values were determined by unpaired t-test (**b,c**). **d-f,** Schematics of qPCR study (**d**). CAR T cells were treated with DMSO, JQ1 or dexa at the same dose as cell proliferation assay for 12 hours. Transcripts were normalized to *B2M* for each sample. DMSO normalized *BATF3* and *MYC* levels under JQ1 (**e**) and dexa (**f**) treatment. Multiple unpaired t-tests corrected by BKY method (**e,f**). **g,** Graphical model summarizing the results. Data in **b,c, e,f** is presented as mean±SD (n=4)

CHAPTER 5

SUV39H1 disruption enhances functional persistence of CD28 costimulated CAR T cells

Introduction

In the previous chapters, we explored the role of *TET2* in CAR T cell function. In this chapter, we study the effect of disruption of histone methyl transferase, *SUV39H1*, in CAR T cell function. We focused on the Rv-1928z CAR in this study as *TET2*-editing did not improve anti-tumor efficacy in T cells expressing this CAR design.

Results

SUV39H1 disruption improves anti-tumor efficacy of Rv-1928z CAR T cells

We employed the same CAR T cell generation protocol as was used in the *TET2* study (Figure 5.1a). We were able to achieve a ~80% genome editing efficiency of the SUV39H1 locus (Figures 5.1b-c). SUV39H1 disruption was confirmed at the protein level (Figure 5.1d). SUV39H1 is a H3K9 methyltransferase, therefore, we compared global H3K9me3 levels in unedited and *SUV39H1*-edited T cells at 2 days and 5 days after electroporation (Figures 5.2a-b). We did not observe significant differences in *SUV39H1*-edited and unedited T cells (scrambled gRNA treated), 2 days after electroporation (Left panel, Figure 5.2b). However, H3K9me3 levels were reduced in *SUV39H1*-edited T cells as compared to unedited T cells at 5 days post electroporation (Middle panel, Figure 5.2b). Interestingly, H3K9me3 levels increased from day 2 to day 5 post electroporation in unedited T cells (Right panel, Figure 5.2b).

We employed the NALM6 B-ALL xenograft model for assessing differences in anti-tumor activity of Rv-1928z upon *SUV39H1* editing (Figure 5.1a). *SUV39H1* editing did not significantly affect CAR transduction and pre-infusion differentiation phenotype (Figures 5.3a-b). *SUV39H1* editing enhanced the anti-tumor efficacy of Rv-1928z CAR T cells relative to their unedited counterparts, with 9/10 NALM6 bearing mice treated with *SUV39H1*-edited Rv-1928z CAR T cells (*SUV^{etd}* Rv-1928z) surviving over the duration of observation (90 days) as compared to 1/12 mice treated with unedited Rv-1928z CAR T cells (WT Rv-1928z) (Figure 5.1e). NALM6 have been engineered to express GFP-

luciferase, which allows us to monitor tumor burden in mice. We noted very similar primary tumor clearance (first 10 days post CAR T cell injection) in WT Rv-1928z and *SUV^{etd}* Rv-1928z CAR T cells (Figure 5.1f). However, mice treated with WT Rv-1928z relapsed after initial tumor clearance in contrast to mice treated with *SUV^{etd}* Rv-1928z CAR T cells which maintain durable tumor control (Figure 5.1f). To confirm that the observed effects were not due to an off-target effect of the gRNA, we setup an *invitro* model of repeated CAR T cell stimulation (Figure 5.4a). We identified the top 10 predicted off-target sites, which included 2 genomic sites with 2 mismatches to the SUV39H1 gRNA and 8 genomic sites with 3 mismatches to the *SUV39H1* gRNA (Figure 5.4b). There were no genomic sites with 1 mismatch to the gRNA. The assay was designed to first find the rate of editing at the top 10 predicted off-target sites before CAR stimulation (Figure 5.4a). Editing efficiency at the top 10 predicted off-target sites was then assessed after 4 rounds of CAR stimulation (Figure 5.4b). We also assessed editing efficiency at the *SUV39H1* locus at both those time points, hypothesizing that there would be an enrichment for *SUV39H1* editing after 4 rounds of CAR stimulation. All editing efficiencies were analyzed through sequencing of the PCR product encompassing the editing site. The false discovery rate (FDR) of this assay was determined through amplifying an unrelated genomic locus of T cells that were electroporated with only Cas9. The FDR of this assay was 0.06% (Figure 5.4c). All off-target sites (except off-target site 9, OT-9) were edited at a frequency near FDR (Figure 5.4c). OT-9 was edited at a frequency of 1%. No enrichment was observed in any of the 10 off-target sites after 4 rounds of CAR stimulation (Figure 5.4c). *SUV39H1* editing before CAR stimulation (day 7) was 72.7%, it increased to 83.7% after 4 rounds

of CAR stimulation (Figure 5.4c). These observations allow us to rule out an off-target genome editing event resulting in improved CAR T cell function.

SUV39H1 disruption enhances early CAR T cell proliferation and persistence

We then assessed the effect of SUV39H1 disruption on *in vivo* CAR T cell proliferation and persistence. We chose 3 time points to quantify CAR T cell numbers (in bone marrow) – day 10, day 17 and day 60 (post CAR T cell infusion). Day 10 represents early tumor rejection phase for both WT and *SUV^{etd}* Rv-1928z CAR T cells (Figure 5.1f). At day 17, *SUV^{etd}* Rv-1928z CAR T cells contract post primary tumor clearance while WT Rv-1928z CAR T cells start experiencing activation due to relapsing tumor (Figure 5.1f). Day 60 CAR T cell quantification provides an insight into their long-term persistence. For day 60 analysis, we treat NALM6 bearing mice with 4e5 CAR T cells, which is twice the stress test dose. This results in effective early tumor clearance (generally by day 10-15) and allows assessment of persistence in absence of CAR activation. *SUV39H1* editing enhanced early CAR T cell accumulation (day 10, Figure 5.5a) and long-term persistence (day 60, Figure 5.5c). Day 17 CAR T cell numbers were not significantly different between *SUV39H1*-edited and unedited groups (Figure 5.5b). Flow cytometry analysis revealed increased CD27 expression at day 17 in WT Rv-1928z CAR T cells as compared to *SUV^{etd}* Rv-1928z CAR T cells, suggesting increase activation, likely due to tumor relapse (Figures 5.5c-d). CD27 levels were not significantly different between *SUV^{etd}* Rv-1928z CAR T and WT Rv-1928z CAR T cells at day 10 (Figures 5.5c-d). IL7Rα, a marker for memory phenotype in T cells, was elevated at both

day 10 and day 17 in *SUV*^{etd} Rv-1928z CAR T as compared to WT Rv-1928z CAR T cells (Figures 5.5c-d). Flow cytometry analysis of inhibitory receptor expression (PD1, LAG3, TIM3) at both day 10 and day 17 showed a slight decrease in PD1 expression at day 10 in *SUV*^{etd} Rv-1928z CAR T as compared to WT Rv-1928z CAR T cells (Figures 5.6a-b) but no significant differences otherwise (Figures 5.6a-c).

Single cell transcriptional analysis reveals *SUV39H1* editing limits effector differentiation, enhances memory phenotype and improves clonal diversity

We performed single cell transcriptional analysis on *SUV*^{etd} Rv-1928z CAR T cells and WT Rv-1928z CAR T cells to characterize the effect of *SUV39H1* disruption on Rv-1928z CAR T cells (Figure 5.7a). We chose 3 time points for this analysis – pre-infusion in mice (day 0), 9 days post CAR T cell infusion and 16 days post CAR T cell infusion (Figure 5.7b). Across both genotypes and all 3 time points, we identified 16 sub-populations of CD4's and 11 sub-populations of CD8's (Figures 5.7b-d). As expected, the populations transition from naïve-like to effector over time (Figure 5.7e).

In line with the previously discussed CAR T cell quantification data, we find higher fraction of proliferating CAR T cells (both $CD4^+$ and $CD8^+$) in *SUV39H1*-edited group as compared to unedited group at day 9 (Figure 5.8a). Gene set enrichment analysis and differential gene expression analysis suggested reduced effector differentiation in *SUV*^{etd} Rv-1928z CAR T cells at both day 9 and day 16 (Figures 5.8b-e). We confirmed reduced cytokine secretion in

SUV^{etd} Rv-1928z CAR T as compared to WT Rv-1928z CAR T cells in an *in vitro* model of repeated CAR stimulation (Figures 5.9a-b). Strong effector differentiation leads to limited long-term persistence and function[107]. Therefore, we assessed the clonal diversity of CAR T cells by analyzing their TCRβ sequence. As expected, the pre-infusion population was quite diverse in both *SUV39H1*-edited and unedited groups leading to a TCRβ sequence capture of only a small fraction of the population (Figures 5.10a-b). However, at day 16, *SUV*^{etd} Rv-1928z CAR T cells display a higher clonal diversity as compared to WT Rv-1928z CAR T cells, suggestive of their superior fitness (Figures 5.10a-b). Mitochondrial capacity has been implicated in CAR T cell persistence[106]. This led us to assess glycolytic and mitochondrial function of *SUV*^{etd} Rv-1928z CAR T cells and WT Rv-1928z CAR T cells over time, under conditions of repeated CAR stimulation (Figure 5.11a). We did not find significant differences in mitochondrial capacity between *SUV*^{etd} Rv-1928z CAR T cells and WT Rv-1928z after 2 rounds of CAR stimulation (Figure 5.11b, left panel). However, *SUV*^{etd} Rv-1928z CAR T cells have improved mitochondrial function after 3rd and 4th round of CAR stimulation, suggestive of their improved cellular fitness (Figure 5.11b, middle and right panel). The glycolytic rates were not significantly different between WT and *SUV*^{etd} Rv-1928z CAR T cells (Figure 5.11c).

SUV39H1 disruption enhances the ability of Rv-1928z CAR T cells upon multiple rechallenges

SUV39H1 deficient CD8^{+} T cells demonstrated poor ability to eliminate *Listeria monocytogenes* infection upon rechallenge due to poor effector

differentiation[152]. To assess the ability of *SUV^{etd}* Rv-1928z CAR T cells to eliminate tumor upon rechallenge, we modified the previously discussed xenograft model such that mice are rechallenges with NALM6 multiple times (3-5 times, Figure 5.12a). In this setting, we found that *SUV^{etd}* Rv-1928z CAR T cells outperformed WT RV-1928z CAR T cells in their ability to reject tumor (Figures 5.12b-c). CAR T cell quantification in the bone marrow and spleen after 5 rounds of rechallenge showed increased CAR T cell numbers upon *SUV39H1* editing (Figure 5.12d). We also performed paired transcriptional and chromatin accessibility (ATACseq) analysis of WT and *SUV^{etd}* Rv-1928z CAR T cells that had undergone 3 rounds of rechallenge (Figure 5.12a). Transcriptional analysis revealed increased expression of memory associated transcription factors and receptors such as *TCF7*, *LEF1*, *CCR7* and *IL7R* in *SUV^{etd}* Rv-1928z CAR T cells as compared to WT Rv-1928z CAR T cells (Figure 5.12e). WT Rv-1928z CAR T cells expressed increased levels of effector/terminal-effector state associated transcription factors such as *TBX21*, *EOMES* and *PRDM1* (Figure 5.12e). Increased expression of various inhibitory receptors such as *PDCD1*, *LAG3*, *HAVCR2*, *CTLA4*, *CD38*, *KLRG1* And *TIGIT* was also observed in WT Rv-1928z CAR T cells (Figure 5.12e). Geneset enrichment analysis revealed increased enrichment of human T cell exhaustion associated genes in WT Rv-1928z CAR T cells (Figure 5.12f). ATACseq revealed increased global accessibility in *SUV^{etd}* Rv-1928z CAR T cells as compared to WT Rv-1928z CAR T cells, which is expected, given SUV39H1's role in mediating methylation at H3K9 and maintaining heterochromatin structure (Figure 5.12g). Interestingly, while global chromatin accessibility was higher in *SUV^{etd}* Rv-1928z CAR T cells, we observed reduced chromatin

accessibility of several inhibitory receptors and effector/terminal-effector state associated transcription factors in *SUV^{etd}* Rv-1928z CAR T cells as compared to WT Rv-1928z CAR T cells (Figure 5.12h). We confirmed some of these findings by flow cytometry in CAR T cells that had undergone 5 rounds of stimulation (over 70 days post infusion in mice, Figures 5.13a-b). Motif analysis of genes that were upregulated in *SUV^{etd}* Rv-1928z as compared to WT Rv-1928z CAR T cells showed an enrichment of E2F motif (Figure 5.12i). E2F transcription factors are mediators of cellular proliferation[177]. Therefore, motif analysis in conjunction with the previously discussed single cell transcriptional analysis and CAR T cell quantification suggests increased proliferation in *SUV^{etd}* Rv-1928z CAR T cells under conditions of rechallenge. Motif analysis of genes that were downregulated in *SUV^{etd}* Rv-1928z as compared to WT Rv-1928z CAR T cells showed an enrichment of *TCF7 (*Protein TCF1)/*LEF1* motif (Figure 5.12j). TCF1 and LEF1 are homologous proteins that have both transcriptional activating and inhibitory domains[178]. TCF1/LEF1 have also been shown to remodel chromatin during T cell development[179]. TCF1/LEF1 repress transcriptional factors that mediate effector differentiation (*ID2*, *PRDM1*)[180] and inhibitory receptors (*PDCD1*, *LAG3*, *CTLA4*)[178] and are in turn inhibited by effector state associated transcription factors[181] and effector cytokines[181,182]. With the context of transcriptional and chromatin accessibility analysis, enrichment of *TCF7*/*LEF1* motif in genes that are downregulated in *SUV^{etd}* Rv-1928z CAR T cells suggests that the increased expression of *TCF7* and *LEF1* in *SUV^{etd}* Rv-1928z results in suppression of terminal effector differentiation of *SUV^{etd}* Rv-1928z CAR T cells allowing for increased CAR T cell proliferation and persistence leading to improved tumor control.

Discussion

In this chapter we show that the disruption of *SUV39H1* in Rv-1928z CAR T cells enhances their anti-tumor efficacy. Disruption of *SUV39H1* in human T cells leads to significant reduction of global H3K9me3 levels as early as 5 days post *SUV39H1* editing. *SUV^{etd}* Rv-1928z CAR T cells have reduced cytokine secretion as compared to WT Rv-1928z CAR T cells. However, the differences in cytokine secretion disappear after repeated CAR stimulation. Several reports have identified metabolic changes associated with different cytokines[183]. Memory T cells rely on fatty acid oxidation (FAO) while effector T cells favor glycolysis[184]. Although early metabolic features are indistinguishable in unedited and *SUV^{etd}* Rv-1928z CAR T cells. Over time, *SUV^{etd}* Rv-1928z CAR T cells display improved mitochondrial capacity while maintaining similar glycolytic rate as unedited Rv-1928z CAR T cells. Whether these late-stage metabolic differences are due to differences in cytokine secretion or due to continued expression of memory associated transcription factors needs to delineated.

SUV39H1 editing enhances early and late Rv-1928z CAR T cell numbers. Single cell transcriptional analysis reveals improved late-stage clonal diversity of *SUV^{etd}* Rv-1928z CAR T cells. Several studies have shown that *SUV39H1* and other histone methyl transferases interact with E2F transcription factors through their association with retinoblastoma (*RB1*) during cell cycle which leads to deposition of H3K9me3 marks on E2F target genes such as CyclinE and CyclinA2 resulting in their silencing[185,186]. As a result, CyclinE and CyclinA2 activity are elevated in *SUV39H1* null fibroblast[186]. Whether similar processes

are happening in CAR T cells needs to be studied. Single cell transcriptional analysis also shows that only a few CAR T cell sub-populations show enhanced cell cycle signature in the *SUV39H1*-edited group as compared to unedited group. Why *SUV39H1* disruption only affects proliferation in specific subpopulations of CAR T cells is intriguing and warrants further study?

The effect of *SUV39H1* editing on cytokine secretion and proliferation of Rv-1928z CAR T cells is similar to the effect of mutation of the two distal ITAM domains of the CD3z in the 1928z CAR, termed the Rv-1928z-1xx CAR[107]. Like *SUV^{etd}* Rv-1928z, Rv-1928z-1xx CAR outperforms the Rv-1928z CAR in both, *in vivo* anti-tumor efficacy at limiting CAR T cell dose and under repeated *in vivo* tumor rechallenges. Both *SUV^{etd}* Rv-1928z and Rv-1928z-1xx CAR T cells allow for durable tumor control at a dose where Rv-1928z CAR treated mice begin to relapse after early tumor control. However, there is one significant difference when comparing the *in vivo* performance of *SUV^{etd}* Rv-1928z and 1xx CAR with Rv-1928z CAR T cells. The primary tumor control between *SUV^{etd}* Rv-1928z and Rv-1928z CAR T cells is very similar. However, Rv-1928z-1xx has a slower kinetics of primary tumor control as compared to Rv-1928z CAR T cells[107].

CARs (Ex: Rv-19BBz, Rv-1928z-1xx) that have weaker effector differentiation than Rv-1928z, have a higher threshold for antigen levels on target cells to mediate cytolysis[96,104,187]. The effect of *SUV39H1* editing on Rv-1928z antigen recognition sensitivity is an area of future study.

SUV39H1 deficient murine transgenic OT-1 $CD8^+$ T cells show similar primary control of *Listeria monocytogenes* infection as compared to WT OT-1 $CD8^+$ T cells[152]. However, upon rechallenge with *Listeria monocytogenes*, SUV39H1 deficient $CD8^+$ T cells fail to elicit effective effector response[152]. In contrast, *SUV^{etd}* Rv-1928z CAR T cells show an improved ability to reject tumor upon multiple rechallenges as compared to WT Rv-1928z CAR T cells. This difference in phenotype can be due to two reasons – 1) Differences in murine and human T cell biology. 2) Differences in CAR T cell and T cell effector function upon rechallenge. As was discussed in the *TET2* study, Rv-1928z CAR T cells have a very potent effector function. Therefore, it is possible that SUV39H1 deficiency in Rv-1928z CAR T cells allows of residual effector function that can still effectively eliminate tumor upon rechallenge. *TCF7* expression has been identified as a marker in T cells that respond to checkpoint blockade in murine chronic viral infection model[188] as well as in human melanoma[141]. Further evidence of role of *TCF7/LEF1* expression in limiting exhaustion in *SUV^{etd}* Rv-1928z CAR T cells comes from GSEA analysis showing enrichment of gene signature associated with non-responders to checkpoint blockade[141] in unedited Rv-1928z CAR T cells. Therefore, it appears that *SUV39H1* editing in Rv-1928z CAR T cells tunes their effector function such that it allows for continued tumor rejection while maintaining proliferative abilities. Whether *SUV39H1* editing will enhance the anti-tumor efficacy of T cell expressing other CAR designs that differ in their effector function and proliferative properties from retrovirally encoded CD28-CAR still needs to be determined.

In summary we find that *SUV39H1* editing enhances the anti-tumor efficacy of Rv-1928z CAR T cells by enhancing their proliferation, persistence and limiting the onset of exhaustion due to continued expression of memory transcription factors, particularly *TCF7* and *LEF1*.

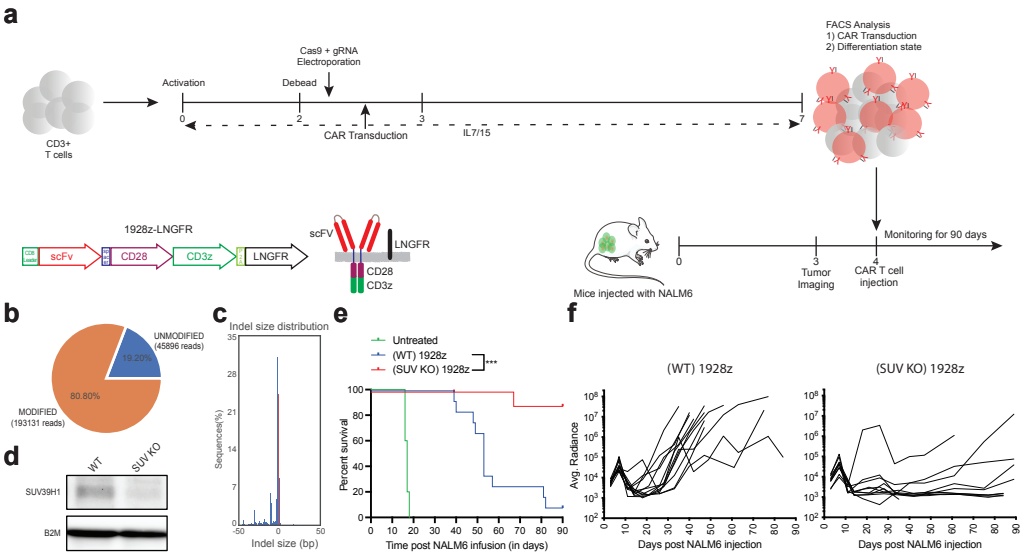

Figure 5.1:*SUV39H1* disruption improves anti-tumor efficacy of Rv-1928z CAR T cells. **a,** Schematics of CAR T cell generation protocol and murine NALM6 model. **b-c,** gRNA editing efficiency (**b**) and indel distribution (**c**). **d,** Western blot showing *SUV39H1* disruption at protein level (**d**). **e-f,** Mice survival (**e**) and tumor radiance (**f**) under Rv-1928z (dose: 1e5, n=5 for untreated, n=12 for WT, and n=10 for *SUV39H1*-edited) CAR T cell treatment. p values were determined through log-rank Mantel–Cox test (**e**).

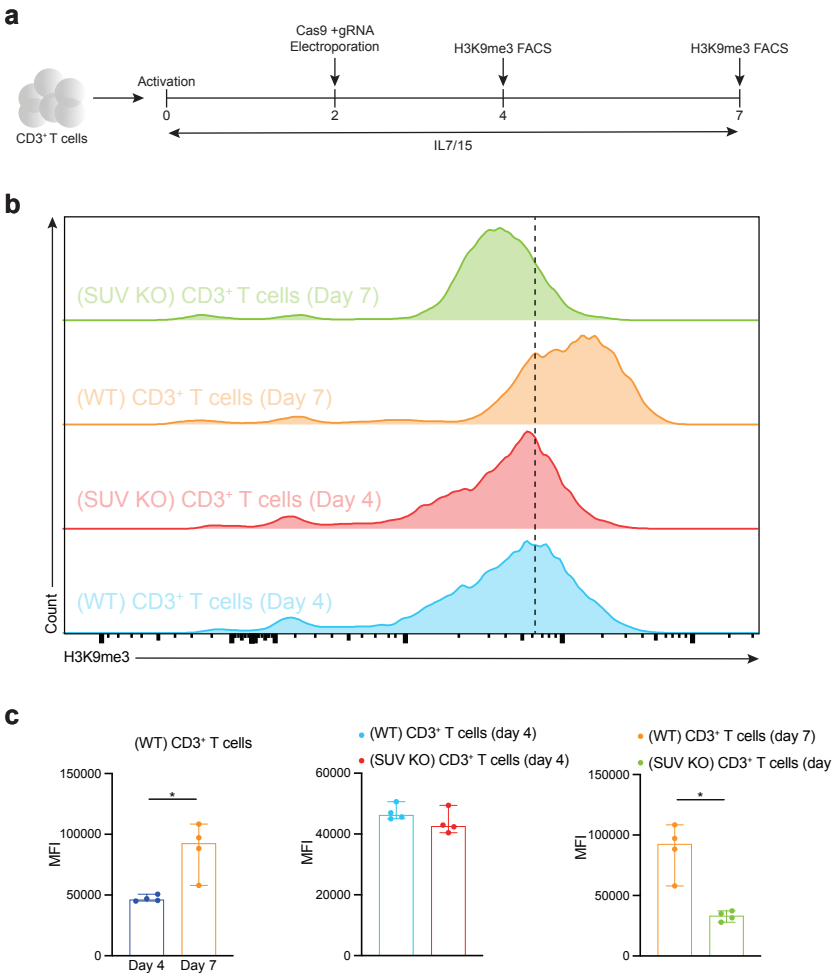

Figure 5.2: *SUV39H1* disruption reduces global H3K9me3 levels in T cells.
a, Schematics of H3k9me3 FACS assay, **b,** Representative H3K9me3 flow data for each time point. **c,** Summary data from two replicates per donor (2 donors). p values were determined by Mann-Whitney (**c**).

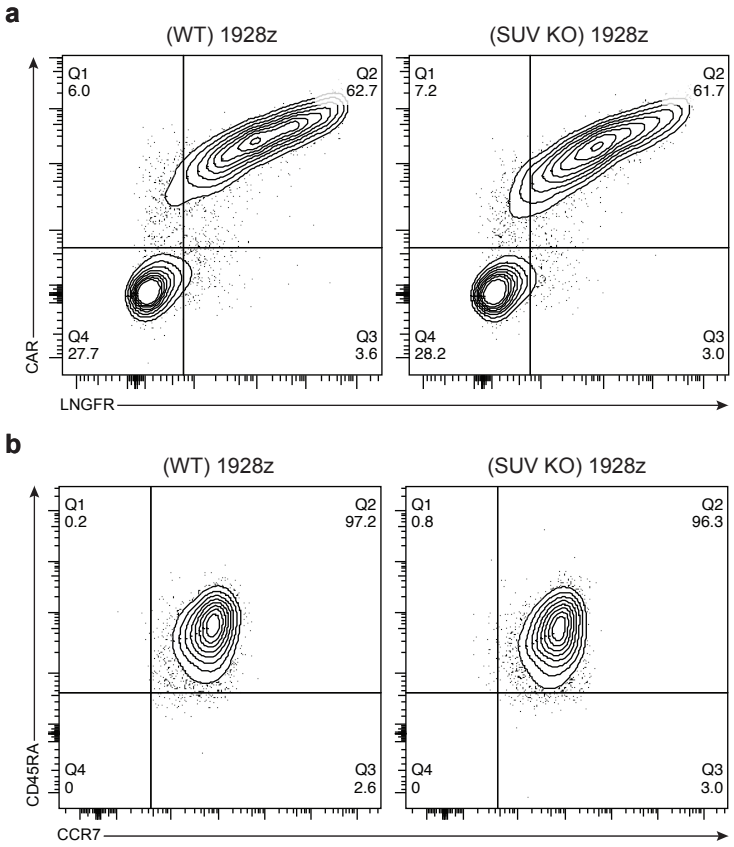

Figure 5.3: Pre-infusion CAR transduction efficiency and differentiation profile.
a-b, Pre-infusion CAR transduction efficiency (**a**) and CAR T cell differentiation profile (**b**) of (WT) and (SUVKO) Rv-1928z CAR T cells.

a

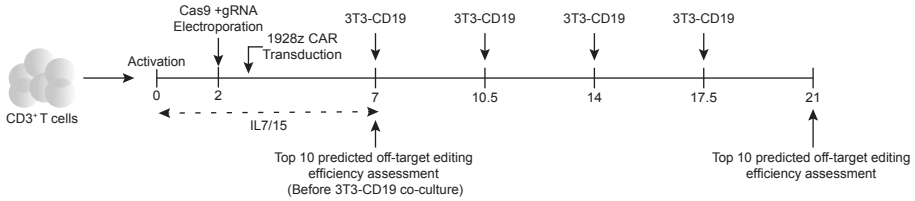

b

OT1- GCTGCAGGACCCGCGCCGCC

OT2- GCTGCAGGACCTGTGCTCCC

OT3- GCTGCAGGACCTGAGCAGTC

OT4- GCTGCAGGGCCTCTGCCGGC

OT5- GCTGCAGGACCTGGGCCTCT

OT6- GCTGGAGGAACTGTGACGCC

OT7- GCTGCAGGAGCTGGGCCTCC

OT8- CCTGCAGGACCTCTGCTGCC

OT9- GCTGCAGGAGCTGTGTCACC

OT10- GCTGCAGGCCCTGTGTCACC

c

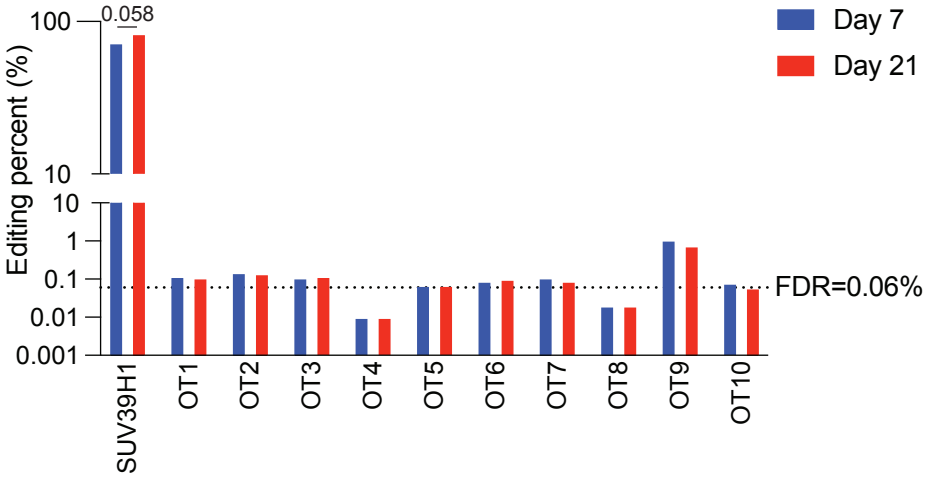

Figure 5.4: Off-target editing of the *SUV39H1* gRNA.
a, Schematics of the assay design for assessing gRNA editing efficiency. **b,** Top 10 predicted off-target sites. Mismatches are highlighted in red. **c,** Editing efficiencies at day 7 (before CAR stimulation) and at day 21 (after 4 rounds of CAR stimulation).p values were determined through $\chi 2$ test (**c**).

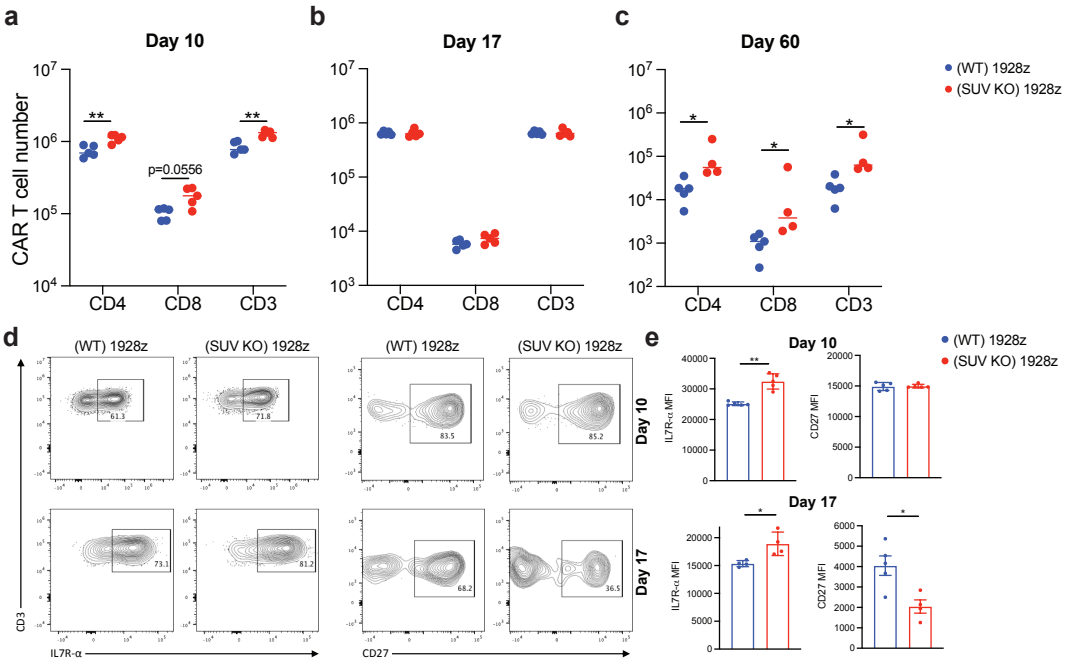

Figure 5.5: *SUV39H1* disruption enhances early 1928z CAR T cell proliferation and persistence.

a-c, CAR T cell quantification in the bone marrow at day 10 **(a)**, day 17 **(b),** and day 60 **(c).** (n=4-5 group for each day). **d,** Representative CAR T cell IL7R-α (Left) and CD27 (Right) flow cytometry plots at day 10 (Top panel) and day 17 (Bottom panel). **e,** Summary data for IL7R-α and CD27 flow cytometry plot replicates. p values were determined by Mann-Whitney (**a-c, e**)

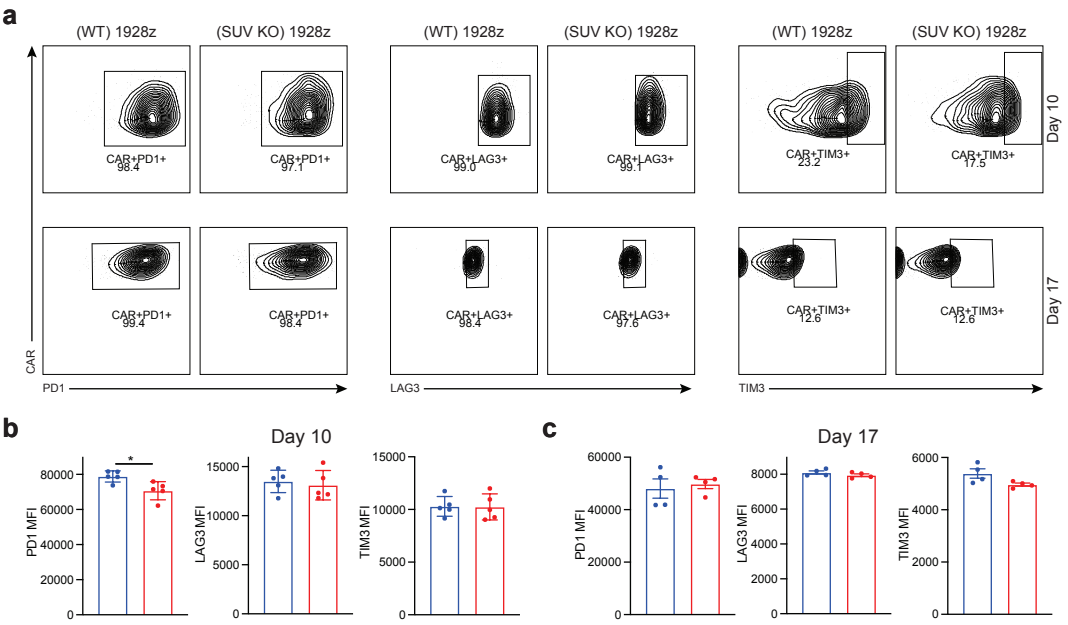

Figure 5.6: CAR T cell inhibitory receptor expression.
a, Representative CAR T cell PD1, LAG3, TIM3 flow cytometry plots at day 10 (Top panel) and day 17 (Bottom panel). **b-c,** Summary data for PD1, LAG3, TIM3 flow cytometry plot replicates at day 10 (**b**) and day 17 (**c**). Data is represented as mean±SD (**b,c**). p values were determined by Mann-Whitney (**b**).

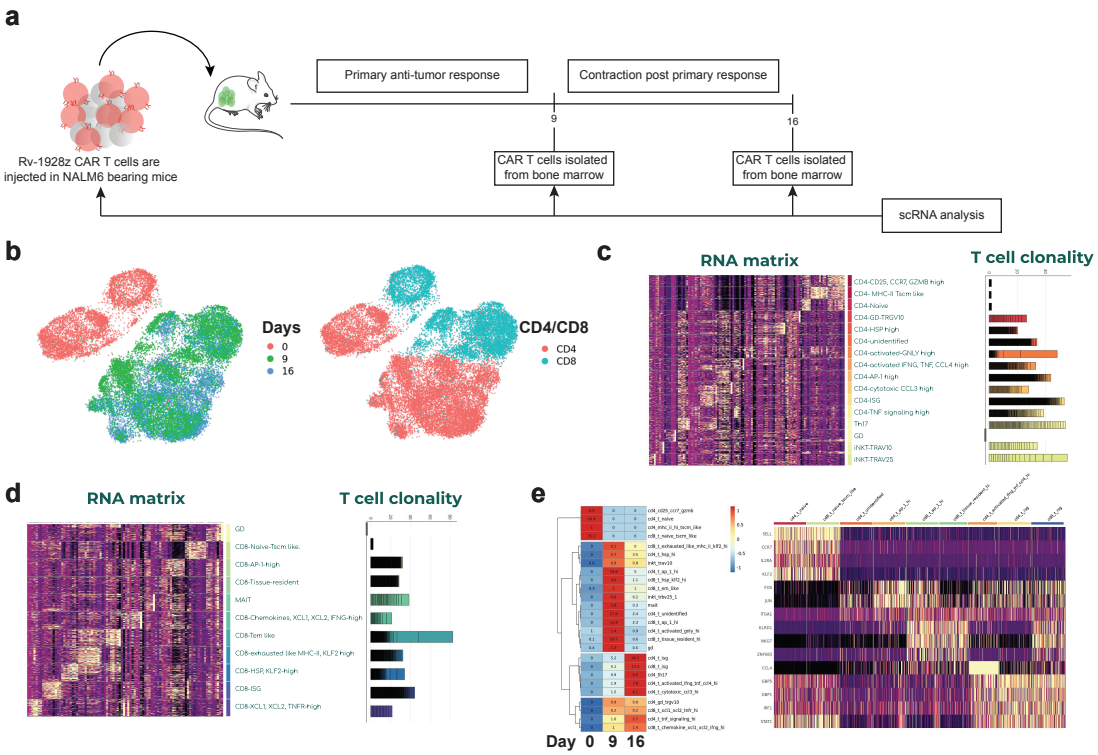

Figure 5.7: Single cell transcriptional profiling of CAR T cells.
a, Design of single cell transcriptional profiling. Single cell RNA sequencing was performed at three time points: Pre-infusion (day 0), day 9, and day 16. **b,** Uniform Manifold Approximation and Projection (UMAP) for all three time points (Left panel) and CD4's and CD8's (Right panel). **c,d** Sub-populations of CD4's (**c**) anf CD8's (**d**) identified through single cell profiling. **e,** Changes in population composition over time (Left panel, **e**) and gene expression associated with sub-populations (Right panel, **e**)

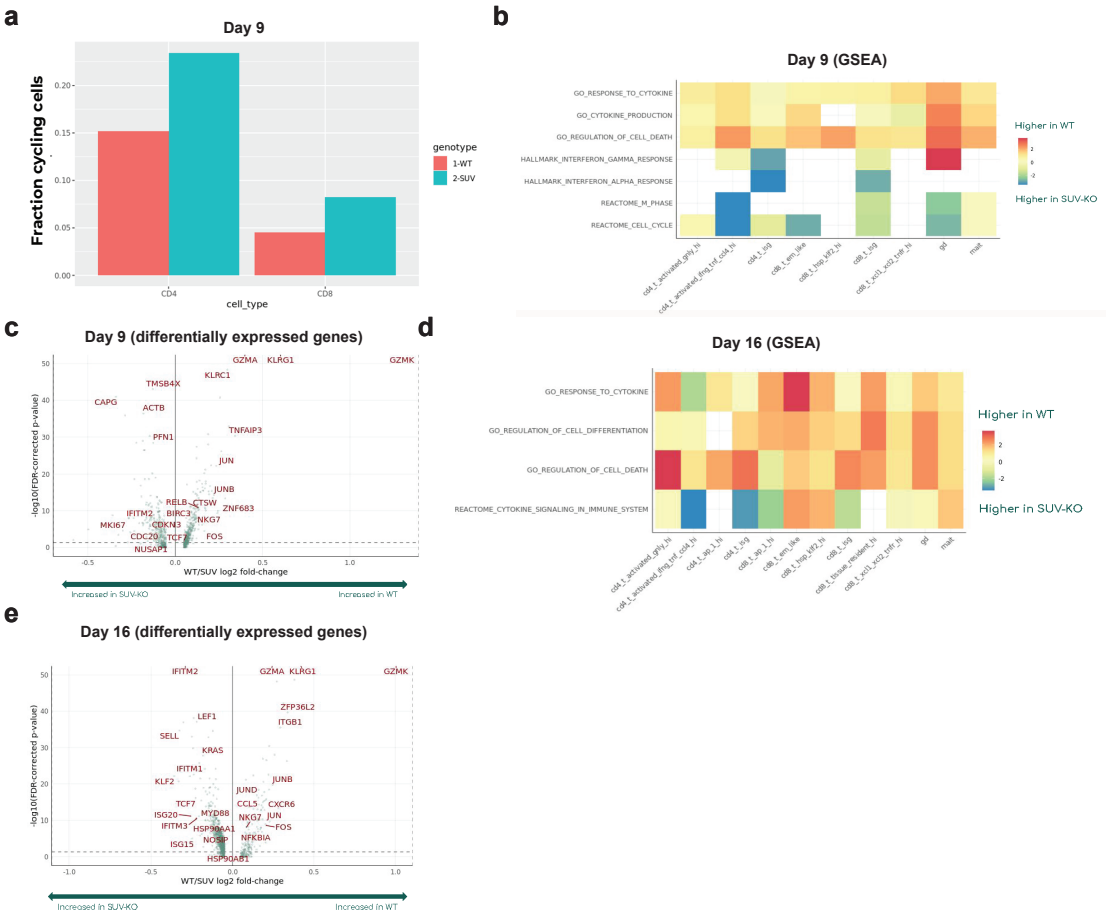

Figure 5.8: Increased proliferation and reduced effector function in Rv-1928z CAR T cells upon *SUV39H1* disruption.

a, Frequency of cycling cells at day 9 between unedited and *SUV39H1*-edited Rv-1928z CAR T cells. **b,** GSEA analysis at day 9. **c,** Differentially expressed genes between unedited and *SUV39H1*-edited Rv-1928z CAR T cells at day 9. **d,** GSEA analysis at day 16. **c,** Differentially expressed genes between unedited and *SUV39H1*-edited Rv-1928z CAR T cells at day 16.

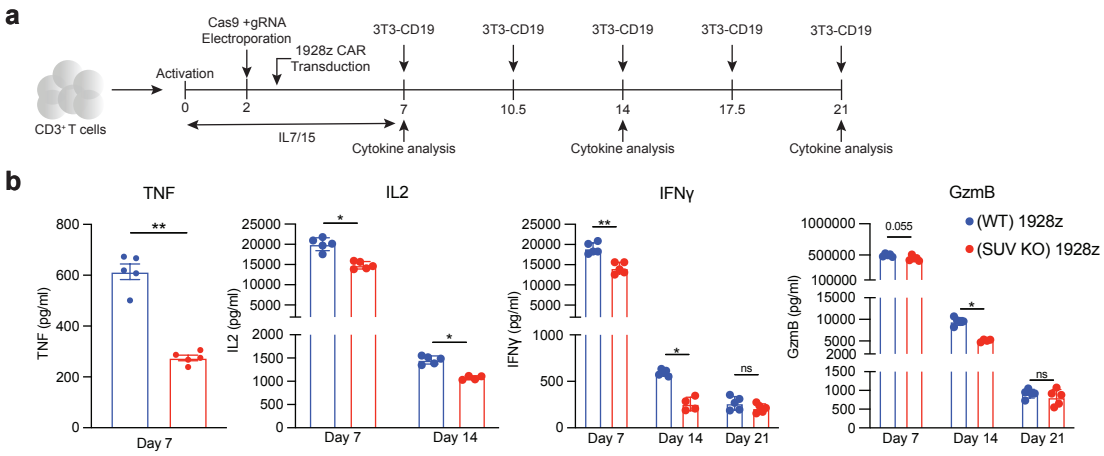

Figure 5.9: Cytokine secretion upon repeated CAR stimulation.
a, Schematics of repeated CAR stimulation assay. Cytokines were measured in the media 24 hours after co-culture with target cells at indicated time points (**a**). **b,** Cytokine quantification for unedited and *SUV39H1*-edited Rv-1928z CAR T cells. TNF was below assay detection limit at day 14 and day 21 while IL2 was below detection limit at day 21. Data is represented as mean±SD (**b**). p values were determined by Mann-Whitney (**b**).

a

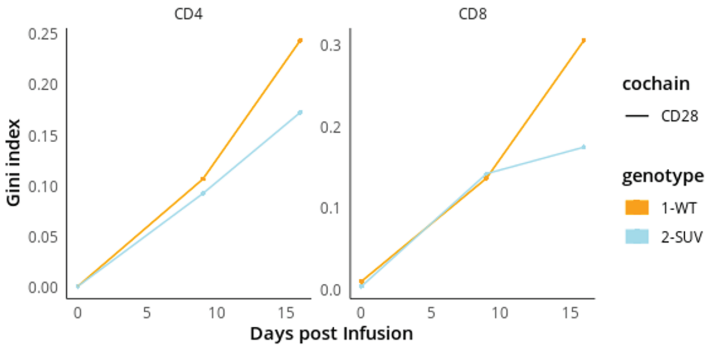

b

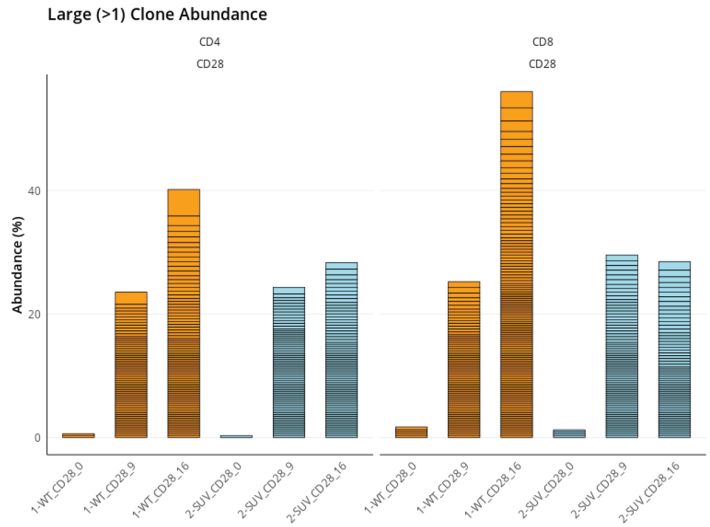

Figure 5.10: *SUV39H1*-editing enhances clonal diversity of Rv-1928z CAR T cells. **a,** Progression of Gini index over time. Gini index is reflective of “inequality” of TCRs in a given population. The lower the index, higher is the diversity. **b,** Distribution of large clones (Clone size>1) at day 0, 9, and 16 between unedited and *SUV39H1*-edited Rv-1928z CAR T cells.

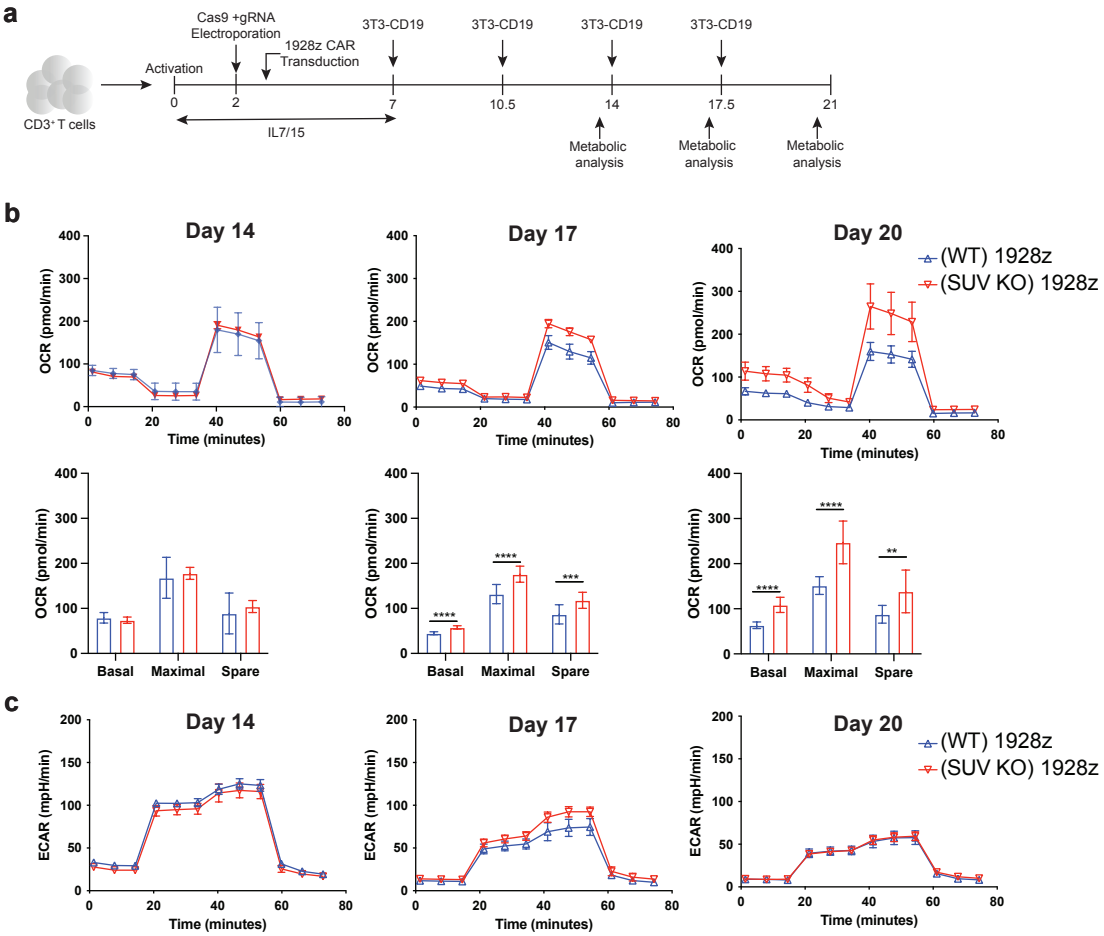

Figure 5.11: Metabolic assessment of unedited and *SUV39H1*-edited CAR T cells under conditions of repeated stimulation.

a, Schematics of repeated CAR stimulation assay. Oxygen consumption rate (OCR, **b**) and extra cellular acidification rate (ECAR,**c**) were measured three days CAR stimulation. **b-c,** OCR **(b)** and ECAR **(c)** rates of unedited and *SUV39H1*-edited Rv-1928z CAR T cells were assessed at the indicated time points. Data is represented as mean±SD (**b, c**). p values were calculated by unpaired t-test (**b**).

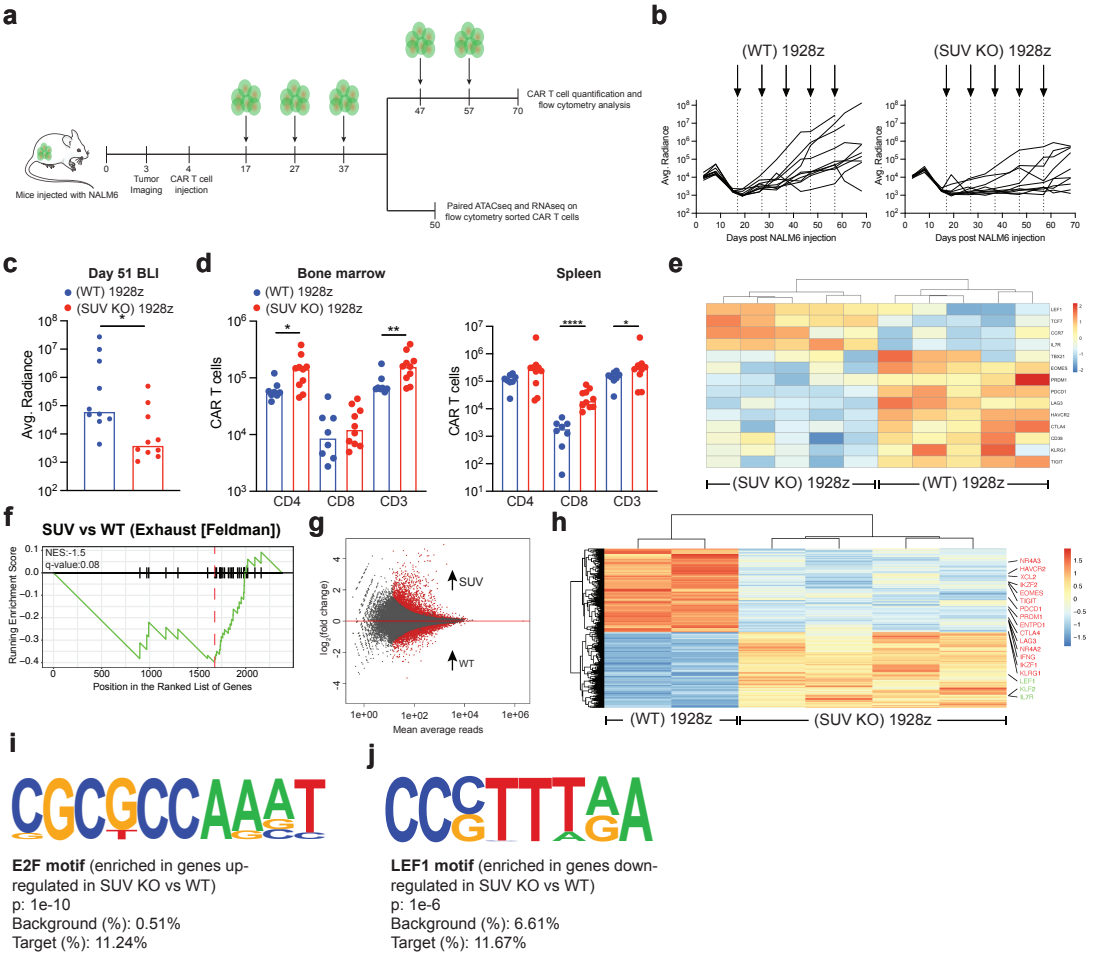

Figure 5.12: *SUV39H1*-editing enhances the ability of Rv-1928z CAR T cells to reject tumor upon multiple rechallenges.

a, Design of the rechallenge study. Mice were treated with 2e5 Rv-1928z CAR T cells. Tumor rechallenge was done with 2e6 NALM6. **b,** Tumor radiance over time. Tumor rechallenge is indicated by arrowheads. **c,** Comparing tumor radiance between unedited and *SUV39H1*-edited Rv-1928z CAR T cells at day 51 (last time point [tumor radiance measurement] when all unedited Rv-1928z CAR T cells are alive). **d,** CAR T cell quantification in bone marrow and spleen. **e,** RNAseq heatmap of memory, effector, and inhibitory receptor genes. **f,** GSEA showing enrichment of human T cell exhaustion signature in unedited Rv-1928z CAR T cells. **g,** Mean average plot (ATACseq). Red dots are peaks with p_{adj}<0.1. **h,** ATACseq heatmap, most significant peak associated with memory, effector, and inhibitory receptor genes is highlighted. **i,j** Motif enrichment analysis identifies E2F motif (**i**) enriched in genes up-regulated in *SUV39H1*-edited Rv-1928z CAR T cells and LEF1 motif (**j**) in genes down-regulated in *SUV39H1*-edited Rv-1928z CAR T cells. p values were determined by Mann-whitney (**c,d**)

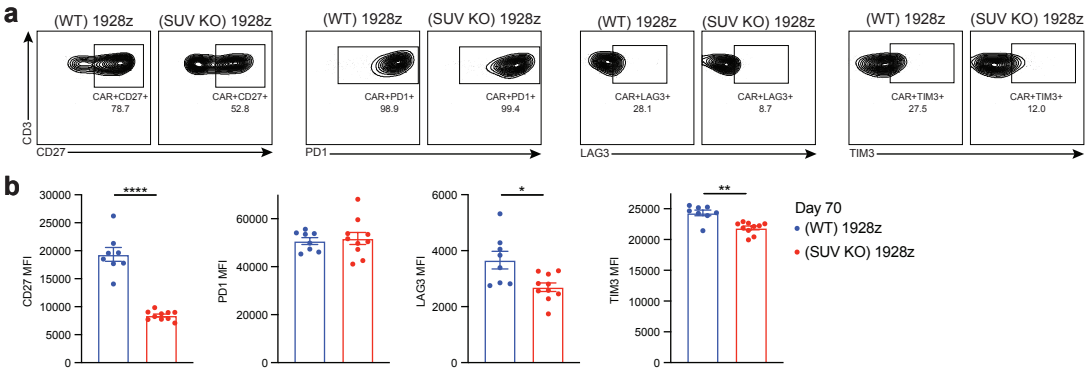

Figure 5.13: Activation and inhibitory receptor expression in CAR T cells after repeated tumor rechallenge.

a, Representative CAR T cell CD27, PD1, LAG3, TIM3 flow cytometry plots at day 70. **b,** Summary data for CD27, PD1, LAG3, TIM3 flow cytometry plot replicates at day 70. Data is represented as mean±SD (**b**). p values were determined by Mann-Whitney (**b**)

CHAPTER 6

Concluding Remarks

This thesis describes the effects of disruption of epigenetic factors, *TET2* and *SUV39H1*, in T cells expressing different CAR designs. We find that the CAR properties determine whether a T cell would gain enhanced anti-tumor properties upon *TET2* disruption. The CAR also determines the frequency with which a clone would enter an antigen independent hyper-proliferative state. These observations highlight the need to consider the nature of CAR properties into devising engineering strategies to improve their function. Improving CAR T cell therapy for a particular tumor type can involve several different parameters, some T cell extrinsic such as tumor-cell death programs, tumor microenvironment, access to tumor site among others. Others require optimizing elements of T cell biology such as proliferation, persistence, effector function, resistance to immune inhibitory mechanisms, and antigen sensitivity. The above-mentioned properties of T cells are inextricably linked to one another, modulating one will inevitably have consequences on the other. For example, Rv-1928z CAR T cells have strong effector function and exquisite antigen sensitivity as compared to Rv-19BBz CAR T cells that allows them to eliminate low antigen expressing tumors[96]. However, Rv-1928z CAR T cells have limited persistence which may lead to tumor relapse[107]. As a result, the likelihood of success with one size fits all approach in engineering next generation of improved CAR therapies is low. A more deliberate approach considering the constraints imposed by both T cell intrinsic and extrinsic factors

and engineering approaches to overcome those limitations is more likely to succeed.

Another important takeaway from our *TET2* study is the often-overlooked element of safety while engineering potent CAR T cell therapies. While T cells appear to be intrinsically resistant to transformation[44], multiple clonal expansions in patients receiving CAR T cells have been reported[42,81,189]. While none of the clonal CAR T cell expansions have been lethal, there is a risk of pathogenicity as we continue to engineer more potent CAR therapies. It is therefore important to develop pre-clinical models and frameworks to assess risk of new CAR engineering approaches.

Pre-clinical modeling of CAR T cell therapy is inherently difficult – working with human T cells necessitates use of immune deficient mouse models. On the other hand, syngeneic murine models require working with murine T cells. In fact, CRS, the most significant toxicity associated with CAR T cell therapy was not observed in the early pre-clinical CAR T cell models. Nevertheless, most CAR T cell studies focus on anti-tumor efficacy in murine models over relatively short duration (<50 days). Therefore, there is a danger of missing out on toxicities that become evident only after a long time. We anticipate that the use of curative CAR T cell doses to assess long-term monitoring, along with clone tracking, retroviral integration site analysis, and exome analysis will provide a framework to study safety of CAR T cells in a pre-clinical setting.

The effects of *SUV39H1* disruption on Rv-1928z CAR T cells highlights the potential of epigenetic engineering strategies to affect T cell phenotype even under the influence of potent CAR designs. It further highlights the importance of choosing the right engineering strategy to improve the deficiencies of a particular CAR design. While *SUV39H1*-edited Rv-1928z CAR T cells have reduced effector function, they appear to compensate for reduced effector function by displaying enhanced proliferation that allows for indistinguishable primary anti-tumor response when compared to unedited Rv-1928z CAR T cells. Post-primary tumor clearance, *SUV39H1*-edited Rv-1928z CAR T cells outperform unedited Rv-1928z CAR T cells in maintaining durable remission as well as in eliminating tumor upon rechallenge.

Future Perspectives

The results discussed in this thesis on *TET2* and *SUV39H1* disruption in CAR T cells highlights the power of epigenetic programming in affecting CAR T cell function and the need to carefully evaluate the long-term consequences of applying these methodologies in CAR T cells. The current work is limited to a snapshot of an epigenetic state that is ultimately achieved in *TET2* and *SUV39H1* deficient CAR T cells, but we do not know the intermediate states that eventually culminate in the described epigenetic state for both TET2 and SUV39H1 deficient CAR T cells in this study. Furthermore, the transcriptional and epigenetic analysis in this thesis for *TET2* and *SUV39H1* was limited to Rv-1928z+41BBL and Rv-1928z CAR T cells respectively. Therefore, there is a need to extend this analysis to other CAR designs to identify similarities and differences owing to CAR design. In the case of *TET2* study, we are conducting

experiments to test the role of *BATF3* more directly in driving the proliferation of TET2-deficient CAR T cells. While biallelically edited *TET2* CAR T cells enter a state of antigen independent expansion, a strategy in which *TET2* disruption (but not total elimination) might result in improved CAR T cell efficacy without the risk of antigen independent expansion might still be possible and needs further exploration. For *SUV39H1* study, we are conducting experiments to ascertain the role of candidate transcription factors in mediating improved proliferation and persistence of Rv-1928z CAR T cells. The role of H3K9me3 in silencing of memory associated transcription factors has also still not been conclusively established.

Another avenue for research is in the solid tumor model system, especially in the context of *SUV39H1* editing. Solid tumors are generally associated with chronic T cell activation due to restricted access of T cells to tumors (Sterner et al., 2021). *SUV39H1* editing by allowing for continued expression of memory factors in CAR T cells under conditions of chronic activation might enable T cell to maintain their effector function and eliminate the tumor.

Both, *TET2* and *SUV39H1*, were evaluated by disrupting these genes individually and studying their effect on CAR T cells. With the advent of CRISPR/Cas9 technology, it has become possible to perform genome wide pooled screens to identify factors that, when disrupted, will lead to improved T cell function. These strategies have already been applied to CAR T cells[135,136], but a lot remains to be explored regarding modeling different clinical scenarios. Another approach is to over-express a library of genes in conjunction with CAR

to identify factors that improve CAR function. Recently, a report by Legut et al. employing this approach to identify lymphotoxin-β receptor (LTBR) as a receptor that improves CAR T cell function was published[191]. As with knock out screens, over-expression screens in CAR T cells have only just been explored. Co-opting these strategies to identify epigenetic regulators of CAR T cell function is likely to be an interesting area of future study.

Patient monitoring and retrospective analysis of CAR T cells have also yielded new insights into CAR T cell biology. *TET2* was identified by integration site analysis during clonal expansion of CAR T cells[42]. Similar analyses have also identified insertional mutagenesis of other genes resulting in clonal expansions such as transforming growth factor-beta receptor type 2 (*TGFBR2*)[189], neural EGFL like 2 (*NELL2*), and glucocorticoid-induced transcript 1 protein (*GLCCI1*)[192]. Concurrently, transcriptional, and epigenetic profiling technologies are being employed to characterize CAR T cells in patients to understand changes in their cell state and their associations with patient response[81,90,91,143]. Understanding relationships between CAR T cell state and patient response will provide us with insights into engineering next generation of CAR therapies.

APPENDIXES

1) Figure1.1 is adapted under license from the template “Stem cell differentiation from bone marrow” by BioRender (2022, https://biorender.com/).
2) Figure1.2 is adapted under license from the template “T-Cell Development in Thymus” by BioRender (2022).
3) Figure 1.3 was created with BioRender (2022).

BIBLIOGRAPHY

1) Rothschild, B.M., Tanke, D.H., Helbling, M., and Martin, L.D. (2003). Epidemiologic study of tumors in dinosaurs. Naturwissenschaften *90*, 495–500.
2) Faguet, G.B. (2015). A brief history of cancer: Age-old milestones underlying our current knowledge database. Int. J. Cancer *136*, 2022–2036.
3) Siegel, R.L., Miller, K.D., Fuchs, H.E., and Jemal, A. (2022). Cancer statistics, 2022. CA. Cancer J. Clin. *72*, 7–33.
4) Balkwill, F., and Mantovani, M. (2001). Inflammation and cancer: back to Virchow?
5) Coley, W.B. (1891). II. Contribution to the Knowledge of Sarcoma. Annals of Surgery
6) Wang, D., Wei, X., Kalvakolanu, D. V., Guo, B., and Zhang, L. (2021). Perspectives on Oncolytic Salmonella in Cancer Immunotherapy—A Promising Strategy. Front. Immunol. *12*, 1–17.
7) McCarthy, E.F. (2006). The toxins of William B. Coley and the treatment of bone and soft-tissue sarcomas. Iowa Orthop. J. *26*, 154–158.
8) Janeway's Immunobiology, Ninth Edition. 2016. Garland Science: New York, New York. ISBN: (Paperback) 978-0815345053. 2016.
9) Abel, A.M., Yang, C., Thakar, M.S., and Malarkannan, S. (2018). Natural killer cells: Development, maturation, and clinical utilization. Front. Immunol. *9*, 1–23.
10) Spits, H. (2002). Development of αβ T cells in the human thymus. Nat. Rev. Immunol. *2*, 760–772.
11) Radtke, F., Wilson, A., Stark, G., Bauer, M., Van Meerwijk, J., MacDonald, H.R., and Aguet, M. (1999). Deficient T cell fate specification in mice with an induced inactivation of Notch1. Immunity *10*, 547–558.
12) Radtke, F., Wilson, A., Stark, G., Bauer, M., Van Meerwijk, J., MacDonald, H.R., and Aguet, M. (1999). Deficient T cell fate specification in mice with an induced inactivation of Notch1. Immunity *10*, 547–558.
13) Zhao, Y., Niu, C., and Cui, J. (2018). Gamma-delta (γδ) T Cells: Friend or Foe in Cancer Development. J. Transl. Med. *16*, 1–13.
14) Littman, D.R. (2016). How Thymocytes Achieve Their Fate. J. Immunol. *196*, 1983–1984.
15) Carlson, C.M., Endrizzi, B.T., Wu, J., Ding, X., Weinreich, M. a, Walsh, E.R., Wani, M. a, Lingrel, J.B., Hogquist, K. a, and Jameson, S.C. (2006). Kruppel-like factor 2 regulates thymocyte and T-cell migration. Nature *442*, 299–302.
16) Zhang, Z., Lu, M., Qin, Y., Gao, W., Tao, L., Su, W., and Zhong, J. (2021). Neoantigen: A New Breakthrough in Tumor Immunotherapy. Front. Immunol. *12*, 1–9.
17) Nathanson, L. (1976): Spontaneous regression of malignant melanoma: a review of the literature on incidence, clinical features, and possible mechanisms: conference on spontaneous regression of cancer. Natl. Cancer Inst. Monogr. 44:67, 1976.
18) Mackensen, A., Ferradini, L., Carcelain, G., et al. (1993). Evidence for in situ amplification of cytotoxic T-lymphocytes with antitumor activity in a human regressive melanoma. Cancer Res. 53:3569, 1993

19) Halliday, G.M., Patel, A., Hunt, M.J., Tefany, F.J., and Barnetson, R.S.C. (1995). Spontaneous regression of human melanoma/nonmelanoma skin cancer: Association with infiltrating CD4+ T cells. World J. Surg. *19*, 352–358.
20) Brunet, J.F., Denizot, F., Luciani, M.F., Roux-Dosseto, M., Suzan, M., Mattei, M.G., and Golstein, P. (1988). A new member of the immunoglobulin superfamily-CTLA-4. Nature *328*, 267–270.
21) Ishida, Y., Agata, Y., Shibahara, K., and Honjo, T. (1992). Induced expression of PD-1, a novel member of the immunoglobulin gene superfamily, upon programmed cell death. EMBO J. *11*, 3887–3895.
22) Zappasodi, R., Merghoub, T., and Wolchok, J.D. (2018). Emerging Concepts for Immune Checkpoint Blockade-Based Combination Therapies. Cancer Cell *33*, 581–598.
23) Waldman, A.D., Fritz, J.M., and Lenardo, M.J. (2020). A guide to cancer immunotherapy: from T cell basic science to clinical practice. Nat. Rev. Immunol. *20*, 651–668.
24) Nadler SH, Moore GE. (1969). Immunotherapy of malignant disease. Arch. Surg. 99:376–81
25) Santos GW. (1979). Bone marrow transplantation. Adv. Intern. Med. 24:157–82
26) Sadelain, M. (2017). Chimeric antigen receptors: A paradigm shift in immunotherapy. Annu. Rev. Cancer Biol. *1*, 447–466.
27) Allison JP, McIntyre BW, & Bloch D (1982) Tumor-specific antigen of murine T-lymphoma defined with monoclonal antibody. Journal of immunology (Baltimore, Md.: 1950) 129(5):2293–2300.
28) Rosenberg, S.A., Spiess., P., Lafreniere, R. (1986). A new approach to the adoptive immunotherapy of cancer with tumor-infiltrating lymphocytes. Science 233:1318–21
29) Kasid, A., Morecki, S., Aebersold, P., Cornetta, K., Culver, K., Freeman, S., Director, E., Lotze, M.T., Blaese, R.M., Anderson, W.F., et al. (1990). Human gene transfer: Characterization of human tumor-infiltrating lymphocytes as vehicles for retroviral-mediated gene transfer in man. Proc. Natl. Acad. Sci. U. S. A. *87*, 473–477.
30) Mavilio, F., Ferrari, G., Rossini, S., Nobili, N., Bonini, C., Casorati, G., Traversari, C., and Bordignon, C. (1994). Peripheral blood lymphocytes as target cells of retroviral vector-mediated gene transfer. Blood *83*, 1988–1997.
31) Bunnell, B.A., Muul, L.M., Donahue, R.E., Blaese, R.M., and Morgan, R.A. (1995). High-efficiency retroviral-mediated gene transfer into human and nonhuman primate peripheral blood lymphocytes. Proc. Natl. Acad. Sci. U. S. A. *92*, 7739–7743.
32) Gallardo, H.F., Tan, C., and Sadelain, M. (1997). The internal ribosomal entry site of the encephalomyocarditis virus enables reliable coexpression of two transgenes in human primary T lymphocytes. Gene Ther. *4*, 1115–1119.
33) Poznansky, M., Lever, A., Bergeron, L., Haseltine, W., and Sodroski, J. (1991). Gene transfer into human lymphocytes by a defective human immunodeficiency virus type 1 vector. J. Virol. *65*, 532–536.

34) Shimada, T., Fujii, H., Mitsuya, H., and Nienhuis, A. W. (1991) Targeted and highly efficient gene transfer into $CD4^+$ cells by a recombinant human immunodeficiency virus retroviral vector. *J. Clin. Invest.***88**, 1043–1047.
35) Corbeau P., Kraus G., Wong-Staal F. (1996). Efficient gene transfer by a human immunodeficiency virus type 1 (HIV-1)-derived vector utilizing a stable HIV packaging cell line. Proc Natl Acad Sci USA 1996.
36) Matsuoka, H., Miyake. K., Shimada, T. (1998). Improved methods of HIV vector mediated gene transfer. Int J Hematol 1998; 67: 267–273.
37) Wang, X., and Rivière, I. (2016). Clinical manufacturing of CAR T cells: Foundation of a promising therapy. Mol. Ther. - Oncolytics *3*, 16015.
38) Ellis, G.I., Sheppard, N.C., and Riley, J.L. (2021). Genetic engineering of T cells for immunotherapy. Nat. Rev. Genet. *22*, 427–447.
39) Hacein-Bey-Abina, S., Pai, S.-Y., Gaspar, H.B., Armant, M., Berry, C.C., Blanche, S., Bleesing, J., Blondeau, J., de Boer, H., Buckland, K.F., et al. (2014). A Modified γ-Retrovirus Vector for X-Linked Severe Combined Immunodeficiency. N. Engl. J. Med. *371*, 1407–1417.
40) Cartier N, Hacein-Bey-Abina S, Bartholomae CC, Veres G, Schmidt M, Kutschera I, et al. Hematopoietic stem cell gene therapy with a lentiviral vector in X-linked adrenoleukodystro- phy. Science. 2009;326:818–23.
41) Maldarelli F, Wu X, Su L, Simonetti FR, Shao W, Hill S, et al. HIV latency. Specific HIV integration sites are linked to clonal expansion and persistence of infected cells. Science. 2014;345:179–83.
42) Fraietta, J.A., Nobles, C.L., Sammons, M.A., Lundh, S., Carty, S.A., Reich, T.J., Cogdill, A.P., Morrissette, J.J.D., DeNizio, J.E., Reddy, S., et al. (2018). Disruption of TET2 promotes the therapeutic efficacy of CD19-targeted T cells. Nature *558*, 307–312.
43) Milone, M.C., and O'Doherty, U. (2018). Clinical use of lentiviral vectors. Leukemia *32*, 1529–1541.
44) Newrzela, S., Cornils, K., Li, Z., Baum, C., Brugman, M.H., Hartmann, M., Meyer, J., Hartmann, S., Hansmann, M., Fehse, B., et al. (2008). Resistance of mature T cells to oncogene transformation. *112*, 2278–2287.
45) Gogol-Doring, A., Ammar, I., Gupta, S., Bunse, M., Miskey, C., Chen, W., Uckert, W., Schulz, T.F., Izsvak, Z., and Ivics, Z. (2016). Genome-wide profiling reveals remarkable parallels between insertion site selection properties of the MLV retrovirus and the piggyBac transposon in primary human CD4+ T cells. Mol. Ther. *24*, 592–606.
46) Chicaybam, L. et al. CAR T cells generated using Sleeping Beauty transposon vectors and expanded with an EBV-transformed lymphoblastoid cell line display antitumor activity in vitro and in vivo. Human Gene Ther. 30, 511–522 (2019).
47) Roth, T.L., Puig-Saus, C., Yu, R., Shifrut, E., Carnevale, J., Li, P.J., Hiatt, J., Saco, J., Krystofinski, P., Li, H., et al. (2018). Reprogramming human T cell function and specificity with non-viral genome targeting. Nature *559*, 405–409.
48) Chandran, S.S., and Klebanoff, C.A. (2019). T cell receptor-based cancer immunotherapy: Emerging efficacy and pathways of resistance. Immunol. Rev. *290*, 127–147.

49) Van Den Berg, J.H., Gomez-Eerland, R., Van De Wiel, B., Hulshoff, L., Van Den Broek, D., Bins, A., Tan, H.L., Harper, J. V., Hassan, N.J., Jakobsen, B.K., et al. (2015). Case Report of a Fatal Serious Adverse Event Upon Administration of T Cells Transduced with a MART-1-specific T-cell Receptor. Mol. Ther. *23*, 1541–1550.
50) Johnson, L.A., Morgan, R.A., Dudley, M.E., Cassard, L., Yang, J.C., Hughes, M.S., Kammula, U.S., Royal, R.E., Sherry, R.M., Wunderlich, J.R., et al. (2009). Gene therapy with human and mouse T-cell receptors mediates cancer regression and targets normal tissues expressing cognate antigen. Blood *114*, 535–546.
51) Parkhurst, M.R., Yang, J.C., Langan, R.C., Dudley, M.E., Nathan, D.A.N., Feldman, S.A., Davis, J.L., Morgan, R.A., Merino, M.J., Sherry, R.M., et al. (2011). T cells targeting carcinoembryonic antigen can mediate regression of metastatic colorectal cancer but induce severe transient colitis. Mol. Ther. *19*, 620–626.
52) Kuwana, Y., Asakura, Y., Utsunomiya, N., Nakanishi, M., Arata, Y., Itoh, S., Nagase, F., and Kurosawa, Y. (1987). Expression of chimeric receptor composed of immunoglobulin-derived V resions and T-cell receptor-derived C regions. Biochem. Biophys. Res. Commun. 149, 960–968.
53) Gross, G., Waks, T., and Eshhar, Z. (1989). Expression of immunoglobulin-T-cell receptor chimeric molecules as functional receptors with antibody-type specificity. Proc. Natl. Acad. Sci. U. S. A. *86*, 10024–10028.
54) Brocker, T., Peter, A., Traunecker, A., and Karjalainen, K. (1993). New simplified molecular design for functional T cell receptor. Eur. J. Immunol. *23*, 1435–1439.
55) Brocker, T. (2000). Chimeric Fv-ζ or Fv-ε receptors are not sufficient to induce activation or cytokine production in peripheral T cells. Blood *96*, 1999–2001.
56) Krause, A, Guo, H.F., Latouche, J.B., Tan, C., Cheung, N.K., and Sadelain, M. (1998). Antigen-dependent CD28 signaling selectively enhances survival and proliferation in genetically modified activated human primary T lymphocytes. J. Exp. Med. *188*, 619–626.
57) Finney, H.M., Lawson, A.D., Bebbington, C.R., and Weir, A.N. (1998). Chimeric receptors providing both primary and costimulatory signaling in T cells from a single gene product. J. Immunol. *161*, 2791–2797.
58) June, C.H., Ledbetter, J. a, Gillespie, M.M., Lindsten, T., and Thompson, C.B. (1987). T-cell proliferation involving the CD28 pathway is associated with cyclosporine-resistant interleukin 2 gene expression. Mol.Cell.Biol. *7*, 4472–4481.
59) Chen, L., and Flies, D.B. (2013). Molecular mechanisms of T cell co-stimulation and co-inhibition. Nat. Rev. Immunol. 13, 227–242.
60) MacKay, M., Afshinnekoo, E., Rub, J., Hassan, C., Khunte, M., Baskaran, N., Owens, B., Liu, L., Roboz, G.J., Guzman, M.L., et al. (2020). The therapeutic landscape for cells engineered with chimeric antigen receptors. Nat. Biotechnol. *38*, 233–244.
61) Wang, K., Wei, G., and Liu, D. (2012). CD19: a biomarker for B cell development, lymphoma diagnosis and therapy. Exp. Hematol. Oncol. *1*, 1–7.

62) Nagro, C.J. Del, Otero, D.C., Anzelon, A.N., Omori, S.A., and Kolla, R. V, Rickert, R.C. (2005). CD19 CD21 B cell PI3-kinase Co-receptor Germinal center Marginal zone B-1 cell CD19 Function in Central and Peripheral B-Cell Development. 119–131.
63) LeBien, T.W. and Tedder, T.F. (2008) B Lymphocytes: How They Develop and Function. Blood, 112, 1570-1580.
64) Brentjens, R.J., Latouche, J.B., Santos, E., Marti, F., Gong, M.C., Lyddane, C., King, P.D., Larson, S., Weiss, M., Rivière, I., et al. (2003). Eradication of systemic B-cell tumors by genetically targeted human T lymphocytes co-stimulated by CD80 and interleukin-15. Nat. Med. *9*, 279–286.
65) Kowolik, C.M., Topp, M.S., Gonzalez, S., Pfeiffer, T., Olivares, S., Gonzalez, N., Smith, D.D., Forman, S.J., Jensen, M.C., and Cooper, L.J.N. (2006). CD28 costimulation provided through a CD19-specific chimeric antigen receptor enhances in vivo persistence and antitumor efficacy of adoptively transferred T cells. Cancer Res. *66*, 10995–11004.
66) Brentjens, R.J., Santos, E., Nikhamin, Y., Yeh, R., Matsushita, M., La Perle, K., Quintás-Cardama, A., Larson, S.M., and Sadelain, M. (2007). Genetically targeted T cells eradicate systemic acute lymphoblastic leukemia xenografts. Clin. Cancer Res. *13*, 5426–5435.
67) Imai, C., Mihara, K., Andreansky, M., Nicholson, I.C., Pui, C.H., Geiger, T.L., and Campana, D. (2004). Chimeric receptors with 4-1BB signaling capacity provoke potent cytotoxicity against acute lymphoblastic leukemia. Leukemia *18*, 676–684.
68) Milone, M.C., Fish, J.D., Carpenito, C., Carroll, R.G., Binder, G.K., Teachey, D., Samanta, M., Lakhal, M., Gloss, B., Danet-Desnoyers, G., et al. (2009). Chimeric receptors containing CD137 signal transduction domains mediate enhanced survival of T cells and increased antileukemic efficacy in vivo. Mol. Ther. *17*, 1453–1464.
69) Kochenderfer, J.N., Wilson, W.H., Janik, J.E., Dudley, M.E., Stetler-Stevenson, M., Feldman, S.A., Maric, I., Raffeld, M., Nathan, D.A.N., Lanier, B.J., et al. (2010). Eradication of B-lineage cells and regression of lymphoma in a patient treated with autologous T cells genetically engineered to recognize CD19. Blood *116*, 4099–4102.
70) Kalos, M., Levine, B.L., Porter, D.L., Katz, S., Grupp, S.A., Bagg, A., and June, C.H. (2011). T cells with chimeric antigen receptors have potent antitumor effects and can establish memory in patients with advanced leukemia. Sci. Transl. Med. *3*, 1–12.
71) Brentjens, R.J., Rivière, I., Park, J.H., Davila, M.L., Wang, X., Stefanski, J., Taylor, C., Yeh, R., Bartido, S., Borquez-Ojeda, O., et al. (2011). Safety and persistence of adoptively transferred autologous CD19-targeted T cells in patients with relapsed or chemotherapy refractory B-cell leukemias. Blood *118*, 4817–4828.
72) Neelapu, S.S., Locke, F.L., Bartlett, N.L., Lekakis, L.J., Miklos, D.B., Jacobson, C.A., Braunschweig, I., Oluwole, O.O., Siddiqi, T., Lin, Y., et al. (2017). Axicabtagene Ciloleucel CAR T-Cell Therapy in Refractory Large B-Cell Lymphoma. N. Engl. J. Med. *377*, 2531–2544.
73) Maude, S.L., Laetsch, T.W., Buechner, J., Rives, S., Boyer, M., Bittencourt, H., Bader, P., Verneris, M.R., Stefanski, H.E., Myers, G.D., et

al. (2018). Tisagenlecleucel in Children and Young Adults with B-Cell Lymphoblastic Leukemia. N. Engl. J. Med. *378*, 439–448.

74) Davila, M.L., Riviere, I., Wang, X., Bartido, S., Park, J., Curran, K., Chung, S.S., Stefanski, J., Borquez-Ojeda, O., Olszewska, M., et al. (2014). Efficacy and toxicity management of 19-28z CAR T cell therapy in B cell acute lymphoblastic leukemia. Sci. Transl. Med. *6*, 224ra25.

75) Lee, D.W., Gardner, R., Porter, D.L., Louis, C.U., Ahmed, N., Jensen, M., Grupp, S.A., and Mackall, C.L. (2014). Current concepts in the diagnosis and management of cytokine release syndrome. Blood *124*, 188–195.

76) Teachey, D.T., Lacey, S.F., Shaw, P.A., Melenhorst, J.J., Maude, S.L., Frey, N., Pequignot, E., Gonzalez, V.E., Chen, F., Finklestein, J., et al. (2016). Identification of predictive biomarkers for cytokine release syndrome after chimeric antigen receptor T-cell therapy for acute lymphoblastic leukemia. Cancer Discov. *6*, 664–679.

77) June, C.H., and Sadelain, M. (2018). Chimeric Antigen Receptor Therapy | Enhanced Reader. New Engl. J. Med. Rev.

78) Grupp, S.A., Kalos, M., Barrett, D., Aplenc, R., Porter, D.L., Rheingold, S.R., Teachey, D.T., Chew, A., Hauck, B., Wright, J.F., et al. (2013). Chimeric Antigen Receptor–Modified T Cells for Acute Lymphoid Leukemia. N. Engl. J. Med. *368*, 1509–1518.

79) Giavridis, T., Van Der Stegen, S.J.C., Eyquem, J., Hamieh, M., Piersigilli, A., and Sadelain, M. (2018). CAR T cell-induced cytokine release syndrome is mediated by macrophages and abated by IL-1 blockade letter. Nat. Med. *24*, 731–738.

80) Kochenderfer, J.N., Dudley, M.E., Feldman, S.A., Wilson, W.H., Spaner, D.E., Maric, I., Stetler-Stevenson, M., Phan, G.Q., Hughes, M.S., Sherry, R.M., et al. (2012). B-cell depletion and remissions of malignancy along with cytokine-associated toxicity in a clinical trial of anti-CD19 chimeric-antigen-receptor-transduced T cells. Blood *119*, 2709–2720.

81) Melenhorst, J.J., Chen, G.M., Wang, M., Porter, D.L., Chen, C., Collins, M.K.A., Gao, P., Bandyopadhyay, S., Sun, H., Zhao, Z., et al. (2022). Decade-long leukaemia remissions with persistence of CD4+ CAR T cells. Nature *602*, 503–509.

82) Turtle, C.J., Hanafi, L., Berger, C., Gooley, T.A., Cherian, S., Hudecek, M., Sommermeyer, D., Melville, K., Pender, B., Budiarto, T.M., et al. (2016). CD19 CAR – T cells of defined $CD4^+$:$CD8^+$ composition in adult B cell ALL patients. J Clin Invest *1*, 1–16.

83) Park, J.H., Rivière, I., Gonen, M., Wang, X., Sénéchal, B., Curran, K.J., Sauter, C., Wang, Y., Santomasso, B., Mead, E., et al. (2018). Long-Term Follow-up of CD19 CAR Therapy in Acute Lymphoblastic Leukemia. N. Engl. J. Med. *378*, 449–459.

84) Maude, S.L., Frey, N., Shaw, P.A., Aplenc, R., Barrett, D.M., Bunin, N.J., Chew, A., Gonzalez, V.E., Zheng, Z., Lacey, S.F., et al. (2014). Chimeric Antigen Receptor T Cells for Sustained Remissions in Leukemia. N. Engl. J. Med. *371*, 1507–1517.

85) Fry, T.J., Shah, N.N., Orentas, R.J., Stetler-Stevenson, M., Yuan, C.M., Ramakrishna, S., Wolters, P., Martin, S., Delbrook, C., Yates, B., et al. (2018). CD22-targeted CAR T cells induce remission in B-ALL that is naive or resistant to CD19-targeted CAR immunotherapy. Nat. Med. *24*, 20–28.

86) Lee DW, Kochenderfer JN, Stetler-Ste- venson M, et al. T cells expressing CD19 chimeric antigen receptors for acute lym- phoblastic leukaemia in children and young adults: a phase 1 dose-escalation trial.
87) Kochenderfer, J.N., Dudley, M.E., Kassim, S.H., Somerville, R.P.T., Carpenter, R.O., Maryalice, S.S., Yang, J.C., Phan, G.Q., Hughes, M.S., Sherry, R.M., et al. (2015). Chemotherapy-refractory diffuse large B-cell lymphoma and indolent B-cell malignancies can be effectively treated with autologous T cells expressing an anti-CD19 chimeric antigen receptor. J. Clin. Oncol. *33*, 540–549.
88) Schuster, S.J., Svoboda, J., Chong, E.A., Nasta, S.D., Mato, A.R., Anak, Ö., Brogdon, J.L., Pruteanu-Malinici, I., Bhoj, V., Landsburg, D., et al. (2017). Chimeric Antigen Receptor T Cells in Refractory B-Cell Lymphomas. N. Engl. J. Med. *377*, 2545–2554.
89) Cappell, K.M., Sherry, R.M., Yang, J.C., Goff, S.L., Vanasse, D.A., McIntyre, L., Rosenberg, S.A., and Kochenderfer, J.N. (2020). Long-Term Follow-Up of Anti-CD19 Chimeric Antigen Receptor T-Cell Therapy. J. Clin. Oncol. *38*, 3805–3815.
90) Fraietta, J.A., Lacey, S.F., Orlando, E.J., Pruteanu-Malinici, I., Gohil, M., Lundh, S., Boesteanu, A.C., Wang, Y., O'connor, R.S., Hwang, W.T., et al. (2018). Determinants of response and resistance to CD19 chimeric antigen receptor (CAR) T cell therapy of chronic lymphocytic leukemia. Nat. Med. *24*, 563–571.
91) Deng, Q., Han, G., Puebla-Osorio, N., Ma, M.C.J., Strati, P., Chasen, B., Dai, E., Dang, M., Jain, N., Yang, H., et al. (2020). Characteristics of anti-CD19 CAR T cell infusion products associated with efficacy and toxicity in patients with large B cell lymphomas. Nat. Med. *26*, 1878–1887.
92) Singh, N., Lee, Y.G., Shestova, O., Ravikumar, P., Hayer, K.E., Hong, S.J., Lu, X.M., Pajarillo, R., Agarwal, S., Kuramitsu, S., et al. (2020). Impaired Death Receptor Signaling in Leukemia Causes Antigen-Independent Resistance by Inducing CAR T-cell Dysfunction. Cancer Discov. *10*, 552–567.
93) Sotillo, E., Barrett, D.M., Black, K.L., Bagashev, A., Oldridge, D., Wu, G., Sussman, R., Lanauze, C., Ruella, M., Gazzara, M.R., et al. (2015). Convergence of acquired mutations and alternative splicing of CD19 enables resistance to CART-19 immunotherapy. Cancer Discov. *5*, 1282–1295.
94) Gardner, R., Wu, D., Cherian, S., Fang, M., Hanafi, L.A., Finney, O., Smithers, H., Jensen, M.C., Riddell, S.R., Maloney, D.G., et al. (2016). Acquisition of a CD19-negative myeloid phenotype allows immune escape of MLL-rearranged B-ALL from CD19 CAR-T-cell therapy. Blood *127*, 2406–2410.
95) Ruella, M., Xu, J., Barrett, D.M., Fraietta, J.A., Reich, T.J., Ambrose, D.E., Klichinsky, M., Shestova, O., Patel, P.R., Kulikovskaya, I., et al. (2018). Induction of resistance to chimeric antigen receptor T cell therapy by transduction of a single leukemic B cell. Nat. Med. *24*, 1499–1503.
96) Hamieh, M., Dobrin, A., Cabriolu, A., van der Stegen, S.J.C., Giavridis, T., Mansilla-Soto, J., Eyquem, J., Zhao, Z., Whitlock, B.M., Miele, M.M., et al. (2019). CAR T cell trogocytosis and cooperative killing regulate tumour antigen escape. Nature *568*, 112–116.

97) Spiegel, J.Y., Patel, S., Muffly, L., Hossain, N.M., Oak, J., Baird, J.H., Frank, M.J., Shiraz, P., Sahaf, B., Craig, J., et al. (2021). CAR T cells with dual targeting of CD19 and CD22 in adult patients with recurrent or refractory B cell malignancies: a phase 1 trial. Nat. Med. *27*, 1419–1431.
98) Cordoba, S., Onuoha, S., Thomas, S., Pignataro, D.S., Hough, R., Ghorashian, S., Vora, A., Bonney, D., Veys, P., Rao, K., et al. (2021). CAR T cells with dual targeting of CD19 and CD22 in pediatric and young adult patients with relapsed or refractory B cell acute lymphoblastic leukemia: a phase 1 trial. Nat. Med. *27*, 1797–1805.
99) Chmielewski, M., Hombach, A., Heuser, C., Adams, G.P., and Abken, H. (2004). T Cell Activation by Antibody-Like Immunoreceptors: Increase in Affinity of the Single-Chain Fragment Domain above Threshold Does Not Increase T Cell Activation against Antigen-Positive Target Cells but Decreases Selectivity. J. Immunol. *173*, 7647–7653.
100) Ghorashian, S., Kramer, A.M., Onuoha, S., Wright, G., Bartram, J., Richardson, R., Albon, S.J., Casanovas-Company, J., Castro, F., Popova, B., et al. (2019). Enhanced CAR T cell expansion and prolonged persistence in pediatric patients with ALL treated with a low-affinity CD19 CAR. Nat. Med. *25*, 1408–1414.
101) Srivastava, S., and Riddell, S.R. (2015). Engineering CAR-T cells: Design concepts. Trends Immunol. *36*, 494–502.
102) Hudecek, M., Lupo-Stanghellini, M.T., Kosasih, P.L., Sommermeyer, D., Jensen, M.C., Rader, C., and Riddell, S.R. (2013). Receptor affinity and extracellular domain modifications affect tumor recognition by ROR1-specific chimeric antigen receptor T cells. Clin. Cancer Res. *19*, 3153–3164.
103) Hudecek, M., Sommermeyer, D., Kosasih, P.L., Silva-Benedict, A., Liu, L., Rader, C., Jensen, M.C., and Riddell, S.R. (2015). The nonsignaling extracellular spacer domain of chimeric antigen receptors is decisive for in vivo antitumor activity. Cancer Immunol. Res. *3*, 125–135.
104) Majzner, R.G., Rietberg, S.P., Sotillo, E., Dong, R., Vachharajani, V.T., Labanieh, L., Myklebust, J.H., Kadapakkam, M., Weber, E.W., Tousley, A.M., et al. (2020). Tuning the antigen density requirement for car T-cell activity. Cancer Discov. *10*, 702–723.
105) Zhao, Z., Condomines, M., van der Stegen, S.J.C., Perna, F., Kloss, C.C., Gunset, G., Plotkin, J., and Sadelain, M. (2015). Supplementary Structural Design of Engineered Costimulation Determines Tumor Rejection Kinetics and Persistence of CAR T Cells. Cancer Cell *28*, 415–428.
106) Kawalekar, O.U., O'Connor, R.S., Fraietta, J.A., Guo, L., McGettigan, S.E., Posey, A.D., Patel, P.R., Guedan, S., Scholler, J., Keith, B., et al. (2016). Distinct Signaling of Coreceptors Regulates Specific Metabolism Pathways and Impacts Memory Development in CAR T Cells. Immunity *44*, 380–390.
107) Feucht, J; Sun J; Eyquem, J; Ho, Yu-jui; Zhao Z; Leibold, J; Dobrin, A; Cabriolu, A; Hamieh, M. (2018). Calibrated CAR activation potential directs alternative T cell fates and therapeutic potency. Nat. Med. Press.
108) Guedan, S., Madar, A., Casado-Medrano, V., Shaw, C., Wing, A., Liu, F., Young, R.M., June, C.H., and Posey, A.D. (2020). Single residue in CD28-costimulated CAR-T cells limits long-term persistence and antitumor durability. J. Clin. Invest. *130*, 3087–3097.

109) Kuhn, N.F., Purdon, T.J., van Leeuwen, D.G., Lopez, A. V., Curran, K.J., Daniyan, A.F., and Brentjens, R.J. (2019). CD40 Ligand-Modified Chimeric Antigen Receptor T Cells Enhance Antitumor Function by Eliciting an Endogenous Antitumor Response. Cancer Cell *35*, 473-488.e6.
110) Katsarou, A., Sjöstrand, M., Naik, J., Mansilla-Soto, J., Kefala, D., Kladis, G., Nianias, A., Ruiter, R., Poels, R., Sarkar, I., et al. (2021). Combining a CAR and a chimeric costimulatory receptor enhances T cell sensitivity to low antigen density and promotes persistence. Sci. Transl. Med. *13*, 1–17.
111) Cherkassky, L., Sadelain, M., Prasad, S., Invest, J.C., Cherkassky, L., Morello, A., Villena-vargas, J., Feng, Y., Dimitrov, D.S., Jones, D.R., et al. (2016). Human CAR T cells with cell-intrinsic PD-1 checkpoint blockade resist tumor-mediated inhibition Find the latest version: Human CAR T cells with cell-intrinsic PD-1 checkpoint blockade resist tumor-mediated inhibition.
112) Liu, X., Ranganathan, R., Jiang, S., Fang, C., Sun, J., Kim, S., Newick, K., Lo, A., June, C.H., Zhao, Y., et al. (2016). A chimeric switch-receptor targeting PD1 augments the efficacy of second-generation CAR T cells in advanced solid tumors. Cancer Res. *76*, 1578–1590.
113) Rafiq, S., Hackett, C.S., and Brentjens, R.J. (2020). Engineering strategies to overcome the current roadblocks in CAR T cell therapy. Nat. Rev. Clin. Oncol. *17*, 147–167.
114) Pegram, H. J. et al. (2012). Tumor-targeted T cells modified to secrete IL-12 eradicate systemic tumors without need for prior conditioning. Blood 119, 4133–4141 (2012).
115) Koneru, M., Purdon, T. J., Spriggs, D., Koneru, S. & Brentjens, R. J. (2015). IL-12 secreting tumor- targeted chimeric antigen receptor T cells eradicate ovarian tumors in vivo. Oncoimmunology 4, e994446.
116) Krenciute, G. et al. (2017). Transgenic expression of IL15 improves antiglioma activity of IL13Rα2-CAR T cells but results in antigen loss variants. Cancer Immunol. Res. 5, 571–581.
117) Chen, Y. et al. Eradication of neuroblastoma by T cells redirected with an optimized GD2-specific chimeric antigen receptor and interleukin-15. Clin. Cancer Res. 25, 2915–2924 (2019).
118) Chmielewski, M. & Abken, H. CAR T cells releasing IL-18 convert to T-Bet^{high} FoxO1^{low} effectors that exhibit augmented activity against advanced solid tumors. Cell Rep. 21, 3205–3219 (2017).
119) Hu, B. et al. Augmentation of antitumor immunity by human and mouse CAR T cells secreting IL-18. Cell Rep. 20, 3025–3033 (2017).
120) Adachi, K. et al. IL-7 and CCL19 expression in CAR- T cells improves immune cell infiltration and CAR- T cell survival in the tumor. Nat. Biotechnol. 36, 346–351 (2018).
121) Chen, Y. & Lu, B. Guided delivery of the “alarming” cytokine IL-33 to tumor by chimeric antigen receptor T cells. J. Immunol. 198, 204.223 (2017).
122) Li, X. D., A., Lopez, A., Purdon, T. & Brentjens, R. Augmenting CAR T cell mediated antitumor efficacy through genetic modification to secrete a novel cytokine IL-36γ. Mol. Ther. 27, 432–433 (2019).
123) Lynn, R.C., Weber, E.W., Sotillo, E., Gennert, D., Xu, P., Good, Z., Anbunathan, H., Lattin, J., Jones, R., Tieu, V., et al. (2019). c-Jun

overexpression in CAR T cells induces exhaustion resistance. Nature *576*, 293–300.
124) Seo, H., González-Avalos, E., Zhang, W., Ramchandani, P., Yang, C., Lio, C.W.J., Rao, A., and Hogan, P.G. (2021). BATF and IRF4 cooperate to counter exhaustion in tumor-infiltrating CAR T cells. Nat. Immunol. *22*, 983–995.
125) Zhou, J. e., Yu, J., Wang, Y., Wang, H., Wang, J., Wang, Y., Yu, L., and Yan, Z. (2021). ShRNA-mediated silencing of PD-1 augments the efficacy of chimeric antigen receptor T cells on subcutaneous prostate and leukemia xenograft. Biomed. Pharmacother. *137*, 111339.
126) Osborn, M.J., Webber, B.R., Knipping, F., Lonetree, C.L., Tennis, N., DeFeo, A.P., McElroy, A.N., Starker, C.G., Lee, C., Merkel, S., et al. (2016). Evaluation of TCR gene editing achieved by TALENs, CRISPR/Cas9, and megaTAL nucleases. Mol. Ther. *24*, 570–581.
127) Qasim, W., Zhan, H., Samarasinghe, S., Adams, S., Amrolia, P., Stafford, S., Butler, K., Rivat, C., Wright, G., Somana, K., et al. (2017). Molecular remission of infant B-ALL after infusion of universal TALEN gene-edited CAR T cells. Sci. Transl. Med. *9*, 1–9.
128) Liu, X., Zhang, Y., Cheng, C., Cheng, A.W., Zhang, X., Li, N., Xia, C., Wei, X., Liu, X., and Wang, H. (2017). CRISPR-Cas9-mediated multiplex gene editing in CAR-T cells. Cell Res. *27*, 154–157.
129) Eyquem, J., Mansilla-Soto, J., Giavridis, T., van der Stegen, S.J.C., Hamieh, M., Cunanan, K.M., Odak, A., Gönen, M., and Sadelain, M. (2017). Targeting a CAR to the TRAC locus with CRISPR/Cas9 enhances tumour rejection. Nature *543*, 113–117.
130) Hu, W., Zi, Z., Jin, Y., Li, G., Shao, K., Cai, Q., Ma, X., and Wei, F. (2019). CRISPR/Cas9-mediated PD-1 disruption enhances human mesothelin-targeted CAR T cell effector functions. Cancer Immunol. Immunother. *68*, 365–377.
131) Zhang, Q., Chikina, M., Szymczak-Workman, A.L., Horne, W., Kolls, J.K., Vignali, K.M., Normolle, D., Bettini, M., Workman, C.J., and Vignali, D.A.A. (2017). LAG3 limits regulatory T cell proliferation and function in autoimmune diabetes. Sci. Immunol. *2*.
132) Seo, H., Chen, J., González-Avalos, E., Samaniego-Castruita, D., Das, A., Wang, Y.H., López-Moyado, I.F., Georges, R.O., Zhang, W., Onodera, A., et al. (2019). TOX and TOX2 transcription factors cooperate with NR4A transcription factors to impose CD8+ T cell exhaustion. Proc. Natl. Acad. Sci. U. S. A. *116*, 12410–12415.
133) Tang, N., Cheng, C., Zhang, X., Qiao, M., Li, N., Mu, W., Wei, X.F., Han, W., and Wang, H. (2020). TGF-β inhibition via CRISPR promotes the long-term efficacy of CAR T cells against solid tumors. JCI Insight *5*.
134) Wei, J., Long, L., Zheng, W., Dhungana, Y., Lim, S.A., Guy, C., Wang, Y., Wang, Y.-D., Qian, C., Xu, B., et al. (2019). Targeting REGNASE-1 programs long-lived effector T cells for cancer therapy. Nature *576*.
135) Gurusamy, D., Henning, A.N., Yamamoto, T.N., Yu, Z., Zacharakis, N., Krishna, S., Kishton, R.J., Vodnala, S.K., Eidizadeh, A., Jia, L., et al. (2020). Multi-phenotype CRISPR-Cas9 Screen Identifies p38 Kinase as a Target for Adoptive Immunotherapies. Cancer Cell *37*, 818-833.e9.
136) Wang, D., Prager, B.C., Gimple, R.C., Aguilar, B., Alizadeh, D., Tang, H., Lv, D., Starr, R., Brito, A., Wu, Q., et al. (2021). Crispr screening of car t

cells and cancer stem cells reveals critical dependencies for cell-based therapies. Cancer Discov. *11*, 1192–1211.
137) Youngblood, B. et al. (2013) Cutting edge: prolonged exposure to HIV reinforces a poised epigenetic program for PD-1 expression in virus-specific CD8 T cells. J. Immunol. 191, 540–544
138) Youngblood, B. et al. (2017) Effector CD8 T cells dedifferentiate into long-lived memory cells. Nature 552, 404–409
139) Gray, S.M., Amezquita, R.A., Guan, T., Kleinstein, S.H., and Kaech, S.M. (2017). Polycomb Repressive Complex 2-Mediated Chromatin Repression Guides Effector CD8+ T Cell Terminal Differentiation and Loss of Multipotency. Immunity *46*, 596–608.
140) Philip, M., Fairchild, L., Sun, L., Horste, E.L., Camara, S., Shakiba, M., Scott, A.C., Viale, A., Lauer, P., Merghoub, T., et al. (2017). Chromatin states define tumour-specific T cell dysfunction and reprogramming. Nat. Publ. Gr. *545*, 452–456.
141) Sade-Feldman, M., Yizhak, K., Bjorgaard, S.L., Ray, J.P., de Boer, C.G., Jenkins, R.W., Lieb, D.J., Chen, J.H., Frederick, D.T., Barzily-Rokni, M., et al. (2018). Defining T Cell States Associated with Response to Checkpoint Immunotherapy in Melanoma. Cell *175*, 998-1013.e20.
142) Ghoneim, H.E., Fan, Y., Moustaki, A., Neale, G., Thomas, P.G., Youngblood, B., Rejuvenation, P.-B.T.C., Ghoneim, H.E., Fan, Y., Moustaki, A., et al. (2017). Article De Novo Epigenetic Programs Inhibit. Cell *170*, 142-157.e19.
143) Prinzing, B., Zebley, C.C., Petersen, C.T., Fan, Y., Anido, A.A., Yi, Z., Nguyen, P., Houke, H., Bell, M., Haydar, D., et al. (2021). Deleting DNMT3A in CAR T cells prevents exhaustion and enhances antitumor activity. Sci. Transl. Med. *13*, 1–19.
144) Pastor, W.A., Aravind, L., and Rao, A. (2013). TETonic shift: biological roles of TET proteins in DNA demethylation and transcription. Nat. Publ. Gr. *14*, 341–356.
145) Ostrander, E.L., Kramer, A.C., Mallaney, C., Celik, H., Koh, W.K., Fairchild, J., Haussler, E., Zhang, C.R.C., and Challen, G.A. (2020). Divergent Effects of Dnmt3a and Tet2 Mutations on Hematopoietic Progenitor Cell Fitness. Stem Cell Reports *14*, 551–560.
146) Ichiyama, K., Chen, T., Wang, X., Yan, X., Kim, B.S., Tanaka, S., Ndiaye-Lobry, D., Deng, Y., Zou, Y., Zheng, P., et al. (2015). The Methylcytosine Dioxygenase Tet2 Promotes DNA Demethylation and Activation of Cytokine Gene Expression in T Cells. Immunity *42*, 613–626.
147) Carty, S.A., Gohil, M., Banks, L.B., Cotton, R.M., Johnson, M.E., Stelekati, E., Wells, A.D., Wherry, E.J., Koretzky, G.A., and Jordan, M.S. (2018). The Loss of TET2 Promotes CD8 + T Cell Memory Differentiation. J. Immunol. *200*, 82–91.
148) Porter, D.L., Hwang, W.T., Frey, N. V., Lacey, S.F., Shaw, P.A., Loren, A.W., Bagg, A., Marcucci, K.T., Shen, A., Gonzalez, V., et al. (2015). Chimeric antigen receptor T cells persist and induce sustained remissions in relapsed refractory chronic lymphocytic leukemia. Sci. Transl. Med. *7*, 1–13.
149) Allan, R.S., Zueva, E., Cammas, F., Schreiber, H.A., Masson, V., Belz, G.T., Roche, D., Maison, C., Quivy, J.P., Almouzni, G., et al. (2012). An

epigenetic silencing pathway controlling T helper 2 cell lineage commitment. Nature *487*, 249–253.
150) Adoue, V., Binet, B., Malbec, A., Fourquet, J., Romagnoli, P., van Meerwijk, J.P.M., Amigorena, S., and Joffre, O.P. (2019). The Histone Methyltransferase SETDB1 Controls T Helper Cell Lineage Integrity by Repressing Endogenous Retroviruses. Immunity *50*, 629-644.e8.
151) Dobenecker, M.W., Park, J.S., Marcello, J., McCabe, M.T., Gregory, R., Knight, S.D., Rioja, I., Bassil, A.K., Prinjha, R.K., and Tarakhovsky, A. (2018). Signaling function of PRC2 is essential for TCR-driven T cell responses. J. Exp. Med. *215*, 1101–1113.
152) Pace, L., Goudot, C., Zueva, E., Gueguen, P., Burgdorf, N., Waterfall, J.J., Quivy, J.P., Almouzni, G., and Amigorena, S. (2018). The epigenetic control of stemness in CD8+ T cell fate commitment. Science *359*, 177–186.
153) Riviere, I., Brose, K. & Mulligan, R. C. Effects of retroviral vector design on expression of human adenosine deaminase in murine bone marrow transplant recipients engrafted with genetically modified cells. *Proc Natl Acad Sci U S A* **92**, 6733-6737, doi:10.1073/pnas.92.15.6733 (1995).
154) Gallardo, H. F., Tan, C., Ory, D. & Sadelain, M. Recombinant retroviruses pseudotyped with the vesicular stomatitis virus G glycoprotein mediate both stable gene transfer and pseudotransduction in human peripheral blood lymphocytes. *Blood* **90**, 952-957 (1997).
155) Gong, M. C. *et al.* Cancer patient T cells genetically targeted to prostate-specific membrane antigen specifically lyse prostate cancer cells and release cytokines in response to prostate-specific membrane antigen. *Neoplasia* **1**, 123-127, doi:10.1038/sj.neo.7900018 (1999).
156) Stoklasek, T. A., Schluns, K. S. & Lefrancois, L. Combined IL-15/IL-15Ralpha immunotherapy maximizes IL-15 activity in vivo. *J Immunol* **177**, 6072-6080, doi:10.4049/jimmunol.177.9.6072 (2006).
157) Gabriel, R. *et al.* Comprehensive genomic access to vector integration in clinical gene therapy. *Nat Med* **15**, 1431-1436, doi:10.1038/nm.2057 (2009).
158) Paruzynski, A. *et al.* Genome-wide high-throughput integrome analyses by nrLAM-PCR and next-generation sequencing. *Nat Protoc* **5**, 1379-1395, doi:10.1038/nprot.2010.87 (2010).
159) Afzal, S., Wilkening, S., von Kalle, C., Schmidt, M. & Fronza, R. GENE-IS: Time-Efficient and Accurate Analysis of Viral Integration Events in Large-Scale Gene Therapy Data. *Mol Ther Nucleic Acids* **6**, 133-139, doi:10.1016/j.omtn.2016.12.001 (2017).
160) Kong, W., Dimitri, A., Wang, W., Jung, I.Y., Ott, C.J., Fasolino, M., Wang, Y., Kulikovskaya, I., Gupta, M., Yoder, T., et al. (2021). BET bromodomain protein inhibition reverses chimeric antigen receptor extinction and reinvigorates exhausted T cells in chronic lymphocytic leukemia. J. Clin. Invest. *131*, 1–16.
161) Kueberuwa, G., Gornall, H., Alcantar-Orozco, E.M., Bouvier, D., Kapacee, Z.A., Hawkins, R.E., and Gilham, D.E. (2017). CCR7+ selected gene-modified T cells maintain a central memory phenotype and display enhanced persistence in peripheral blood in vivo. J. Immunother. Cancer *5*, 1–14.

162) Subramanian, A., Tamayo, P., Mootha, V.K., Mukherjee, S., Ebert, B.L., Gillette, M.A., Paulovich, A., Pomeroy, S.L., Golub, T.R., Lander, E.S., et al. (2005). Gene set enrichment analysis: A knowledge-based approach for interpreting genome-wide expression profiles. Proc. Natl. Acad. Sci. U. S. A. *102*, 15545–15550.
163) Bowman, R.L., and Levine, R.L. (2017). TET2 in Normal and Malignant Hematopoiesis. Cold Spring Harb. Perspect. Med. *7*, 1–12.
164) Tsagaratou, A., González-Avalos, E., Rautio, S., Scott-Browne, J.P., Togher, S., Pastor, W.A., Rothenberg, E. V., Chavez, L., Lähdesmäki, H., and Rao, A. (2017). TET proteins regulate the lineage specification and TCR-mediated expansion of iNKT cells. Nat. Immunol. *18*, 45–53.
165) Yue, X., Lio, C.J., and Rao, A. Loss of TET2 and TET3 in regulatory T cells unleashes effector function. Nat. Commun. 1–14.
166) Nakagawa, M., Shaffer, A.L., Ceribelli, M., Zhang, M., Wright, G., Huang, D.W., Xiao, W., Powell, J., Petrus, M.N., Yang, Y., et al. (2018). Targeting the HTLV-I-Regulated BATF3/IRF4 Transcriptional Network in Adult T Cell Leukemia/Lymphoma. Cancer Cell *34*, 286-297.e10.
167) Man, K. *et al.* The transcription factor IRF4 is essential for TCR affinity-mediated metabolic programming and clonal expansion of T cells. *Nat Immunol* **14**, 1155-1165, doi:10.1038/ni.2710 (2013).
168) Man, K. *et al.* Transcription Factor IRF4 Promotes CD8(+) T Cell Exhaustion and Limits the Development of Memory-like T Cells during Chronic Infection. *Immunity* **47**, 1129-1141 e1125, doi:10.1016/j.immuni.2017.11.021 (2017).
169) Ataide, M. A. *et al.* BATF3 programs CD8(+) T cell memory. *Nat Immunol* **21**, 1397-1407, doi:10.1038/s41590-020-0786-2 (2020).
170) Eferl, R. & Wagner, E. F. AP-1: a double-edged sword in tumorigenesis. *Nat Rev Cancer* **3**, 859-868, doi:10.1038/nrc1209 (2003).
171) Schreiber, M. *et al.* Control of cell cycle progression by c-Jun is p53 dependent. *Genes Dev* **13**, 607-619, doi:10.1101/gad.13.5.607 (1999).
172) Logan, M. R., Jordan-Williams, K. L., Poston, S., Liao, J. & Taparowsky, E. J. Overexpression of Batf induces an apoptotic defect and an associated lymphoproliferative disorder in mice. *Cell Death Dis* **3**, e310, doi:10.1038/cddis.2012.49 (2012).
173) Liang, H. C. *et al.* Super-enhancer-based identification of a BATF3/IL-2R-module reveals vulnerabilities in anaplastic large cell lymphoma. *Nat Commun* **12**, 5577, doi:10.1038/s41467-021-25379-9 (2021).
174) Genovese, G. *et al.* Clonal hematopoiesis and blood-cancer risk inferred from blood DNA sequence. *N Engl J Med* **371**, 2477-2487, doi:10.1056/NEJMoa1409405 (2014).
175) Zhang, X. *et al.* DNMT3A and TET2 compete and cooperate to repress lineage-specific transcription factors in hematopoietic stem cells. *Nat Genet* 48, 1014-1023, doi:10.1038/ng.3610 (2016).
176) Watatani, Y. *et al.* Molecular heterogeneity in peripheral T-cell lymphoma, not otherwise specified revealed by comprehensive genetic profiling. *Leukemia* 33, 2867-2883, doi:10.1038/s41375-019-0473-1 (2019).
177) Trimarchi, J.M., and Lees, J.A. (2002). Sibling rivalry in the E2F family. Nat. Rev. Mol. Cell Biol. *3*, 11–20.
178) Zhao, X., Shan, Q., and Xue, H.H. (2021). TCF1 in T cell immunity: a broadened frontier. Nat. Rev. Immunol. *13*.

179) Xing, S., Li, F., Zeng, Z., Zhao, Y., Yu, S., Shan, Q., Li, Y., Phillips, F.C., Maina, P.K., Qi, H.H., et al. (2016). Tcf1 and Lef1 transcription factors establish CD8+ T cell identity through intrinsic HDAC activity. Nat. Immunol. *17*, 695–703.
180) Xing, S., Gai, K., Li, X., Shao, P., Zeng, Z., Zhao, X., Zhao, X., Chen, X., Paradee, W.J., Meyerholz, D.K., et al. (2019). Tcf1 and Lef1 are required for the immunosuppressive function of regulatory T cells. J. Exp. Med. *216*, 847–866.
181) Wu, T., Shin, H.M., Moseman, E.A., Ji, Y., Huang, B., Harly, C., Sen, J.M., Berg, L.J., Gattinoni, L., McGavern, D.B., et al. (2015). TCF1 Is Required for the T Follicular Helper Cell Response to Viral Infection. Cell Rep. *12*, 2099–2110.
182) Danilo, M., Chennupati, V., Silva, J.G., Siegert, S., and Held, W. (2018). Suppression of Tcf1 by Inflammatory Cytokines Facilitates Effector CD8 T Cell Differentiation. Cell Rep. *22*, 2107–2117.
183) Bishop, E.L., Gudgeon, N., and Dimeloe, S. (2021). Control of T Cell Metabolism by Cytokines and Hormones. Front. Immunol. *12*, 1–15.
184) Buck, M.D.D., O'Sullivan, D., Klein Geltink, R.I.I., Curtis, J.D.D., Chang, C.H., Sanin, D.E.E., Qiu, J., Kretz, O., Braas, D., van der Windt, G.J.J.W., et al. (2016). Mitochondrial Dynamics Controls T Cell Fate through Metabolic Programming. Cell *166*, 63–76.
185) Vandel, L., Nicolas, E., Vaute, O., Ferreira, R., Ait-Si-Ali, S., and Trouche, D. (2001). Transcriptional Repression by the Retinoblastoma Protein through the Recruitment of a Histone Methyltransferase. Mol. Cell. Biol. *21*, 6484–6494.
186) Nielsen SJ, Schneider R, Bauer UM, Bannister AJ, Morrison A, O'Carroll D, Firestein R, Cleary M, Jenuwein T, Herrera RE, et al. (2001). Rb targets histone H3 methylation and HP1 to promoters. Nature. 412:561-5.
187) Mansilla-Soto, J., Eyquem, J., Haubner, S., Hamieh, M., Feucht, J., Paillon, N., Zucchetti, A.E., Li, Z., Sjöstrand, M., Lindenbergh, P.L., et al. (2022). HLA-independent T cell receptors for targeting tumors with low antigen density. Nat. Med. *28*, 345–352.
188) Jadhav, R.R., Im, S.J., Hu, B., Hashimoto, M., Li, P., Lin, J.X., Leonard, W.J., Greenleaf, W.J., Ahmed, R., and Goronzy, J.J. (2019). Epigenetic signature of PD-1+ TCF1+ CD8 T cells that act as resource cells during chronic viral infection and respond to PD-1 blockade. Proc. Natl. Acad. Sci. U. S. A. *116*, 14113–14118.
189) Nobles, C.L., Melenhorst, J.J., Frederic, D., Nobles, C.L., Sherrill-mix, S., Everett, J.K., Reddy, S., Fraietta, J.A., Porter, D.L., Frey, N., et al. (2019). CD19-targeting CAR T cell immunotherapy outcomes correlate with genomic modification by vector integration. JCI- 2020 Feb 3;130(2):673-685.
190) Sterner, R.C., and Sterner, R.M. (2021). CAR-T cell therapy: current limitations and potential strategies. Blood Cancer J. *11*-4.
191) Legut, M., Gajic, Z., Guarino, M., Daniloski, Z., Rahman, J.A., Xue, X., Lu, C., Lu, L., Mimitou, E.P., Hao, S., et al. (2022). A genome-scale screen for synthetic drivers of T cell proliferation. Nature *603*, 728-735.
192) Narayan, V., et al. (2022). "PSMA-targeting TGFbeta-insensitive armored CAR T cells in metastatic castration-resistant prostate cancer: a phase 1 trial." Nat Med. 28, 724-734.